



Universiteit
Leiden
The Netherlands

The Crab nebula

Woltjer, L.

Citation

Woltjer, L. (1958). The Crab nebula. *Bulletin Of The Astronomical Institutes Of The Netherlands*, 14, 39. Retrieved from <https://hdl.handle.net/1887/6355>

Version: Not Applicable (or Unknown)

License: [Leiden University Non-exclusive license](#)

Downloaded from: <https://hdl.handle.net/1887/6355>

Note: To cite this publication please use the final published version (if applicable).

BULLETIN OF THE ASTRONOMICAL INSTITUTES OF THE NETHERLANDS

1958 JANUARY 16

VOLUME XIV

NUMBER 483

 COMMUNICATION FROM THE OBSERVATORY AT LEIDEN

THE CRAB NEBULA

BY L. WOLTJER

The article describes an empirical as well as theoretical study of the phenomena observed in the Crab nebula. Use has been made of spectra taken by Dr MAYALL with the Crossley reflector of the Lick Observatory and of plates taken by Dr BAADE with the 200-inch telescope.

In Part I a discussion is given of the motion of the shell, the spectrum of the continuum and the space distributions of the optical and radio emission.

Part II contains the photometry of the spectra of the filaments. The excitation of the filaments is shown to be mostly due to the ultraviolet radiation from the inner part of the nebula, with possibly a contribution from the central star. Collisional excitation plays only a minor role. The temperature of the nebula is found to be 17 000° or lower. The electron density in a few strong filaments is about 1500 cm⁻³. The abundances of H, He, N, O, Ne, and S have been derived. The ratio of H and He to the light elements is probably not very abnormal. Helium, however, is at least a factor two overabundant relative to hydrogen. Information on the temperature and density of the filaments has also been obtained from a plate taken by Dr BAADE in the light of the red [SII] lines. From the ionization conditions in the filaments the strength of the far-ultraviolet emission from the inner parts of the nebula has been derived. The differences between the line-intensity ratios in the various filaments may be ascribed to changes in the excitation conditions. The intensity ratio of the [OIII] and [OII] lines shows a systematic dependence on the position in the nebula. This may be due either to anisotropy of the ultraviolet radiation field or to an underestimate of the distance of the nebula, which should possibly be doubled. The nebula would then resemble a prolate instead of an oblate spheroid. The total mass of the visible filaments is found to be slightly less than a tenth of a solar mass, but if the filaments are surrounded by a less dense medium (as indicated in section 38) the total mass of the shell might very well be as large as that of the sun.

In Part III the continuous radiation is discussed. It can be explained as synchrotron radiation produced by relativistic electrons having an energy spectrum $n(E) \propto E^{-\beta}$ with a cut-off at a maximum energy of the order of 10¹² ev. The difference in space distribution between the optical and radio emission cannot be due to their different dependence on the magnetic field. The only possible explanation appears to be a different distribution of the radio electrons and the optical ones. The total energy of the relativistic electrons is of the order of 10⁴⁸ erg if, as appears plausible, for the central parts of the nebula a mean magnetic field of 10⁻⁴ oersted is adopted.

With regard to the possible mechanism for accelerating the electrons it is shown that they cannot have obtained their present energies from a process near the surface of the central star. They may, however, have been accelerated by hydromagnetic waves in the nebula. Under some plausible assumptions the energy spectrum and the maximum energy of the electrons may be computed and a satisfactory agreement with the observed parameters can be obtained.

In Part IV arguments are given to indicate that the magnetic field in the nebula must be of the force-free type. A discussion of such fields is given and the general solution is found for the case where the ratio of current to field strength is constant. The boundary conditions require that a surface current must flow around the region containing the field, if there are no currents outside the region. In the Crab nebula we identify the filaments with such a surface current. A few models of the emission by electrons moving in a force-free field have been constructed, but a detailed comparison with the observations of the polarization in the nebula cannot be made, as the theory of these fields has not been sufficiently developed. An attempt has been made to explain some of the details of the structure of the nebula.

In Part V the expansion of the nebula is discussed. It appears that the magnetic energy must have been much larger in the earlier stages of the evolution of the nebula than at present. The field cannot have been contained in a stellar object. It seems probable that most of the present field originated about one or two years after the explosion of the supernova, as a result of large-scale turbulence in the nebula. The field of the pre-supernova must have been rather strong to make this mechanism effective. The evolution of supernovae and their magnetic fields are briefly discussed. The general results in this paper are consistent with recent theories on element formation in supernovae. Radioactive elements formed during the explosion may be the source of energy for the relativistic electrons as well as for the high activity still persisting in the central star and the nebula.

The filamentary structure of the shell is explained by the pinch effect. It appears probable that the visible filaments are low-temperature condensations in filaments of much lower average density and rather high temperature.

The electrons needed to explain the non-thermal radio emission from the Galactic System may possibly have been formed in supernovae. Additional acceleration in interstellar space or in the galactic halo is possibly of minor importance. It is pointed out that, though objects like the Crab nebula produce too small an amount of cosmic rays, larger numbers of cosmic-ray particles may have been produced in the early stages after a supernova explosion.

PART I. BASIC DATA

1. *Introduction.*

It has been known for some time that the Crab nebula is the remnant of a supernova, which flared up in the year 1054. The nebular spectrum consists of two parts. First there is a strong continuum. The observed brightness of the nebula is largely due to this continuum. In spectra of the nebula or in photographs taken with appropriately chosen narrow band filters we see that besides the continuum there is also some line emission in the nebula. On the photographs it is clearly seen that this line emission is concentrated in filaments (BAADE 1942) and on the spectra we see that these filaments form an expanding, more or less hollow shell (MAYALL 1937). The spectra of the filaments are similar to the spectra of planetary nebulae (MAYALL 1937). The continuum is emitted in regions inside this shell.

The interpretation of the continuum gave large difficulties at first when it was assumed that the continuum was due to free-free transitions in a gas at very high temperature. It now appears much more probable that the continuum is synchrotron radiation (SHKLOVSKY 1954; OORT and WALRAVEN 1956). In the synchrotron mechanism the radiation is due to relativistic electrons spiraling in a magnetic field. The light is emitted in a very narrow cone around the velocity vector of the electron. The emitted radiation is completely polarized with the electric vector perpendicular to the lines of force of the magnetic field. The fact that strong polarization is observed is a confirmation for this theory. On the basis of this mechanism OORT and WALRAVEN (1956) built a theory of the nebula. They found a magnetic field of about 10^{-3} oersted at the centre of the nebula. The relativistic particles would have an energy spectrum similar to, but perhaps somewhat flatter than cosmic rays. The total energies in the magnetic field and in the relativistic particles are then of the same order of magnitude and both equal to a few times 10^{48} erg. The total mass of the relativistic particles is very small. According to OORT and WALRAVEN the filaments can be ionized by the ultraviolet radiation from the inner part.

It seemed of interest, as a plausible theory of the emission of the nebula is now available, to assemble all data that could be obtained to construct a more complete picture of the Crab nebula.

2. *New observational data.*

The new observational data which form the background of the present investigation may be summarized as follows. From Dr BAADE we obtained some

plates taken with the 200-inch telescope, from which we derived the polarization and intensity distribution in the continuum. The results have already been published (L. WOLTJER 1957. In the following we refer to this as Paper I) but the discussion is given in the present paper. These data are important to derive the structure of the magnetic field in the nebula. Dr BAADE also sent us some older plates of the nebula taken with the 100-inch telescope at Mt Wilson. The earliest of these plates was obtained in 1924. These plates are useful for investigating the changes which have taken place in the nebula.

Dr MAYALL sent us a number of spectra of the nebula which he had taken with the Crossley reflector at Lick Observatory, with the aim of measuring radial velocities. These spectra form the basis of our photometric studies of the filaments. Dr BAADE also provided glass copies of photographs of the nebula taken in the light of the forbidden [OII] and [OIII] lines at $\lambda 3727$ A and at $\lambda 5000$ A. Moreover Dr BAADE obtained for us a plate of the nebula in the forbidden [SII] lines at $\lambda 6724$ A. Without all these valuable data, which were put so kindly at our disposal by Dr BAADE and Dr MAYALL, it would have been impossible to make this investigation.

3. *Structure and motion of the filamentary shell.*

The filamentary shell of the nebula is roughly elliptical with semi-axes of $178''$ and $120''$ according to BAADE (1942). The angle between the major axis and the galactic plane is about 20° . The coordinates of the centre of this ellipse referred to the SW component of the central double star are $\Delta\alpha = +6''.9$, $\Delta\delta = +4''.4$. The centre of the optical intensity distribution was derived from the isophotes in Paper I. The coordinates are $\Delta\alpha = -11''.2$, $\Delta\delta = +14''.0$. The difference between the two values seems to be larger than the errors in the determination would allow. The centre of the radio nebula at 400 Mc/s appears to have an intermediate position (SEEGER and WESTERHOUT 1957). From the isophotes in Paper I it appears that the limit of detectability of the optical continuous radiation coincides roughly with the limits of the filamentary system. The radio nebula has the same extent as the optical nebula according to SEEGER and WESTERHOUT (1957). The filamentary shell therefore represents the real physical boundary of the nebula.

We shall tentatively assume that the nebula is an oblate spheroid, with the minor axis perpendicular to the line of sight (cf. however section 17).

In this case the expansion velocity at the end of the major axis must be equal to the radial velocity at the projected centre of the shell. From the radial velocities measured by Dr MAYALL we find for this velocity

1150 km/sec. The proper motions along the major axis have been measured by DUNCAN (1939) and discussed more fully by BAADE (1942), who found at the end of the major axis $\mu = 0''.235/a$. From these data we derive a distance of 1030 pc. Accordingly one minute of arc is 0.300 pc or 9.25×10^{17} cm. The semi-axes of the filamentary system are 0.89 pc and 0.60 pc and the nebular volume becomes 5.9×10^{55} cm³. The average radius is 0.79 pc. The velocities along the major axis are larger than along the minor axis. Assuming that the velocity ellipsoid is an oblate spheroid with an axial ratio equal to the axial ratio of the filamentary system we obtain for the average expansion velocity 1010 km/sec.

In the proper motions DUNCAN and BAADE found indications of an acceleration. When the proper motions along the major axis are extrapolated backwards under the assumption of a constant velocity they indicate a time of origin for the nebula 126 years later than the appearance of the supernova. DEUTSCH and LAVDOVSKY (1940) measured proper motions for seven points in the nebula and obtained a time of origin 100 years too late. It seems therefore probable that this acceleration is real. A new determination of a large number of proper motions, such as is now being made by Dr BAADE, is required to study this question in detail. From DUNCAN's measurements we have the impression that not all filamentary knots have had the same acceleration. It seems for example that in the filamentary bulge at the SW side of the nebula the motions have been retarded.

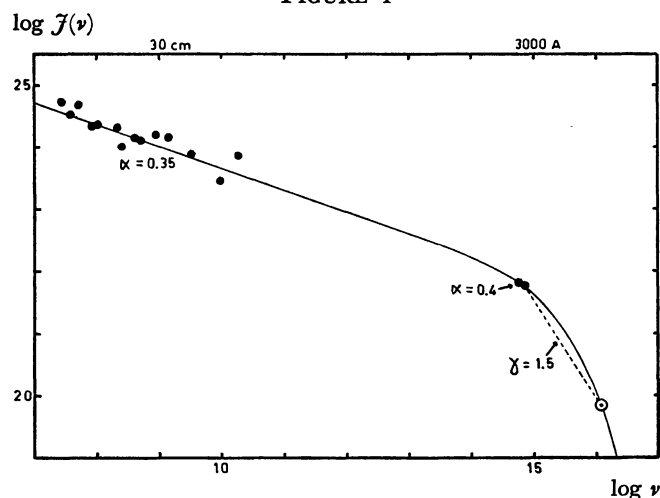
We assume that the acceleration in the motion along the line of sight has been the same as the acceleration in the proper motions along the major axis and that the ratio of acceleration to velocity is independent of the distance to the centre. A filament, with the present radial velocity of 1000 km/sec, has then traversed a distance of 0.79 pc in the radial direction since the supernova outburst. Thus by a measurement of the position of a filament with respect to the projected centre of the nebula, combined with its radial velocity, the filament can be located in space, provided the systematic velocity of the nebula is known. From an inspection of Dr MAYALL's velocities it appears that this velocity is negligible.

Dr TH. WALRAVEN constructed a rough space picture of the filamentary shell using the provisional velocity measurements by Dr MAYALL. This picture, which Dr WALRAVEN kindly put at my disposal, is shown in Plate 3. As Dr WALRAVEN remarks, the picture demonstrates clearly that the filaments represent large-scale structures. They can be followed over large distances around the nebula. Most conspicuous is the long filament encircling the inner part of the nebula.

4. Total intensity and spectrum of the continuum.

The radio spectrum of the nebula seems to be rather well determined. The radio source that has been studied most completely is Cas A. To the observations of this source C. L. SEEGER (1957) fitted a spectrum of the form $J(\nu) \propto \nu^{-\alpha}$ and obtained $\alpha = 0.82$. From a compilation of observations of point sources by SEEGER (1957) we obtained for a number of frequencies the ratio Tau A/Cas A. Following a procedure pointed out to us by SEEGER we obtained our values for Tau A from the smooth spectrum for Cas A and the ratios Tau A/Cas A. The Tau A/Cas A ratios can be represented by the same formula, with $\alpha = -0.47 \pm 0.03$. Thus for Tau A we obtain $\alpha = 0.35$ with an estimated uncertainty of ± 0.05 . We also fitted the formula directly to all observations of Tau A, including a few values which were not included in SEEGER's list. We obtained by least squares $\alpha = 0.31$. This agrees very well with the above determination. In the following we shall adopt $\alpha = 0.35$, but a slightly smaller value appears also possible. At 400 Mc/s we read from the curve for Tau A a flux density of 10.7×10^{-24} watt m⁻² (c/s)⁻¹ in agreement with the result of SEEGER *et al* (1957). Assuming isotropic radiation this corresponds to a total emission $J(4 \times 10^8) = 1.38 \times 10^{24}$ erg sec⁻¹ (c/s)⁻¹. The radio results are shown in Figure 1.

FIGURE 1



The spectrum of the Crab nebula.
The ultraviolet spectrum is discussed in section 16.

The discussion of the optical continuous spectrum is more difficult because of the interstellar extinction. We estimate this extinction from the colour excesses of some O and B stars in the neighbourhood of the nebula, measured by HILTNER (1956). There are four stars in HILTNER's catalogue that are within two degrees from the nebula.

The distances of these stars are between 1200 pc and 1800 pc. This is somewhat larger than the dis-

tance of the nebula adopted here, but the correlation between interstellar absorption and distance is so poor that we did not apply a correction for distance. Moreover we shall discuss in section 17 the possibility that the nebular distance has been underestimated. The values for the colour excess of these stars in the B—V system are $0^m.40$, $0^m.54$, $0^m.54$ and $0^m.64$. We therefore adopt for the colour excess of the nebula $0^m.53$ in the B—V system. This corresponds to a visual absorption of $1^m.59$. We think it improbable that the colour excess could be in error by more than $0^m.15$. The present value for the interstellar absorption is appreciably larger than the value derived by MAYALL and OORT (1942). These authors found a photographic absorption of $1^m.20$ from a catalogue of B stars by STEBBINS *et al* (1940). The difference is largely due to the bluer normal colours used by HILTNER.

The B—V colour of the continuum at the projected centre of the nebula was estimated by WALRAVEN (1957) as $0^m.82$. We estimate the uncertainty in this result as less than $\pm 0^m.10$. The colour corrected for interstellar reddening is therefore $0^m.29$, with an estimated maximum uncertainty of $\pm 0^m.20$. This corresponds to the colour of an F0 star. Adopting a spectral law $J(\nu) \propto \nu^{-\alpha}$ we obtain $\alpha = 0.39$. An error of $\pm 0^m.20$ limits α between $\alpha = -0.1$ and $\alpha = +1.3$.

With our new value of the absorption the spectrophotometric results of BARBIER (1945) indicate $\alpha = 1.76$ around $\lambda = 3900$ Å. This value refers to the integrated colour of the whole nebula. As BARBIER's measurements of the continuous spectrum of the Orion nebula (1944), which was used as standard for the Crab nebula, seem to give a somewhat too low colour temperature (GREENSTEIN 1946) it is possible that his value for α is somewhat too high. MINKOWSKI's (1942) spectrophotometric results give $\alpha = 0.02$ around 4500 Å and $\alpha = 0.31$ around 6000 Å, but these values become higher when a correction for the sky brightness is applied (BARBIER 1945). These values have been corrected for the interstellar extinction determined above. As WALRAVEN's results were obtained photoelectrically they are the most reliable and will be used in the following.

In part III we shall show that the nebular spectrum can be explained satisfactorily when the colour excess is $0^m.10$ less than the colour excess derived above. This difference is well within the limits of possible error.

We now first determine absolute values for the intensity units used in Paper I and then derive the absolute magnitude of the nebula.

One unit of intensity in the intensity table in Paper I corresponds to a surface brightness of 0.775 stars of the 25th magnitude per square second of arc. After correction for visual interstellar absorption this

becomes 3.35 such stars. The photovisual magnitude of the sun is $m_{pv} = -26.88$ (GOLDBERG 1953). Applying a correction for the blanketing effect of about $0^m.06$ derived from MICHARD's (1950) tables, we obtain for the solar continuum $m_{pv} = -26^m.94$. As the area of the solar disc is 2.89×10^6 square seconds of arc, we obtain for the solar surface brightness around 5500 Å, 2.06×10^{14} stars of the 25th magnitude per square second of arc. From the data compiled by MINNAERT (1953) we find that the surface brightness of the solar continuum at 5500 Å is 9.28×10^6 erg A⁻¹ cm⁻² sec⁻¹. Therefore our intensity units correspond to a surface brightness of 1.51×10^{-7} erg A⁻¹ cm⁻² sec⁻¹ at 5500 Å. This is equivalent to 1.52×10^{-18} erg cm⁻² sec⁻¹ (c/s)⁻¹. The total visual magnitude of the nebula was found in paper I as $m_v = 8^m.64$. With the above data we find for the total emission per frequency unit at 5500 Å

$$J(5.45 \times 10^{14}) = 6.54 \times 10^{21} \text{ erg sec}^{-1} \text{ (c/s)}^{-1}.$$

When we now try to fit the whole region between the radio spectrum and the optical spectrum by one spectral law $J(\nu) \propto \nu^{-\alpha}$ we obtain $\alpha = 0.38$, thus almost the same value of α that is valid for the radio spectrum (cf. Figure 1).

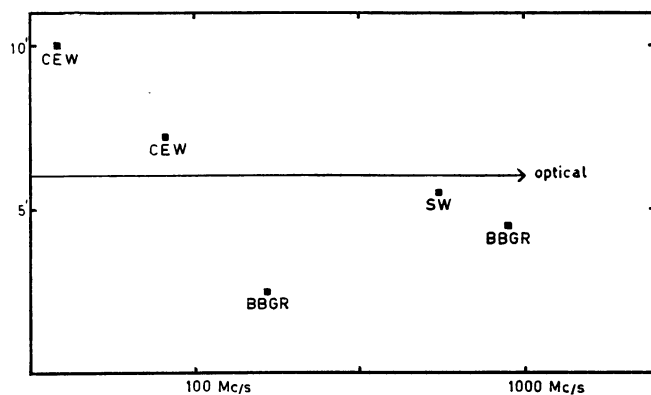
If we assume that the electron energy spectrum has some resemblance to the energy spectrum of cosmic rays, it is unlikely that α would decrease anywhere when proceeding from radio to optical frequencies. We conclude that α should be larger than about 0.4 in the optical region. The uncertainty in the value of α for the optical spectrum is therefore reduced to between $\alpha = +0.4$ and $\alpha = +1.3$. But, although we do not know the exact optical spectral index, it is certain that α must be about 0.38 from the radio spectrum to some wavelength close to the optical spectrum, say 15000 Å. For if the optical spectrum were characterized for example by $\alpha = 1.3$ up to 55000 Å, then we would have for this wavelength $J(5.45 \times 10^{13}) = 1.308 \times 10^{23}$ erg sec⁻¹ (c/s)⁻¹. If we would now represent the spectrum between this frequency and 400 Mc/s by one spectral index, we would obtain $\alpha = 0.20$. This is smaller than in the radio spectrum, which seems highly unpalatable. Slight changes in the parameters do not alter this conclusion.

5. The intensity distribution across the nebula.

In Paper I the optical intensity distribution was derived. The radio brightness distribution can be determined best from occultation observations; but every occultation only gives us a brightness strip distribution. Occultation observations were made by BOISCHOT *et al* (1956) at 900 Mc/s and at 169 Mc/s, by COSTAIN *et al* (1956) at 81 Mc/s and 38 Mc/s, and by SEEGER and WESTERHOUT (1957) at 400 Mc/s.

The observations at 900 Mc/s and at 38 Mc/s are not very reliable. It is difficult to judge the reliability of the observations of BOISCHOT *et al* for 169 Mc/s. But from their published curves we do not think that their results are very accurate. The Cambridge results were obtained with an interferometer, which had a fixed orientation during the whole occultation. The occultation curve was obtained by a comparison of the records at the occultation day and records made at other days. The observations of SEEGER and WESTERHOUT, made with the Dwingeloo 25 metre parabola, which followed the nebula during the occultation, are more direct. Therefore we are inclined to give the largest weight to their results.

FIGURE 2



The maximum extent of Tau A from occultation observations at various frequencies.

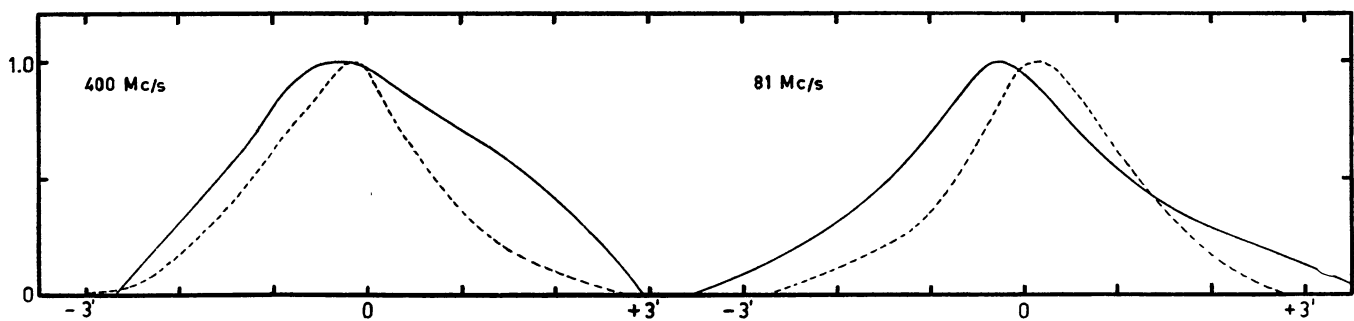
In Figure 2 we have plotted the maximum extent of the radio nebula derived by the various observers. The results show that the 169 Mc/s observations give much too small a diameter. There is no clear indication of a change of the diameter of the radio nebula as a function of the frequency. The results appear to be consistent with our conclusion that the filamentary shell forms the physical boundary of the nebula.

SEEGER and WESTERHOUT give radio strip brightness distributions derived from their occultation curves. They also give the corresponding strip brightness distributions for the optical radiation, which they computed from the intensities given in Paper I. Their results for the occultation on November 13, 1955 are not very accurate. We have therefore not used these results. In view of the large discrepancies between different observations we neglect all details in the occultation curves. Therefore we have averaged their results for the two series of observations on November 30, 1955, and drawn a smooth curve through the points. The result is shown in Figure 3.

COSTAIN *et al* at 81 Mc/s also give a radio strip distribution. For this occultation we computed a comparable optical strip distribution from the intensities in Paper I. These strip brightness distributions are also shown in Figure 3.

The brightness distributions in Figure 3 clearly indicate that the radio brightness distribution is much flatter than the optical distribution. Although the curves at 400 Mc/s and at 81 Mc/s are not strictly comparable, owing to the different path of the moon

FIGURE 3



A comparison of optical- and radio strip brightness distributions
The radio brightness is indicated by a full-drawn line, the optical brightness by a broken line.

in the two occultations, it seems that the 400 Mc/s results indicate a flatter distribution than the results at 81 Mc/s. As we argued above that the 400 Mc/s results are the most reliable, we will consider this flatter distribution as representative for the entire radio region. The preceding discussion shows that the conclusion of COSTAIN *et al* that the radio distribution becomes flatter with decreasing frequency is unfounded.

PART II. THE FILAMENTS

6. The measurements.

In the winter season of the years 1954 and 1955 Dr MAYALL obtained some spectra of the Crab nebula with the Crossley reflector of the Lick Observatory. Similar spectra, taken earlier, have been described by Dr MAYALL (1937). All spectra were taken with a slit of $6'.3 \times 8''.2$ orientated in position

angle 125° , i.e. parallel to the major axis of the nebula. The dispersion is about 430 Å/mm at H_γ . The sensitivity of the plates decreases rapidly at 5000 Å toward the red, but the nebular lines are still well visible. Dr MAYALL also obtained some calibration plates with sensitometer marks. These plates were developed together with the spectra. Dr MAYALL very kindly sent all these beautiful plates to Leiden and thus afforded us the opportunity to measure line intensities on them.

All spectra were analysed with a recording microphotometer. On every spectrum some knots, representing filaments crossing the slit, are visible. We measured about fifty of these knots by making tracings parallel to the dispersion. The lines that could be measured in these tracings are given in Table 1. All spectra were measured once with a roughly square slit, the linear dimension of which was 33 microns on the plate, corresponding to about 5.6 seconds of arc. The best spectra were traced a second time with a square slit having a width which was 25 percent smaller. We also made three repeated tracings of each calibration plate. The results of the calibration plates can be used to convert all measures into relative intensities as long as we restrict ourselves to a small part of the spectrum.

TABLE I
Emission lines measured in the Crab nebula.

Ident.	λ	Quality
[OII]	{ 3726.0 3728.8	good
[NeIII]	3868.7	poor
HeI	3888.9	poor
[NeIII]	3967.5	intermediate
[SII]	{ 4068.6 4076.3	intermediate
H_δ	4101.7	intermediate
H_γ	4340.7	rather good
[OIII]	4363.2	intermediate
HeI	4471.5	intermediate
HeII ¹⁾	4685.7	very poor
H_β	4861.3	rather good
[OIII]	{ 4959.5 5007.6	rather good

¹⁾ Probably blended with [FeIII] $\lambda 4658$.

We need information on the colour sensitivity of the plates to obtain relative intensities at different wavelengths. The spectrum of the nebular continuum is known, although not very accurately. Thus by measurements of the continuum on the plates for different wavelengths, but for the same spot in the nebula, we can determine the colour sensitivity of the plate. The surface brightness of the continuum is known all over the nebula (Paper I) and we can,

therefore, convert all measurements on the filaments to absolute values of the surface brightness. The detailed procedure was as follows. We made the plausible assumption, which afterwards proved to be essentially correct, that the *form* of the calibration curve does not depend on the wavelength. The *scale* of the intensities in the calibration curve is different for each wavelength and for each plate and this scale can be determined from the continuum. The continuum on the plates is disturbed by sky light. For every plate and for various wavelengths we plotted the measured continuum intensities (on an arbitrary scale) against the intensities found in Paper I for the same spots. A straight line was drawn through the points. The slope of this line determines the scale of the intensities. The measured intensity at the point where the real intensity is zero represents the sky light and is eliminated. From a comparison of points with different intensities on the same plate it appeared that our assumption of a constant form of the calibration curve is roughly valid.

In all computations we assumed that the continuum varies as $\nu^{-1.15}$. The value for the exponent was taken from the work of OORT and WALRAVEN. From the discussion in part III it appears that the colour of the nebula is perhaps somewhat more blue than is implied by this formula. Slight changes in the exponent do not change our results very much.

We shall refer all results to the emission in the continuum at 4250 Å. In section 4 we found that one of the intensity units of the continuum in Paper I corresponds to a surface brightness of 1.51×10^{-7} erg $\text{Å}^{-1} \text{cm}^{-2} \text{sec}^{-1}$ at 5500 Å. When $J(\nu) \propto \nu^{-1.15}$, i.e. $J(\lambda) \propto \lambda^{-0.85}$, these units correspond to 1.88×10^{-7} erg $\text{Å}^{-1} \text{cm}^{-2} \text{sec}^{-1}$ at 4250 Å. This figure will be used in all calculations. Then the total emission from the nebula at the frequency corresponding to 4250 Å is given by

$$J(7.06 \times 10^{14}) = 4.85 \times 10^{21} \text{ erg sec}^{-1} (\text{c/s})^{-1}.$$

If a change of this figure would be necessary, then all results in Table 2 have to be changed by the same factor.

7. The line intensities.

As the line width seems to be mostly instrumental we derived the surface brightness in the lines by integrating over the whole profile of the line. When the angular width of a filamentary knot parallel to the slit of the spectrograph is not too small ($> 10''$), the effect of instrumental broadening in that direction is negligible. When however a narrow filament crosses the slit of the spectrograph at right angles, the measured width will be largely instrumental. It might be expected that this has some influence on the measured intensity ratio between very strong and very

weak lines because of the non-linearity of the calibration curve. It is very difficult to measure this width accurately for weaker knots because of the small size of the spectra and because it is very difficult to obtain tracings perpendicular to the dispersion without disturbance from neighbouring filaments. The photometer slit width was chosen so that the readings do not deviate perceptibly from the readings for a much smaller slit. On the other hand we found by measuring some narrow strong knots in a micrometer that the width perpendicular to the dispersion is not larger than twice the photometer slit width. Therefore we expect the effect in the ratio of line intensities between very strong and very weak lines to be much less than a factor two. Moreover the effect is only present when a filament crosses the slit of the spectrograph at nearly right angles, because otherwise the real length of the filament perpendicular to the dispersion is already larger than the photometer slit width, and the real width of the filament is probably the same for all lines.

The greatest difficulty in the determination of the absolute values of the surface brightness is that most filaments occupy only part of the slit width of the spectrograph. This causes the measured ratio of filament to continuum to be generally smaller than the real ratio of surface brightnesses. As the location of the spectrograph slits is not known very precisely, the estimates of this effect must remain uncertain.

We discuss the correction for a few cases. When a long filament is at right angles to the slit the last correction is not needed. We must, however, multiply the results by the ratio of the width of the filament perpendicular to the dispersion in the spectrum and the real width of the filament. The real diameters of the filaments are difficult to determine. We used for this purpose a glass copy of a plate taken by Dr BAADE with the 200" telescope in the light of the [OII] $\lambda 3727$ line and found for the width values around one second of arc. The correction factor to be applied to the measured surface brightness then becomes about 7. If the filament is orientated parallel to the slit the correction factor is equal to the ratio of the slit width of the spectrograph to the real filament width and is therefore about 8.2. If thicker filaments are present, or some filaments are together in the slit of the spectrograph, the corrections become much smaller. For those filaments which are situated at the edges of the slit it is impossible to find any correction factors, because the exact location of the slit is not known. For the cases in which the correction factors could be found they have been given in Table 4.

In Table 2 we have given the results of our measurements without applying corrections to the surface brightness. The real surface brightness will on the average be about a factor five larger. In the first column the number of the plate is given. Then follow

respectively the identification with the knots measured by Dr MAYALL, the approximate coordinates in minutes of arc referred to the south-west component of the central double star, and the velocity of the filament as measured by Dr MAYALL. Dr MAYALL states that these velocities are not very reliable because of the large width of the slit of the spectrograph. In the next columns are given the real distance from the centre of the nebula in parsecs, determined as indicated in section 3, and the intensity of the continuum in the units of Paper I at the location of the filament. In the eighth column we give the quality of the spectrum as follows: For a spectrum that was measured twice we have A very good; B good; C poor. For spectra which we measured only once, D means reasonable and E very poor. The weight of the spectra classified C or D will be about equal. When the lines are sharp the quality is supplemented by a letter s, when they are broad by a letter b, and when the lines are clearly double due to superposition of filaments with different velocities the letter d has been used.

The lines [NeIII] $\lambda 3869$ and HeI $\lambda 3889$ are frequently blended. When we observe an apparent separation it may be that the second component is due to helium, but it is also possible that when two filaments are superposed, giving a broad but unresolved [OII] $\lambda 3727$ line, the components are separately visible in [NeIII]. It is therefore by no means certain that the entries for HeI $\lambda 3889$ do not represent partly [NeIII] radiation. The reflected solar spectrum on observing nights when the moon is present causes on some spectra the H and K lines of CaII to be visible as well as the G band. The K line falls near the same wavelength as the [NeIII] $\lambda 3968$ line and therefore tends to make the measured intensities for this line too small. When the H line is clearly observed we give its intensity under the remarks in the last column. The [SII] lines at $\lambda 4068$ and $\lambda 4076$ frequently form a blend with H_β . When these lines could not be separated a common entry is given. The same is true for the lines H_γ and [OIII] $\lambda 4363$, which are never very well separated. Moreover, the line [OIII] $\lambda 4363$ is blended with an Hg line at $\lambda 4358$ from the city lights. This line has usually about the same intensity as $\lambda 4363$. Unless the contrary is stated we corrected for this line by measuring its intensity well outside the nebula.

The line HeII $\lambda 4686$ is almost always much broader than H_β . In the few instances where the line appears double it seems to be blended with a line of about equal intensity at a wavelength about 4660 \AA .

The average intensity of this line in the unresolved blends is probably about equal to one quarter of the total measured intensity. The only possible identification that we have found is [FeIII] $\lambda 4658$. This is the strongest [FeIII] line in the Orion nebula. The spectra are not good enough to be certain about the

TABLE 2

Line intensities in the filaments of the Crab nebula.

The unit of intensity is 1.20×10^{-6} erg cm^{-2} sec^{-1} but a correction for the rather large width of the slit must still be applied, and will probably amount to about a factor five in most cases. The x and y coordinates are measured in minutes of arc from the south-west component of the central double star. The radius vector r is measured in parsecs from the centre of the filamentary system, and represents the real distance in space between this centre and a filament.

The velocities in the fifth column were all measured by Dr N. U. MAYALL.

Plate	Filament	x	y	Vel.	r	Cont.	Qual.	[OII] 3727	[NeIII] 3869	HeI 3889	[NeIII] 3968	[SII] 4075	H δ 4101	H γ 4340	[OIII] 4363	HeI 4471	HeII 4686	H β 4861	[OIII] 5000	Remarks
2100	v6 a	+0.65	-0.24	- 870	0.73	161	Bb	4200	776	437	343	118:	195:	260	68	237	738b	645	Large	spectrum overexposed all lines very broad
	v6 b	+0.43	-0.40	- 870	0.72	176	Db	3130	936		276	102		268		×	455	518	[8900]	
	v7/v8	+1.36	+0.28	- 320	0.52	86	ABs	2170	382	158:	125	61	16:	69:	47	26:	220b	233	3410	
	r11	+2.54	+1.14	+ 10	0.86	15	Es	320	×	×	×	×	×	×	24	×	×	×	300	probably H β present
	r5	-0.55	-1.08	+ 120	0.38	90	Bs	1620	430		144	226:		134		68	192b	322b	3510	
	r3	-1.26	-1.55	+ 250	0.63	23	Cs	1440	286		82	68	—	14	60	—	×	72:	1580	
	v2	-1.09	-1.44	- 810	0.83	32	BCd	1410	248		×	124		30	33:	39:	39:	44	1520	H = 36:
	v3	-0.84	-1.26	-1190	1.04	44	DEd	820	×	×	×	×	49	12	2	—	57b	111b	1380	
2101	v13	+1.44	+1.64	- 400	0.73	80	D	540	57		30	—	19	×	×	×	×	×	490	
	v4/v5	-1.46	-0.44	(- 740)	0.72	69	E	420	48	28	57	×	×	×	×	×	×	×	×	
	v2	-2.01	-0.79	- 540	0.76	57	BCs	1070	142	39	×	91	—	×	—	—	×	91	1520	
	v3	-1.85	-0.69	-1170	1.08	64	C	950	144	46	48	35:	×	—	—	—	53:b	×	820	
	v4	-1.64	-0.56	- 760	0.78	76	D	700		128	42	×	—	—	—	×	×	×	920	
	r1	-2.80	-1.32	+ 600	1.02	7	Cs	620	75	17	×	30	×	8	—	×	×	×	350	
2102	r10/r11	+1.54	+2.34	(+ 500)	0.93	24	E	350	×	×	×	×	×	—	—	×	×	×	340	
	r9	+0.65	+1.07	+ 170	0.55	84	As	1830	344		107	102	61	230	64	81	171b	363	2790	
	v10	+0.05	+1.23	- 240	0.40	111	Bs	1900	355	109	73	247:	×	216	31	—	×	481	2780	
	r5	-1.03	+0.47	+ 630	0.58	85	Cd	1400	300:	162:	66	×	×	110	—	—	238b	271	2410	
	r2/r3	-1.92	-0.12	+ 240	0.58	28	Es	1130	150	34	×	×	167	18	36	—	×	×	1170	
	Sv1	-2.72	-0.66			7	Cs	1860	183		46:	44:	17:	20:	33	×	×	×	1620	
	v5	-1.52	+0.14	- 730	0.71	12	As	2280	590		117	25	39	218	38b	245b	260	4240	H = 63	
2103	v14	+1.84	+1.60	- 180	0.76	49	DEs	800	135	19	×	33	28	34	4	×	42b	34	900	
	v13	+1.49	+1.34	- 860	0.84	99	D	740	88		28	46	—	33	33	—	74b	80	950	
	v4	-1.43	-0.73	-1120	1.00	92	E	650	90	62	28	34	—	×	×	—	×	×	670	
	v3	-1.73	-0.92	- 830	0.87	77	As	1330	191	46	125	149	45	60	28	×	110	1860		
2104	r11	+0.99	+0.56	+1780	1.45	111	Ed	810	×	×	×	×	×	×	×	×	×	×	1050	
	r7	-0.61	-0.58	+ 690	0.60	147	E	1340	×	×	—	×	×	×	×	×	×	×	168b	2430
	r6	-0.78	-0.69	+1050	0.88	105	E	930	×	×	×	×	×	×	×	×	×	×	1150	
	r3	-1.77	-1.36	- 40	0.66	21	Es	1560	79	—	×	50	25	×	×	×	×	187b	1430	
2126	v9	+1.99	+0.27	- 140	0.65	30	E	840	×	×	×	×	×	×	×	×	×	×	×	
	r8	+1.70	+0.06	+ 590	0.72	26	Es	1490	283	101	×	65	—	21	7	—	×	85b	1770	
	r7	+1.47	-0.11	+ 580	0.66	57	BCs	2060	387	100	77	×	—	68:	×	×	109d	152	2760	
	r5	+1.14	-0.35	+ 830	0.77	35	Bs	2550	495	123	114	48:	38	120	57	164	331b	4850		
	v1	-1.41	-2.13	- 90	0.77	3	Es	680	×	×	×	×	×	×	×	×	×	×	980	
2127	r8	+1.36	-0.73	+ 450	0.62	37	A	1450	×	×	80	×	×	×	147	49	×	175	2850	
	Sv1	-1.02	-2.33	(0)	0.77	3	Ds	620	355	69	55	63b	—	22	—	×	×	33	1340	
	r5, v5	+0.68	-1.21	{ + 996 - 328		27	As	2220	460	53	178	47	51	264	—	—	148b	318	3850	H = 83
	v4	+0.43	-1.40	- 80	0.47	4	Bs	1550	357	91	91	35:	37:	133	38	×	181	180	3460	H = 28
	v1	+0.04	-1.66	- 90	0.53	15	Bs	1040	114	46	×	76	—	78	9:	×	86b	56b	1990	
2130	r4	-0.48	-1.19	+ 180	0.42	61	ABs	1300	321		75	158	33:	130	49	57	93	219	2400	
	v11	+1.54	+0.25	- 60	0.50	61	Bs	1730	278	107	88	37:	18:	54	41:	×	180b	147	2930	
	v12	+2.27	+0.78	- 150	0.76	17	Es	830	60	97	×	×	×	7	×	×	×	×	820	
	r1	-1.69	-2.01	+ 160	0.79	4	C	720		114	×	29	10:	24	2	×	43:	900:		
2131	r8	-0.19	+1.31	+ 170	0.45	31	As	1830	283	132	127	155	43:	166b	12	52	202b	300	2250	H = 45
	r5	-1.20	+0.80	+ 640	0.64	51	BC	700	111		57	×	23:	54	×	×	×	58	920	
	v6	-1.45	+0.61	-1090	0.96	29	BCd	730	106	70	×	×	—	45	18	—	62	1320		
	v4+r2	-2.33	+0.03	{ + 111 - 526		6	Bs	820	100	18	×	27:	7:	78	—	×	70	960		

* not corrected for Hg line from city lights.

presence or absence of other [FeIII] lines. In the Orion nebula $\lambda 4658$ has an intensity equal to about one tenth of the intensity of [NeIII] $\lambda 3869$. In the Crab nebula the intensity ratio seems to be about 0.2. When the [FeIII] lines are present it is also possible that [FeII] could be observed. Unfortunately the strongest [FeII] line is at $\lambda 4359$. If this line is present it might contribute some intensity to [OIII] $\lambda 4363$, but as no other [FeII] lines are observed it is not possible to estimate this contribution. In the Orion nebula [FeII] $\lambda 4359$ has not been observed, because of the much larger strength of [OIII] $\lambda 4363$. From some other [FeII] lines we estimate that in the Orion nebula [FeII] $\lambda 4359$ /[FeIII] $\lambda 4658$ should be about 0.4. If this were also the case in the Crab nebula and if the line at $\lambda 4658$ is really due to [FeIII], we find that

[FeII] $\lambda 4359$ would account for two fifths of the measured $\lambda 4363$ intensity. Because of the higher excitation in the Crab nebula we could expect the [FeII] lines to be weaker. But as the radiation field in the Crab nebula is very different from that in planetary nebulae no certain conclusion can be reached.

The nebularium lines are seldom resolved well enough to give separate intensities, so we give only one entry for them. The plate sensitivity is decreasing very steeply at this wavelength.

We expect that the errors in the results for not too faint lines on spectra qualified A or B are in general below 25 percent. The results for the [NeIII] $\lambda 3869$ and the HeII $\lambda 4686$ lines frequently show a larger scatter.

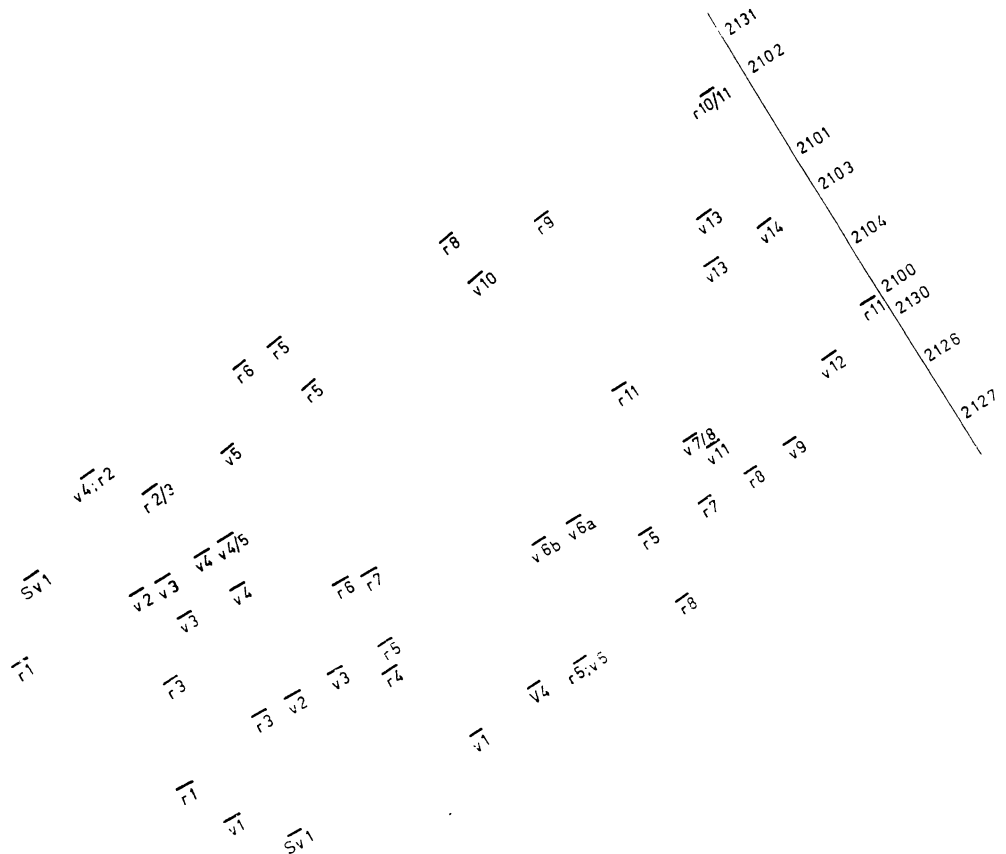
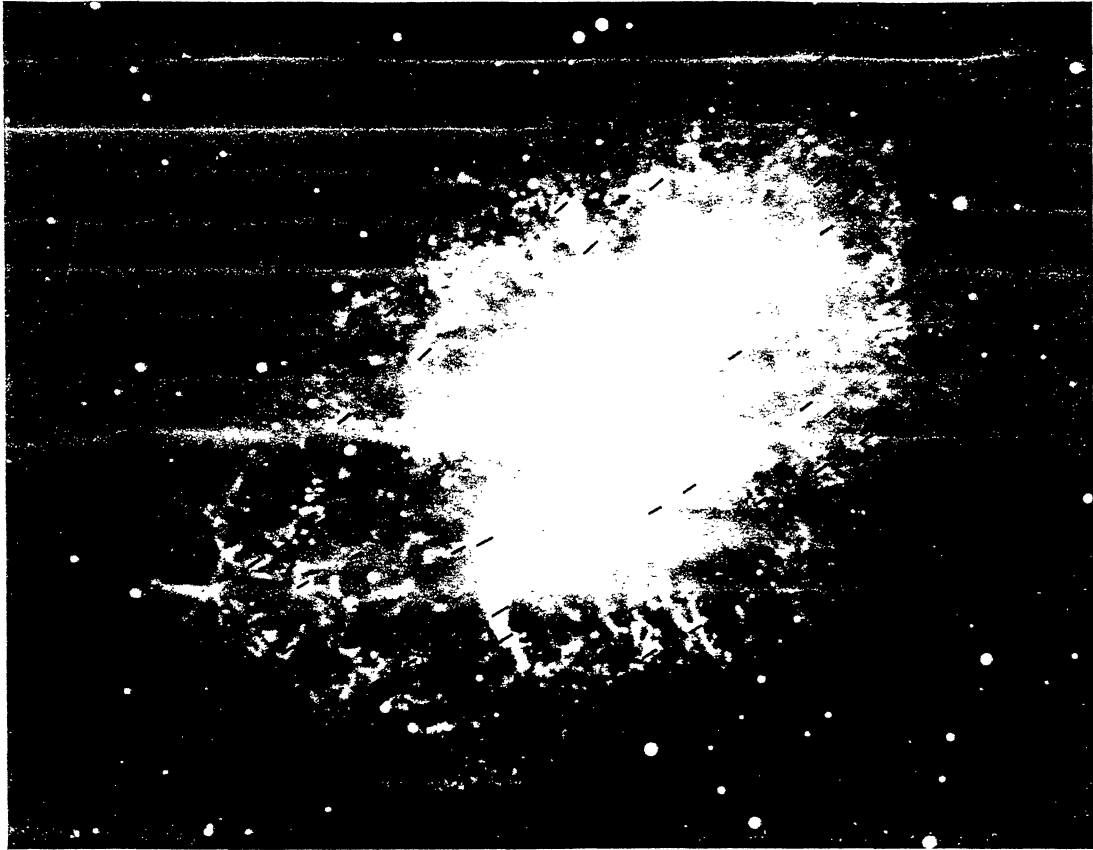


Plate 1. Identification chart for the filaments in Table 2.

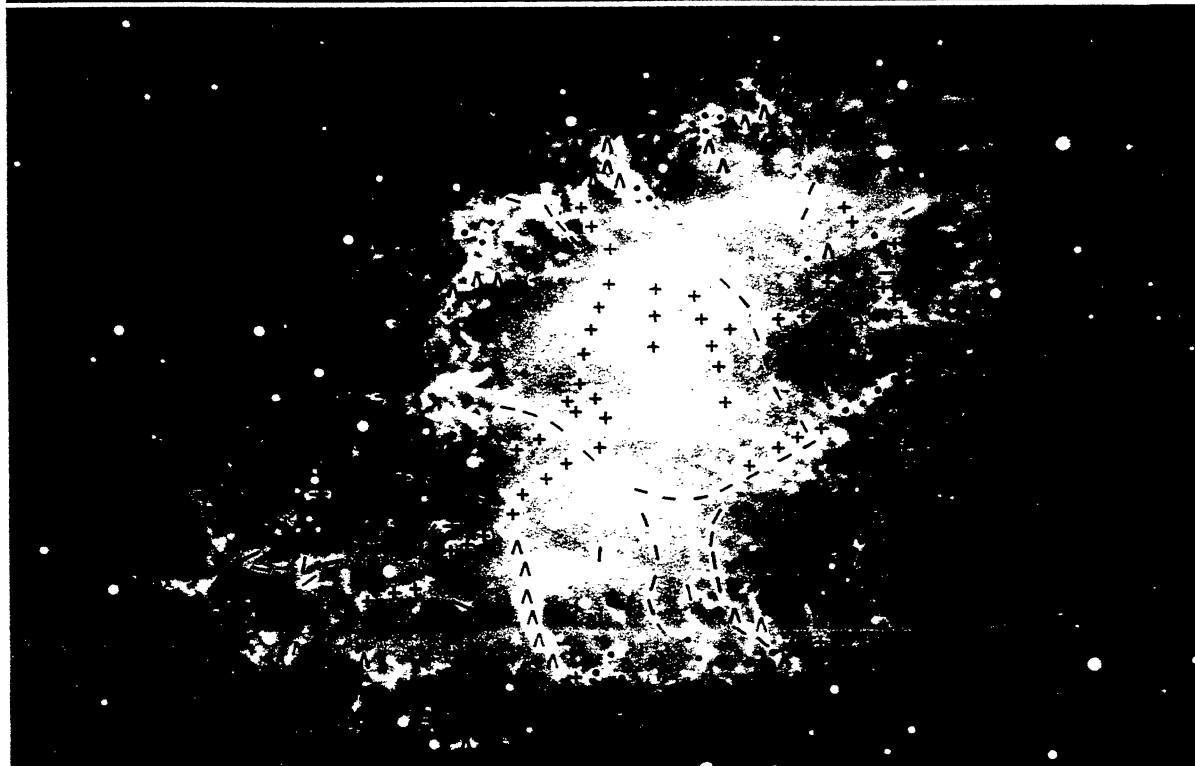
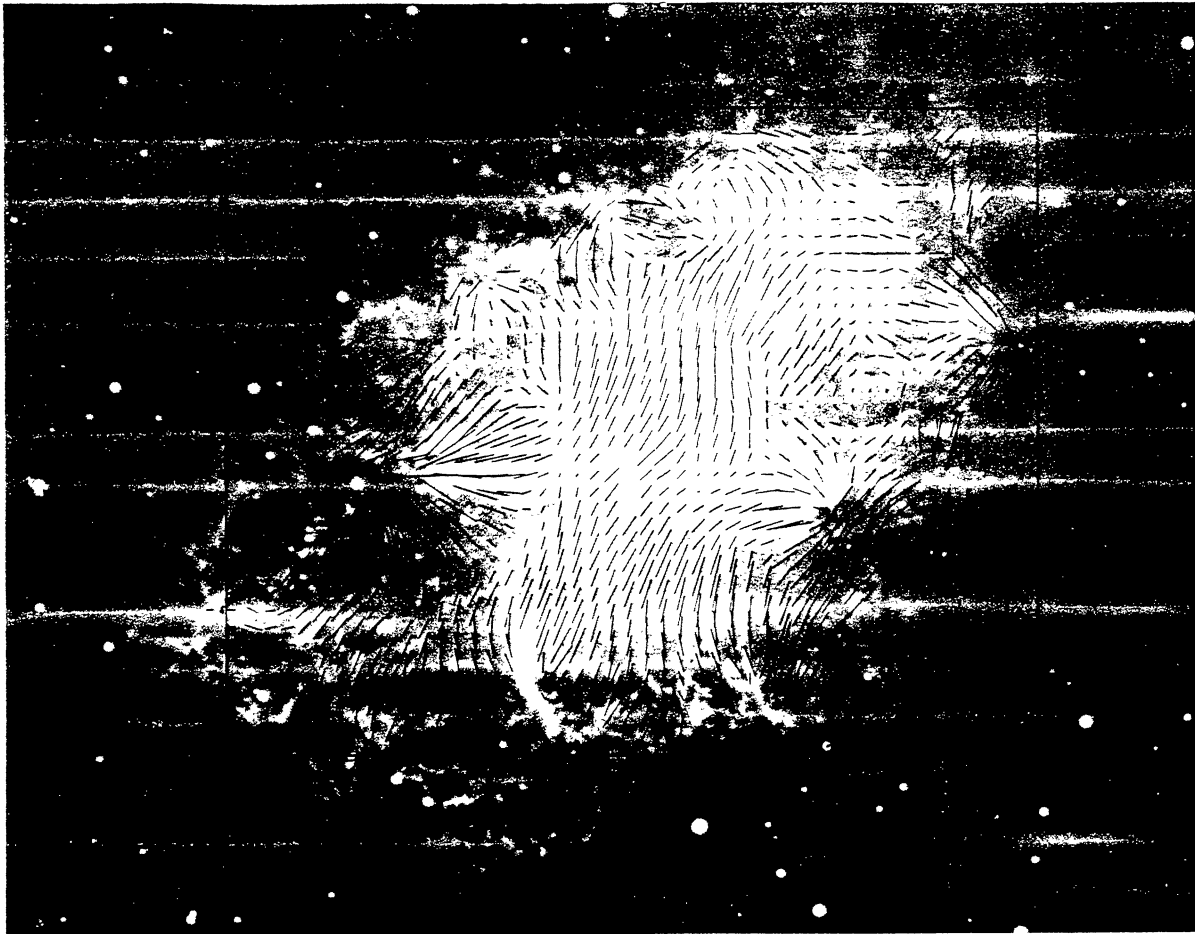


Plate 2. The polarizations of Paper I, projected against a photograph of the Crab nebula taken by Dr W. BAUDE in the light of the [SII] lines.

Plate 3. A space picture of the filamentary shell as constructed by Dr TH. WALRAVEN on the basis of the radial velocities obtained by Dr N. U. MAYALL.

+ $V_r > +500$ km/sec; Δ $+500$ km/sec $\geq V_r \geq 0$ km/sec; \bullet 0 km/sec $\geq V_r \geq -500$ km/sec; $-$ -500 km/sec $\geq V_r$

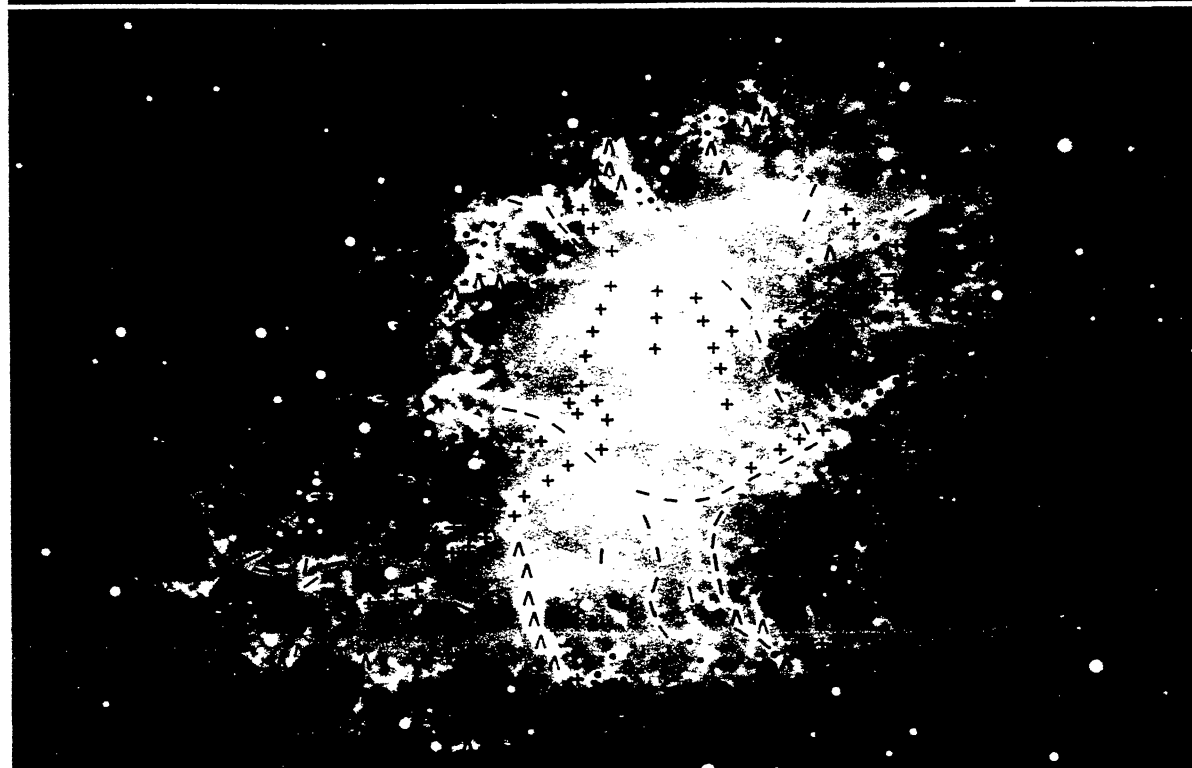
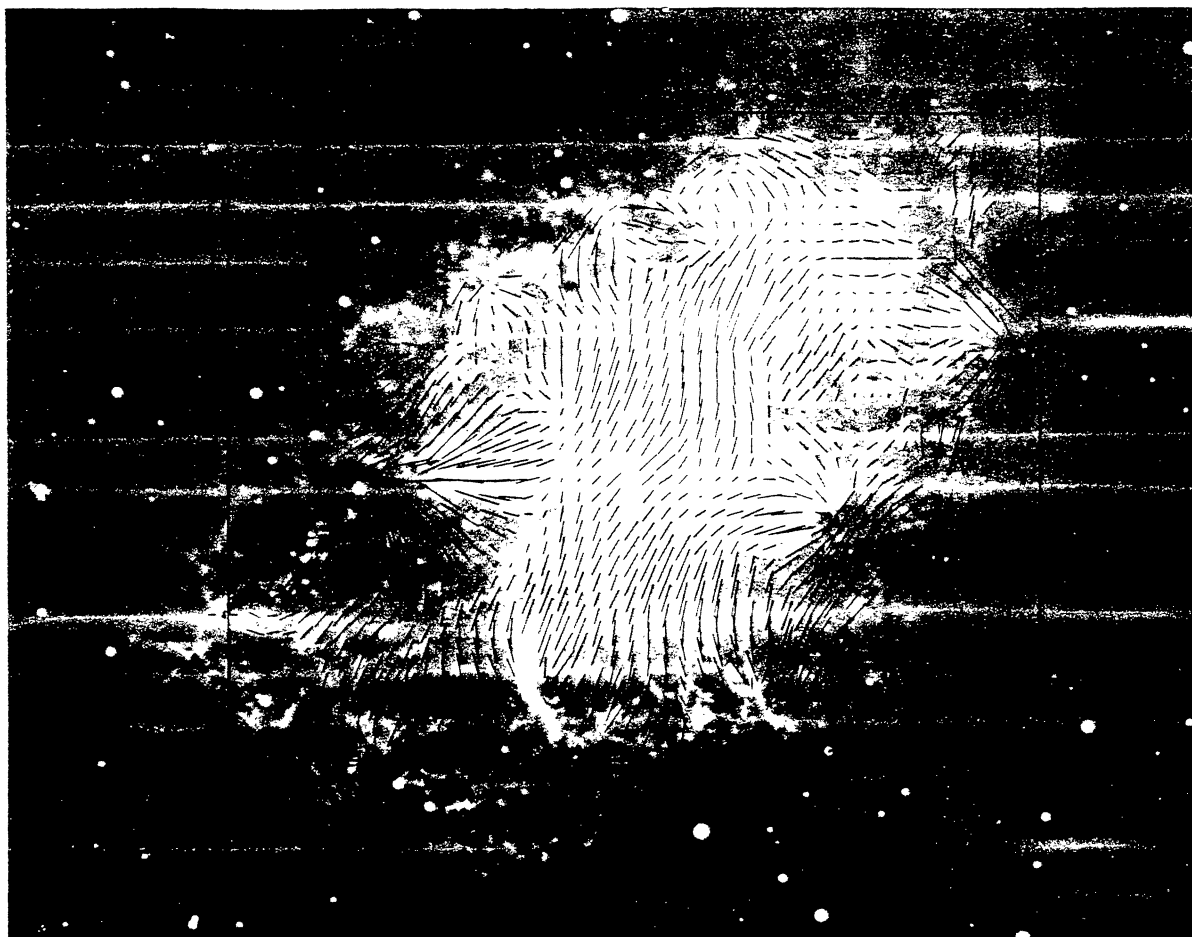


Plate 2. The polarizations of Paper I. projected against a photograph of the Crab nebula taken by Dr W. BAUDE in the light of the [SII] lines.

Plate 3. A space picture of the filamentary shell as constructed by Dr TH. WALRAVEN on the basis of the radial velocities obtained by Dr N. U. MAYALL.

+ $V_r > +500$ km/sec; Δ $+500$ km/sec $> V_r > 0$ km/sec; \bullet 0 km/sec $> V_r > -500$ km/sec; $-$ -500 km/sec $> V_r$

When we were reasonably certain that no observable line was present at a certain wavelength in the spectrum this is indicated in the table by a dash. When it was not possible to measure a line or when because of a plate defect we did not know whether a line was present or not this is indicated by a cross. Uncertain values are indicated by a colon. A line has an abnormal width (in most cases spurious) when a letter b is attached to the intensity value for that line.

8. *The source of excitation of the filaments.*

Probably a large part of the energy needed to ionize the filaments and to compensate their emission losses is derived from the ultraviolet radiation of the amorphous part of the nebula. But part of this energy might also be due to interstellar atoms swept up by the nebula. These atoms act as a brake for the expansion and transform energy from the orderly motion of the expanding shell into a kind of thermal energy. We also cannot exclude the possibility that the central star of the nebula has a large emission in the far ultraviolet. BAADE (1942) has given some reasons for believing that the south-west component of the central double star is associated with the nebula. The star does not have a high colour temperature, but its spectrum is continuous without any detectable lines (MINKOWSKI 1942). We shall further discuss the possible role of the central star in section 9 and in part V. It is also possible that an amount of radioactive substances is present in the filaments and that part of the decay energy is available to heat the filaments. This possibility will also be discussed in part V.

To proceed further we must make an assumption on the ultraviolet radiation from the amorphous mass. We shall adopt for $\lambda < 4250\text{\AA}$ an emission

$$J(\nu) = J(\nu_0) \left(\frac{\nu}{\nu_0} \right)^{-\gamma} = 4.85 \times 10^{21} \left(\frac{\nu}{\nu_0} \right)^{-\gamma} \text{ erg sec}^{-1} (\text{c/s})^{-1} \quad (8,1)$$

Here $\nu_0 = 7.06 \times 10^{14}$ c/s corresponding with $\lambda = 4250\text{\AA}$. The exponent γ represents the *average* spectral index between 4250\AA and the far ultraviolet. It will be shown in section 16 that γ is about 1.50 between 4250 and 250\AA . The average radius of the shell is 0.79 pc. Therefore the radiation intensity in the shell at 4250\AA is found from (8,1) as $I(\nu_0) = 6.47 \times 10^{-17}$ erg sec $^{-1}$ cm $^{-2}$ (c/s) $^{-1}$. The intensity of the radiation beyond the Lyman limit is then

$$6.47 \times 10^{-17} \int_{\nu_c}^{\infty} \left(\frac{\nu}{\nu_0} \right)^{-\gamma} d\nu = 4.57 \times 10^{-2} \frac{(4.66)^{-(\gamma-1)}}{\gamma-1} \quad (8,2)$$

For $\gamma = 1.50$ we obtain 0.042 erg sec $^{-1}$ cm $^{-2}$.

If there are n atoms per cm 3 in interstellar space the nebula sweeps up $10^8 n$ atoms sec $^{-1}$ cm $^{-2}$. The kinetic energy of an interstellar atom as seen from the moving shell is 10^{-8} erg for a mean atomic weight 1.2. The collisional energy liberated in the shell is therefore n erg sec $^{-1}$ cm $^{-2}$, if the protons lose their energy in the shell.

We conclude therefore that when the density of atoms in interstellar space surrounding the nebula is not much smaller than one tenth per cubic centimetre, the effect of colliding atoms cannot be neglected in the energy balance of the shell. The total mass swept up by the nebula in the course of its existence is rather small, even for $n = 0.1$ cm $^{-3}$. It amounts in that case at most to $6 \times 10^{-3} m_{\odot}$. As the mass of the shell is at least $0.10 m_{\odot}$, the dynamical effects of the interstellar atoms on the shell are rather small.

The collision of interstellar gas atoms with an expanding shell has been discussed by Mrs PELS-KLUYVER (1951). She found that, as the electrons lose their kinetic energy in collisions very rapidly, an electric field is set up which retards the motion of the protons. For an interstellar density of 7 atoms cm $^{-3}$ she found that the distance which a proton can traverse in the shell is about 10^{15} cm when the protons are not retarded by collisions. As we consider here interstellar densities about a hundred times less and as this distance is roughly inversely proportional to the density in interstellar space we see that the electric field cannot greatly retard the motion of the colliding protons through the filaments.

Magnetic fields are probably present in the filaments. All ions will therefore tend to spiral around the lines of force. The path of an ion through a filament is therefore much longer than the diameter of a filament. The cross-sections for charge exchange of protons with helium atoms ($\text{H}^+ + \text{He} \rightarrow \text{H} + \text{He}^+$) and the cross-sections for the ionization of neutral hydrogen and helium are of the order of $\pi a_0^2 = 9 \times 10^{-17}$ cm 2 for proton energies of about 10 kev. The charge exchange and ionization cross-sections of singly ionized helium ions are probably of the same order of magnitude. Along a straight path through a filament there are about 10^{18} neutral hydrogen or helium atoms and singly ionized helium ions per cm 2 . Thus for the longer path length due to the magnetic field a proton from interstellar space may lose an appreciable fraction of its energy in collisions.

However, if the field lines are closed around the filaments and if the field is sufficiently regular, the ions may not reach the inner parts of the filaments. In this case the influence of the colliding ions may be small.

We still have to discuss the influence of the supernova outburst on the surrounding medium. It is easily shown that a particle with radius r cm, density 1 gram cm^{-3} and at a distance of R parsec from the supernova, acquires by the radiation pressure a velocity $V = 2.1 \times 10^{-49} \frac{E}{rR^2}$, where E is the total energy in ergs radiated by the supernova. With $R = 1$, $r = 10^{-5}$ and $E = 3 \times 10^{49}$ erg we obtain a velocity of 6 km/sec for an average interstellar dust grain. The influence on ionized matter will be small and we expect that all neutral atoms will be ionized during the outburst. The supernova outburst by itself has therefore hardly any influence on the state of interstellar matter around the nebula. We only expect a larger degree of ionization, but this does not affect our discussion of the collisions between the shell and interstellar matter.

9. The Balmer decrement.

We first divided the spectra into three groups according to the intensity of H_β . In each group the Balmer decrement was determined by adding the results from all spectra for which the intensities for H_β and H_γ or H_β and H_δ where available. The results are given in Table 3.

TABLE 3

Observed and theoretical Balmer decrements.

	H_α	H_β	H_γ	H_δ	b_4
$H_\beta > 300$		100	47.4	21.5	
$300 > H_\beta > 125$		100	49.5	13.8	
$125 > H_\beta$		100	45.1	26.8	
mean observed		100	47.3	20.6	
$T_e = 10000^\circ$	case B	250	51	31	0.17
	collisional	576	29.1	13.6	1.22
$T_e = 20000^\circ$	case B	259	50	30	0.40
	collisional	479	34.7	16.9	2.32
$T_e = 17000^\circ$ $\mathfrak{f} = 0.07$		337	44.8	25.7	0.46

It will be shown in the next section that the temperature of the nebula is 17000° or perhaps lower. We give some theoretical decrements in Table 3 for $T_e = 10000^\circ$ and $T_e = 20000^\circ$. All these decrements refer to an optically thick nebula. The radiative decrements, known as case B, were taken from BAKER and MENZEL (1938), the collisional decrements from CHAMBERLAIN (1953). The b_n factor for the upper level of H_β is also given. The case where both collisional and radiative excitation are important has

also been treated by CHAMBERLAIN (1953). The results depend on a parameter \mathfrak{f} as follows

$$b_n = (1 - \mathfrak{f}) b_n(B) + \mathfrak{f} b_n(\text{coll}) \quad (9,1)$$

$$\frac{I_{n2}}{H_\beta} = \frac{1 - \mathfrak{f}}{1 - \mathfrak{f} + \mathfrak{f} b_4(\text{coll})/b_4(B)} \left(\frac{I_{n2}}{H_\beta} \right)_B + \frac{\mathfrak{f}}{\mathfrak{f} + (1 - \mathfrak{f}) b_4(B)/b_4(\text{coll})} \left(\frac{I_{n2}}{H_\beta} \right)_{\text{coll}} \quad (9,2)$$

We have computed the Balmer decrement for a few values of \mathfrak{f} and it seems that the rather rough data are best fitted by a decrement with $\mathfrak{f} = 0.07$. No theoretical decrement, however, fits the observations very well. A redetermination of the Balmer decrement would be of considerable interest. CHAMBERLAIN (1953) gives the following relation between \mathfrak{f} and the parameters describing the nebula

$$\mathfrak{f} = \frac{\alpha_k(T_e) T_e^{3/2} N_1}{K G_{T_e} N_e} \quad (9,3)$$

The factor $\alpha_k(T_e)$ depends strongly on the temperature. For $T_e = 17000^\circ$ we interpolate in CHAMBERLAIN's Table 1 a value of about 1.3×10^{-12} . For this temperature we find from a graph by MENZEL and ALLER (1941) $G_{T_e} = 0.22$. For $\mathfrak{f} = 0.07$ we then find for the ratio of the numbers of hydrogen atoms in the ground state to the number of electrons $N_1/N_e = 0.017$. For $T_e = 14000^\circ$ we find $\alpha_k = 1.7 \times 10^{-13}$, $G_{T_e} = 0.19$ and $N_1/N_e = 0.15$. From the observed small value of \mathfrak{f} we thus find that the filaments must be predominantly ionized.

It should be noted that the collisional excitation discussed here is due to the collisions of thermal electrons with atoms. Therefore it is most important for high temperatures. The cause of the temperature is irrelevant. It might be that the temperature is a consequence of collisions between the shell and interstellar atoms but this is not essential. The two kinds of collisions should therefore not be confused.

When the radiation field and the temperature in the nebula are known the value of \mathfrak{f} may be calculated a priori. The expression for \mathfrak{f} given by CHAMBERLAIN can be written as

$$\frac{1 - \mathfrak{f}}{\mathfrak{f}} = \frac{(2\pi mk)^{3/2} K}{N_e \alpha_k h^3} \int_{\nu_c}^{\infty} \frac{W}{e^{h\nu/kT} - 1} \frac{d\nu}{\nu} \quad (9,4)$$

where the arbitrary radiation field is represented as a Planck field with a dilution factor $W(\nu)$ and where we have set the Gaunt factor equal to unity.

Formally we can represent the radiation field in the Crab nebula as diluted Planck radiation, although the dilution factor has then a somewhat awkward form. This representation has the advantage that a number of formulae from the theory of planetary

nebulae can be adapted easily to the case of the Crab nebula. If the radiation were of the Planck type the flux through one cm^2 would be equal to $\frac{2\pi h\nu^3}{c^2} \frac{1}{e^{h\nu/kT} - 1}$.

The real flux through one cm^2 is $6.47 \times 10^{-17} \left(\frac{\nu}{\nu_0}\right)^{-\gamma}$ $\text{erg sec}^{-1} \text{cm}^{-2} (\text{c/s})^{-1}$. We therefore take the dilution factor to be

$$W = 6.47 \times 10^{-17} \left(\frac{\nu}{\nu_0}\right)^{-\gamma} \frac{c^2}{2\pi h\nu^3} (e^{h\nu/kT} - 1) = 3.95 \times 10^{-15} \left(\frac{\nu}{\nu_0}\right)^{-(\gamma+3)} (e^{h\nu/kT} - 1) \quad (9.5)$$

Inserting this expression for W in (9.4) we obtain

$$\frac{1 - \mathfrak{H}}{\mathfrak{H}} = \frac{3.12 \times 10^{-5} (4.66)^{-(\gamma+3)}}{\alpha_k N_e \gamma + 3} \quad (9.6)$$

The resulting values of \mathfrak{H} for $N_e = 10^3$ and for two values of T_e and γ are as follows

$T_e \backslash \gamma$	1.50	2.00
17000°	0.16	0.32
14000°	0.025	0.06

We therefore see that the suggested value for \mathfrak{H} is consistent with a $\nu^{-1.50}$ spectrum for the ultraviolet continuum and an electron temperature in the filaments of about 15000°. This value agrees well with the value of 17000° derived in the following section. If the temperature were lower, collisional excitation would probably be unimportant. The uncertainty in the observations allows also a purely radiative decrement. The results of this section therefore serve mainly to indicate that the temperature is not much higher than 15000°. For if it were higher, the value of \mathfrak{H} would become larger than is indicated by the observations.

10. The temperature in the nebula.

Considering the nebula for the moment as isothermal we can derive the temperature without knowledge of abundance data from the ratio of the intensities of the [OIII] lines. For this ratio SEATON (1954) gives

$$\frac{\lambda 4959 + \lambda 5007}{\lambda 4363} = \frac{8.74 e^{3.30 t_e^{-1}}}{1 + 0.0438 x} \approx 8.74 e^{3.30 t_e^{-1}} \quad (10.1)$$

where the last equality holds when the density is not too large. Here, as usual, $t_e = 10^{-4} \times T_e$ and $x = 10^{-4} \times N_e t_e^{-1/2}$. For the spectra where $\lambda 4363$ is separated from H_γ we determined this ratio dividing the material into two groups, the first with the nebular

lines stronger than 2000 units, the second with these lines weaker. In every group we added all intensities for the nebular lines and all intensities for the $\lambda 4363$ line in order to obtain a significant average. For the two groups we found $T_e = 15700^\circ$ and $T_e = 18200^\circ$, or, on the average 17000°. For those spectra where $\lambda 4363$ was blended with H_γ we computed the intensity for H_γ from the value of H_β , using the mean decrement given in Table 3. The two groups obtained in this way gave $T_e = 16600^\circ$ and $T_e = 17300^\circ$. The very good agreement between these results confirms our determination of the temperature as well as of the Balmer decrement. We therefore adopt in the following calculations $T_e = 17000^\circ$. The main uncertainty in our temperature is caused by the possibility that [OIII] $\lambda 4363$ might be blended with a [FeII] line (cf. section 7). Although this does not seem very probable, we cannot exclude the possibility that the temperature is lower than 17000°, and possibly even much lower.

In principle we may calculate the temperature when the radiation field is known. For a nebula excited only by radiation from a central star with a temperature T_1 , ALLER (1953) finds that the electron temperature in the nebula is related to T_1 by

$$\frac{(k/2hR) T_1 \int_{\nu_1}^{\infty} W_{1\nu} dy / (e^y - 1)}{\int_{\nu_1}^{\infty} W_{1\nu} dy / y (e^y - 1)} = f_2(T_e) + A(T_e) \sum_i \frac{I_i}{I(H_\beta)} \quad (10.2)$$

Here $y = h\nu/kT_1$, $f_2(T_e)$ is a function of the electron temperature given by MENZEL and ALLER (1941), $A(T_e)$ is a function given by ALLER (1953) and $\sum I_i/I(H_\beta)$ represents the ratio of the intensity of all forbidden lines together to the intensity of H_β . Inserting for the dilution factor W the expression given in formula (9.5) of the preceding section we obtain

$$f_1(T_1) = \frac{1}{2} \frac{\gamma + 3}{\gamma + 2} \quad (10.3)$$

Here $f_1(T_1)$ represents the left-hand side of (10.2). When $\gamma = 1.50$ the value of $f_1(T_1)$ is 0.64. In the case of a Planck radiation field with a dilution factor independent of the frequency, $f_1(T_1)$ has this value when $T_1 = 70000^\circ$. For the Crab nebula the ratio of the forbidden line intensities to the intensity of H_β is about 50. The value of $A(T_e)$ for $T_e = 17000^\circ$ is found from ALLER's table to be 4.81×10^{-3} ; from MENZEL and ALLER's results we find for this temperature $f_2(T_e) = 0.55$. The right-hand side of (10.2) is therefore equal to 0.79 and is much larger than

$f_1(T_1)$. Therefore the radiation field in the nebula is not sufficient to maintain the nebula at a temperature of 17000° , or even of the order of only 10000° . Also slight changes in γ are not sufficient to alter the situation. Formula (10,2) refers to a nebula which is optically thin in the Lyman continuum. When the nebula is optically thick $f_2(T_e)$ becomes somewhat larger, as the quanta with high energies are absorbed less than the softer quanta near the Lyman limit. The continuous absorption of helium atoms and ions tends to make the function somewhat smaller for the same value of T_e . It should be noted that the number of quanta does not enter this calculation. Only the distribution function of quanta energies above the Lyman limit is relevant.

To secure agreement between (10,2) and the actual temperature of the nebula we should have about $\gamma = -0.3$. It is impossible that the spectrum of the amorphous mass is characterized by such a low spectral index in the far ultraviolet. In section 16 we shall show that the ionization equilibrium $O^+ \rightleftharpoons O^{++}$ requires $\gamma = 1.5$ in the ultraviolet. This equilibrium depends mainly on the number of quanta beyond the series limit. There are some possible ways out of these difficulties. We might either infer that collisions with interstellar atoms or radioactive matter in the filaments make the temperature high enough, or we must assume a strong far-ultraviolet radiation field from the central star, which also may reduce the discrepancy.

A few remarks may be made about the last possibility. The colour of the central star has been measured by BAADE. After correction for $0^m.59$ reddening in the B-V system this colour corresponds to the colour of an A₃ star. With this low colour temperature it is not possible that Planck radiation in the ultraviolet would be of any importance. Let us assume for a moment that the central star radiates by the synchrotron mechanism. The colour of the star corresponds to a spectral index equal to -0.2 . Let us assume that the same spectral index is valid for the ultraviolet and that the spectral index of the amorphous mass has the value $+1.5$. At 5500\AA the visual magnitude of the nebula is $8^m.64$. For the central star we have $m_b = 15.45$ (BAADE 1942). The nebula radiates at this wavelength 526 times more strongly than the central star. At 500\AA the difference is only a factor 9. As the spectral index of the central star could certainly be somewhat underestimated, it is at present impossible to decide from the observations whether the central star gives an appreciable contribution in the far ultraviolet. We shall discuss in Part V the possible origin of synchrotron radiation in the central star. The possibility of synchrotron radiation from stars is confirmed by the observation of strong polarization in the continuum of a T Tauri star by HUNGER and KRON (1957).

11. Electron densities.

For the filaments in Table 4 we have some knowledge of the surface brightness, as discussed in section 7. For these filaments we estimated the electron density from the intensity of H_β , using the formula given in Table 5. We used $b_4 = 0.46$ from Table 3. In general we made the assumption that the thickness of a filament was equal to its diameter, but when the filament appeared composite we estimated a somewhat smaller value. We considered in this calculation the filaments as long cylinders with radius $d/2$. In this case the surface brightness is $\frac{\pi d^2 E}{4\pi d} = \frac{dE}{4}$, where E represents the volume emissivity. The results are given in Table 4.

TABLE 4

The surface brightness in H_β and the electron density in some filaments.

plate	filament	correction	d	H_β	$\sqrt{N_e N_p}$
2100	v6a	1.5	3"-6"	1110	1170-830
	v6b	(5.0)	(1".6)	(2590)	(2440)
	r5	2.1	3".8	670	810
2102	v10	2.2	1".5	1060	1620
	v5	2.4	1".1	620	1440
2103	v3	8.8	2".0	970	1340
2104	r7	3.0	2".7	500	830
	r3	5.7	1".4	1070	1680
2130	r4	2.9	2".8	640	920
2131	r8	4.7	1".7	1410	1750

From the abundances in section 14 we obtain $N_e = 1.55 N_p$. The values of $\sqrt{N_e N_p}$ must therefore be multiplied by about 1.25 to obtain true electron densities. Although the individual values are quite uncertain it is clear from the results in Table 4 that the electron density is somewhat larger than about $1500 \text{ electrons cm}^{-3}$. This is in good agreement with the results obtained by OSTERBROCK (1957) from the intensity ratio in the [OII] $\lambda 3727$ doublet. OSTERBROCK's point F, where he finds $N_e = 550 \text{ cm}^{-3}$, is identical with filament r7 on plate 2104, where we find $N_e = 1030 \text{ cm}^{-3}$. But very near to this spot OSTERBROCK obtains in point E $N_e = 2400$. OSTERBROCK's point G with $N_e = 850 \text{ cm}^{-3}$ is identical with filament r4 on plate 2130, where we obtain 1150 cm^{-3} . The agreement is satisfactory. If the temperature were 10000° we must use the radiative b_4 value $b_4 = 0.17$. In this case we obtain electron densities that are three percent smaller than the values in Table 4. The results are therefore insensitive to changes in temperature. The main uncertainty in our electron densities is caused by the uncertainties in our values for the correction factors and the diameters of the filaments.

12. Expressions for the line intensities.

From the formulae given by SEATON (1954) it is easily derived that for all forbidden lines in Table 5

except for the violet [SII] lines we can write the intensity emitted in all directions by one cm³ of gas as

$$I_{21} = \frac{8.54 \times 10^{-4} \Omega(1,2) \omega_1 h\nu_{21} e^{-h\nu_{21}/kT_e} x N_1}{1 + \frac{8.54 \times 10^{-4} \Omega(1,2)}{\omega_2 A_{21}} x + \frac{8.54 \times 10^{-4} \Omega(2,3)}{\omega_2} \frac{A_{31}}{A_{21}(A_{31} + A_{32})} e^{-h\nu_{32}/kT_e} x} \quad (12,1)$$

Here the Ω 's are the collision strengths, N_1 is the number of ions in the ground level, whereas the other symbols have their usual meanings. For all ions here of interest, except S^+ , and for electron temperatures below 20000°, the last term in the denominator is less than thirteen percent of the second term. Therefore we neglected this term for these ions. The second term in the denominator is smaller than 0.11 for O° , O^{++} and Ne^{++} for $x < 10$ and was therefore also neglected for these ions. The ground configurations of all these ions contain three energy levels. The population of the upper level can be neglected relative to the population of the second level. For $x < 10$ and $t_e < 2$ the only ions which have an appreciable population in the second level (more than ten percent of the lowest level) are O^+ and S^+ . For the other lines

we may put N_1 equal to the total number of ions. Using also SEATON's formula for the intensity ratio of the red and violet [SII] lines we obtain the results in Table 5. These expressions are valid for $x < 10$ and $t_e < 2$. If the density is low, deviations from these formulae may occur. This depends on the relation between the collision strengths and the statistical weights of the terms. According to SEATON it seems that this relation is such that no very large deviations are to be expected. For convenient reference we give in Table 5 also the formulae for H_β , HeI $\lambda 4471$ and HeII $\lambda 4686$.

13. The mean spectrum of the filaments.

Although large differences occur from filament to filament the general structure of the spectra remains

TABLE 5
Expression for the energy emitted per cm³ in all directions for various lines observed in the nebula.

Ident.	λ	emitted energy
H_β	4861	$2.28 \times 10^{-21} b_4(t_e) t_e^{-1} e^{0.98/t_e} x N_p$
HeI	4471	$1.79 \times 10^{-21} b(t_e) t_e^{-1} e^{0.99/t_e} x N_{He^+}$
HeII	4686	$39.2 \times 10^{-21} b(t_e) t_e^{-1} e^{3.93/t_e} x N_{He^{++}}$
[NII]	$\left\{ \begin{array}{l} 6548 \\ 6584 \end{array} \right.$	$6.86 \times 10^{-16} e^{-2.19/t_e} (1 + 0.10x)^{-1} x N_{N^+}$
[OI]	$\left\{ \begin{array}{l} 6300 \\ 6364 \end{array} \right.$	$1.22 \times 10^{-16} t_e^{1/2} e^{-2.27/t_e} x N_{O^\circ}$
[OII]	$\left\{ \begin{array}{l} 3726 \\ 3729 \end{array} \right.$	$\frac{16.4 \times 10^{-16} e^{-3.86/t_e} x N_{O^+}}{(1 + 1.60x) \{1 + 4 e^{-3.86/t_e} x (1 + 1.60x)^{-1}\}}$
[OIII]	$\left\{ \begin{array}{l} 4959 \\ 5007 \end{array} \right.$	$6.54 \times 10^{-16} e^{-2.89/t_e} x N_{O^{++}}$
[NeIII]	3869	$2.76 \times 10^{-16} e^{-3.71/t_e} x N_{Ne^{++}}$
[SII] _R	$\left\{ \begin{array}{l} 6713 \\ 6728 \end{array} \right.$	$\frac{12.7 \times 10^{-16} e^{-2.13/t_e} x N_{S^+}}{\{1 + 0.16(1 + 2.34 e^{-1.39/t_e})x\} \{1 + 0.40 e^{-2.13/t_e}(1 + 2.34 e^{-1.39/t_e})x(1 + 0.16x)^{-1}\}}$
[SII] _V	$\left\{ \begin{array}{l} 4068 \\ 4075 \end{array} \right.$	$0.116(1 + 5.51x) e^{-1.39/t_e} [SII]_R$

rather constant, except with regard to the sulphur lines. We determined the mean spectrum by adding all entries for a certain line in Table 2 and dividing them by the sum of the corresponding intensities for the [OII] $\lambda 3727$ line. We thus obtain the whole spectrum referred to this line. The result is given in Table 6. The results for the [NeIII] lines were obtained from the spectra where $\lambda 3869$ and $\lambda 3889$ appeared separated. The violet [SII] lines were first studied in the spectra where they appear separated from H_β . Thus we found the value 4.5 relative to 100 for [OII] $\lambda 3727$. For the other spectra we computed H_δ from H_β or H_γ using the mean Balmer decrement from Table 3. This gave a value 5.6. Taking all data together we obtained 4.8. The values for the individual filaments show a very large scatter, so not too much weight should be attached to this result. The result for HeI $\lambda 4471$ depends on a small number of spectra. For HeII $\lambda 4686$ we could do no better than take 3/4

times the observed value, as this line is probably blended with another line, which on the average seems to be somewhat weaker than HeII (cf. section 7). Using the theoretical Balmer decrement, which we fitted to the observations, we can compute the intensity for H_α from the value found for H_β . As MINKOWSKI (1942) has observed that the strength of H_α is on the average equal to the weaker of the [NII] lines at $\lambda 6548$ and $\lambda 6584$, we could derive for these lines an approximate value in our intensity scale. The [NII] lines originate from the same upper level and have therefore a fixed intensity ratio. Using GARSTANG'S (1951) transition probabilities we find that the sum of the two lines is 3.91 times stronger than the weaker component and therefore roughly also 3.9 times stronger than H_α . When the temperature is appreciably lower than 17000° , we must take the purely radiative decrement. The resulting intensity of the [NII] lines is then 1.02 times that of [OII] $\lambda 3727$.

TABLE 6
The mean spectrum of the filaments relative to [OII] $\lambda 3727$.

Ident.	[OII]	[NeIII]	[SII]	HeI	HeII	H_β	[OIII]	H_α	[NII]
λ	3727	3869	$\begin{cases} 4068 \\ 4076 \end{cases}$	4471	4686	4861	$\begin{cases} 4959 \\ 5007 \end{cases}$	6563	$\begin{cases} 6548 \\ 6584 \end{cases}$
Intensity	100	15.5	4.8	1.9	(7.5)	10.3	151	35	137

14. The abundances of some ions.

Knowing the mean temperature of the nebula and the order of magnitude of the electron density the mean spectrum enables us to derive the abundances of various ions. From the expressions in Table 5 we see that for $N_e \approx 10^3$ all intensities are nearly proportional to the electron density. Therefore the relative abundances which we determine will be nearly independent of the density, but not of the temperature. We computed the abundances for $T_e = 17000^\circ$, for $T_e = 10000^\circ$ and for $T_e = 8000^\circ$. At $T_e = 17000^\circ$ we again used $b_4 = 0.46$ in the formula for H_β . For

$T_e = 10000^\circ$ collisions would be of no importance and we took $b_4 = 0.17$. For $T_e = 8000^\circ$ we took $b_4 = 0.11$. For He° we took the b_n value for the radiative case from the computations by MATHIS (1957). For He^+ the b_n factor at T_e is equal to the corresponding b_n factor for hydrogen at $4T_e$. These b factors we found by extrapolating the results of BAKER and MENZEL (1938). For $T_e = 17000^\circ$ we used for He° , $b = 0.223$ and for He^+ , 0.025, for $T_e = 10000^\circ$ He° , $b = 0.110$ and He^+ , $b = 0.004$, and for $T_e = 8000^\circ$ He° , $b = 0.075$ and He^+ , $b = 0.0015$. The abundances obtained are given in Table 7.

TABLE 7
The abundances of some ions in an average filament.

Ion	H^+	He^+	He^{++}	N^+	O^+	O^{++}	Ne^{++}	S^+
$t_e = 1.7$	10000	4820	1370	0.77	0.71	1.36	0.52	0.19
$t_e = 1.0$	10000	3600	940	1.80	3.35	4.14	2.29	1.04
$t_e = 0.8$	10000	3400	770	2.4	9.1	8.9	6.8	2.9

To obtain a rough idea of the abundances of the elements we must make some assumptions. For the moment we put the number of O° and O^{+++} ions equal to one half of the combined number of O^+ and O^{++} ions. Further, we assume most hydrogen and

helium to be ionized. For hydrogen this follows from the discussion of the Balmer decrement if the temperature is high. The discussion in section 16 demonstrates that this condition is also fulfilled at lower values of T_e for both hydrogen and helium. Next we make the

assumptions that $N_{N^+}/N_N = N_{S^+}/N_S = N_{O^+}/N_O$, and $N_{Ne^{++}}/N_{Ne} = N_{O^{++}}/N_O$. These assumptions, although not very accurate, suffice in general to establish the abundances to within a factor of 5. The results obtained in this way are given in Table 8, together with the best values for the mean composition of the planetary nebulae (ALLER 1957). It is seen that the composition of the nebula does not show very large differences with the average planetary nebula, if not too low temperatures are adopted. But helium is overabundant compared with hydrogen. The ratio of H and He on

the one side and the other elements on the other side depends strongly on the temperature. If the temperature were as low as 8000°, the elements N, O, Ne and S would be somewhat overabundant.

The most urgent problem is therefore an accurate determination of the temperature. This can be done best from the ratio of the [OIII] lines when spectra with higher dispersion become available and the question of the presence of the forbidden iron lines can be settled. The simultaneous measurement of the doublet ratio in the [OII] $\lambda 3727$ line and the ratio of

TABLE 8
Abundance of elements in the Crab nebula and in the planetary nebulae.

Element	H	He	N	O	Ne	S	
Crab nebula	$\left\{ \begin{array}{l} T_e = 17000^\circ \\ T_e = 10000^\circ \\ T_e = 8000^\circ \end{array} \right.$	320000	200000	109	100	39	27
		89000	40000	54	100	55	31
		37000	15000	26	100	76	32
Planetary nebulae	170000	32000	40	100	15	9	

this line to the red [OII] lines could also give valuable information on the temperature in the filaments. The same information can also be obtained from the doublet ratio in the red [SII] lines and the ratio of the red to violet [SII] lines, when an accurate theory for this doublet ratio becomes available. Progress in the determination of the relative abundances of N, O, Ne and S will depend mainly on the calculation of accurate radiative ionization cross sections.

15. *The intensity of the red [SII] lines derived from a plate taken by Dr BAADE.*

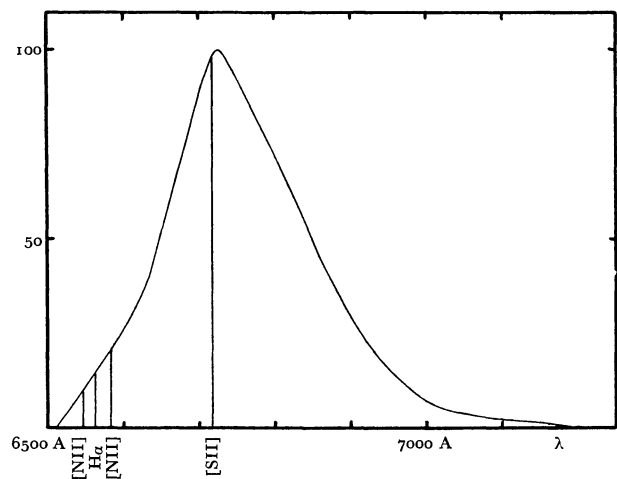
Dr BAADE kindly obtained for us with the 200-inch telescope a photograph of the nebula in the light of the red [SII] lines at $\lambda 6711$ and 6728 . As the intensity ratio of the red and violet [SII] lines depends on the temperature and also strongly on the density, this plate can give us valuable information on the physical conditions in the filaments. The photograph was made through an RG 5 Schott filter on a Kodak 103 aF plate. This combination cuts off most, but not all of the H_α and [NII] radiations.

On this plate the filaments are superposed on the continuum. The continuum was measured at a number of places, and a calibration curve was constructed by plotting the measurements of the continuum on the plate against the known values of the continuum intensity from Paper I. No continuum intensities larger than 300 units are available and we extrapolated the calibration curve to 400 units. A further extrapolation would be too unreliable.

The spectral sensitivity could be determined only from the data given in the catalogues about the plate and the filter. The relative spectral sensitivity so

obtained is shown in Figure 4. The equivalent width of the sensitivity curve is 228 Å and the effective wavelength is at 6751 Å. Adopting again a $\nu^{-1.15}$ law for the continuum we can express the measured [SII] intensities in the units of Table 2.

FIGURE 4



Spectral sensitivity of RG5 Schott filter + Kodak 103 aF plate.

These [SII] intensities must be corrected for the contribution of H_α and the [NII] lines. From the data in section 12 we know the relative intensity values of H_α and the [NII] lines. From the sensitivity curve in Figure 4 we found that the contribution of these lines is corrected for, when we subtract from the measured [SII] intensities 1.03 times the H_α intensity. Using the mean theoretical Balmer decrement of section 9 we find that we must subtract 3.5 times the intensity of H_β .

As we want to compare the red $[\text{SII}]_R$ lines with the violet $[\text{SII}]_V$ lines and as we have to correct for the H_α contribution, useful measurements can be made only for the places where the correction factors for the slit width in Table 2 are known. We derived values for the correction factors from the microphotometer tracings on the $[\text{SII}]$ plate. To compare with the results from Table 2 we divided the $[\text{SII}]$ intensities by these correction factors. In Table 9 we give the measured intensities for some filaments. The further columns show the diameter of the filament in the $[\text{SII}]_R$ lines, the correction factor, the $[\text{SII}]_R$ intensity divided by this factor, the violet $[\text{SII}]_V$ intensities from Table 2, the ratio $[\text{SII}]_R/[\text{SII}]_V$ not corrected for H_α and $[\text{NII}]$, 3.5 times the H_β intensity, the red $[\text{SII}]$ intensities, corrected for H_α and $[\text{NII}]$ lines, and the intensity ratio of red to violet $[\text{SII}]$ lines corrected for H_α and $[\text{NII}]$. For the first two filaments in Table 9 only a minimum value for the intensity could be derived, but we do not expect that the real values are much larger.

From the mean values in Table 9 it would follow that the red $[\text{SII}]$ lines have about the same intensity as H_α . This corresponds to $[\text{SII}]_R/[\text{NII}] = 0.25$. MINKOWSKI (1942) states that the red $[\text{SII}]$ lines have a remarkably high intensity (e.g. in NGC 7027 $[\text{SII}]_R/[\text{NII}] = 0.04$) and when at their strongest give about the same impression on the photographic plate as the $[\text{NII}]$ lines. From the sensitivity curve of Eastman 103 F plates, the plates used by MINKOWSKI, it would follow that this implies $[\text{SII}]_R/[\text{NII}] = 1.4$. The four strongest filaments of Table 9 have a mean measured red $[\text{SII}]$ intensity of 3270 units. After correction for the H_α and $[\text{NII}]$ contribution there remain 1810 units. The $[\text{NII}]$ intensity derived from the mean ratio $[\text{NII}]/H_\alpha$ is 5600 units if H_α is derived using a Balmer decrement with collisions, and 4170 units when we take a purely radiative decrement. This suggests that our correction for H_α and $[\text{NII}]$

might be too large and is perhaps better omitted. In this case the average ratio of the red and violet $[\text{SII}]$ lines becomes 17.6. It is also possible, however, that the $[\text{NII}]$ lines in these filaments are weaker than has been assumed in this discussion, as MINKOWSKI (1942) has observed large relative variations in the ratio of H_α to the $[\text{NII}]$ lines. We are rather safe when we conclude from this that the mean ratio of the red and violet $[\text{SII}]$ lines has a value between 9.1 and 17.6.

The mean electron density that corresponds to the filaments in Table 9 may be found from Table 4. As there is a large amount of helium in the nebula $N_e = 1.55 N_p$ and the results for $\sqrt{N_e N_p}$ must be multiplied by about 1.25 to obtain the electron densities. The mean electron density for the filaments in Table 9 is found to be 1640 electrons cm^{-3} . Inserting this value in the equation for the ratio of the red and violet sulphur lines (Table 5) we obtain for $[\text{SII}]_R/[\text{SII}]_V = 9.1$ a temperature of about 29000° . For a ratio 17.6 we obtain $T_e = 10300^\circ$. As the $[\text{SII}]$ lines are produced predominantly in regions with high density it is probable that these lines originate in the densest part of the filaments. For an effective electron density $N_e = 3280 \text{ cm}^{-3}$, thus twice as large as the value derived from Table 4, we obtain $T_e = 14300^\circ$ and $T_e = 7550^\circ$ for $[\text{SII}]_R/[\text{SII}]_V$ equal to 9.1 and 17.6 respectively.

We computed electron densities for the individual filaments from the $[\text{SII}]_R/[\text{SII}]_V$ ratios. For the uncorrected ratios we took $T_e = 10000^\circ$, for the corrected ratios $T_e = 17000^\circ$. These electron densities are given in Table 9 as $N_{e.u.c.}$ and $N_{e.c.}$ respectively. It appears that the dispersion is smaller for the uncorrected ratios.

The results on the sulphur lines are thus in agreement with the results from MAYALL's spectra. The results can be represented by a temperature of 17000° or somewhat lower. But when the correction for H_α

TABLE 9

Intensities of the red and violet $[\text{SII}]$ lines. The units are the same as in Table 2. All quantities except those in the third column are averaged over the slitwidth of the spectrograph in Table 2.

plate	filament	$[\text{SII}]_R + \left\{ \begin{array}{l} H_\alpha \\ [\text{NII}] \end{array} \right\}$	d	corr.	$[\text{SII}]_R + \left\{ \begin{array}{l} H_\alpha \\ [\text{NII}] \end{array} \right\}$	$[\text{SII}]_V$	$\frac{[\text{SII}]_R + \left\{ \begin{array}{l} H_\alpha \\ [\text{NII}] \end{array} \right\}}{[\text{SII}]_V}$	3.5 H_β	$[\text{SII}]_R$	$\frac{[\text{SII}]_R}{[\text{SII}]_V}$	$N_{e.u.c.}$	$N_{e.c.}$
2100	v6a	> 4000	10".5	1	4000	118	33.9	2260	1740	14.7	4	780
	r5	> 7000	3".7	2.2	3180	160	19.9	1130	2050	12.8	1330	1230
2102	v10	3840	2".8	1.3	3020	247	12.3	1685	1335	5.4	3270	6200
	v5	2350	1".6	2.2	1200	25	48	910	290	11.6	—	1630
2103	v3	5260	2".5	3.2	1645	128	12.9	385	1260	9.8	3050	2360
2104	r3	4690	1".5	5.3	885	50	17.7	655	230	4.6	1730	7680
2130	r4	6600	3".6	2.3	2870	158	18.2	765	2105	13.3	1630	1110
2131	r8	4570	2".8	3.0	1520	155	9.8	1050	470	3.0	4580	13000
mean					2290	130	17.6	1105	1185	9.1	1470	2700

should be omitted the temperature probably does not much exceed 10000°.

16. The ionization.

Neglecting collisional ionizations and three-body recombinations, the ionization equation is readily derived. For a point outside the amorphous mass of the nebula the intensity of the ionizing radiation is $I(\nu) = J(\nu)/4\pi r^2$, when $J(\nu)$ is the total emission at frequency ν and r the distance of the filament to the centre of the amorphous mass. As the ultraviolet emission is probably concentrated still more to the centre than the optical radiation (cf. section 22) all filaments are effectively outside the amorphous mass.

We assume for the ultraviolet continuum, which ionizes the various atoms and ions

$$J(\nu) = J(\nu_i) \left(\frac{\nu}{\nu_i}\right)^{-\gamma_{ci}} = J(\nu_0) \left(\frac{\nu_i}{\nu_0}\right)^{-\gamma_i} \left(\frac{\nu}{\nu_i}\right)^{-\gamma_{ci}} \quad (16,1)$$

Here $h\nu_i$ is the ionization energy of a certain ion. $J(\nu_i)$ is the total emission of the nebula at the frequency ν_i and γ_{ci} is the mean spectral index in the ionizing continuum of that ion. $J(\nu_0)$ refers to the emission at 4250 Å and ν_0 is the corresponding frequency, $J(\nu_0)$ being taken as standard in all calculations in the filaments. The average spectral index between ν_0 and ν_i is represented by γ_i . The ionization equilibrium for any ions A and A⁺ is found by equating the number of radiative ionizations per second to the number of radiative recombinations per second as

$$N_A \int_{\nu_i}^{\infty} \frac{\kappa_A(\nu) J(\nu)}{4\pi r^2 h\nu} d\nu = \frac{N_A J(\nu_0) \left(\frac{\nu_A}{\nu_0}\right)^{-\gamma_A}}{4\pi h r^2} \int_1^{\infty} \kappa_A(y) y^{-(\gamma_{cA} + 1)} dy = \alpha_A + (T_e) N_A + N_e \quad (16,2)$$

Here $\kappa(\nu)$ is the continuous absorption cross-section and $\alpha(T_e)$ represents the recombination coefficient. Inserting numerical values and expressing r in parsecs

$$\frac{N_{A^+}}{N_A} = \frac{1.11 \times 10^{10} \left(\frac{\nu_A}{\nu_0}\right)^{-\gamma_A}}{r^2 \alpha_A + (t_e) N_e} \int_1^{\infty} \kappa_A(y) y^{-(\gamma_{cA} + 1)} dy \quad (16,3)$$

The absorption cross-section for hydrogen is $\kappa(\nu) = 6.3 \times 10^{-18} (\nu/\nu_{H^0})^{-3}$. For He⁺ we have $\kappa(\nu) = 1.6 \times 10^{-18} (\nu/\nu_{He^+})^{-3}$. For He⁰ we can fit the data computed by SU SHU HUANG (1948) to a formula $\kappa(\nu) = 8 \times 10^{-18} (\nu/\nu_{He^0})^{-2.3}$. This is sufficiently accurate for our purpose.

The absorption cross-section for neutral oxygen was computed by BATES and SEATON (1950). Very roughly

we assume $\kappa(\nu) = 4 \times 10^{-18}$ for $\nu/\nu_0 < 1.3$; $\kappa(\nu) = 12 \times 10^{-18}$ for $1.3 < \nu/\nu_0 < 2.5$. For $\nu/\nu_0 > 2.5$ we put $\kappa(\nu) = 12 \times 10^{-18} (\nu/2.5\nu_0)^{-3}$ although no data are available for this region. The exact form of the absorption coefficient in the far ultraviolet is not too important, however, as the number of photons rapidly decreases with frequency. For O⁺ a few cross-sections were computed by BATES (1946). We adopt $\kappa(\nu) = 8.1 \times 10^{-18} (\nu/\nu_{O^+})^{-3}$.

The recombination coefficients are proportional to Z^2 for nuclei and seem to be of the same order for ions with the same charge. From the results by BATES *et al.* (1939) we adopt the following: for protons we obtain approximately $\alpha(t_e) = 2.24 \times 10^{-13} t_e^{-0.7}$, for O⁺ ions $2.16 \times 10^{-13} t_e^{-0.8}$. We therefore adopt for singly charged ions $\alpha(t_e) = 2.20 \times 10^{-13} t_e^{-0.8}$. For ions with charge Z we use a value Z^2 times as large. The results obtained with these parameters are assembled in Table 10.

TABLE 10

N_p/N_{H^0}	$= 31.5 r^{-2} t_e^{0.3} x^{-1} (4.66)^{-\gamma} (\gamma_c + 3)^{-1}$
N_{He^+}/N_{He^0}	$= 40.1 r^{-2} t_e^{0.3} x^{-1} (8.44)^{-\gamma} (\gamma_c + 2.3)^{-1}$
$N_{He^{++}}/N_{He^+}$	$= 1.98 r^{-2} t_e^{0.3} x^{-1} (18.6)^{-\gamma} (\gamma_c + 3)^{-1}$
N_{O^+}/N_{O^0}	$= 20.3 r^{-2} t_e^{0.3} x^{-1} (4.66)^{-\gamma} \frac{1 + 2(1.3)^{-\gamma_c} - 3(2.5)^{-\gamma_c}}{\gamma_c} + \frac{47(2.5)^{-(\gamma_c + 3)}}{\gamma_c + 3}$
$N_{O^{++}}/N_{O^+}$	$= 10.1 r^{-2} t_e^{0.3} x^{-1} (12.03)^{-\gamma} (\gamma_c + 3)^{-1}$

where we have omitted the index i from γ_{ci} and γ_i .

All these formulae have been derived on the assumption that only radiative ionization is important. In the previous sections reasons were given for sup-

posing that collisional excitation might have some influence. But as it appears to be of secondary importance, we do not expect that our ionization formulae will be altered fundamentally. As γ_c is

larger than unity, its precise value is not very critical.

The mean ratio $r^2 N_{O^{++}}/N_{O^+}$ for the filaments in Table 4 (filaments 2100 v6a and v6b are omitted) is found to be 0.658, when $T_e = 17000^\circ$. The mean electron density for these filaments as derived from Table 4 is $N_e = 1610 \text{ cm}^{-3}$. Taking $\gamma_c = 2$ we find from the last formula in Table 11 that $\gamma = 1.41$. For $T_e = 10000^\circ$ the result is $\gamma = 1.42$. The mean ratio $r^2 N_{He^{++}}/N_{He^+}$ can be found from five filaments in Table 4. For $T_e = 17000^\circ$ this ratio is 0.070 for $N_e = 1470 \text{ cm}^{-3}$. Taking again $\gamma_c = 2$, we obtain $\gamma = 1.46$. For $T_e = 10000^\circ$ the result becomes $\gamma = 1.61$. Thus the ionization conditions in the nebula can be explained by adopting an average spectral index $\gamma = 1.5$ from 4250 Å till about 250 Å. We then obtain $J(1.2 \times 10^{16}) = 6.9 \times 10^{19} \text{ erg sec}^{-1} (\text{c/s})^{-1}$ for the emission at the frequency corresponding to 250 Å.

With $\gamma = 1.5$ we obtain for an average filament with $N_e = 10^3$ and $T_e = 17000^\circ$, $N_{He}/N_p \approx 17$. This is somewhat an underestimate as Figure 1 shows that with an average value of γ equal to 1.5 we take the emission at the Lyman limit somewhat too low. Therefore this value of N_{He}/N_p should about be doubled. As $N_p \approx 1000 \text{ cm}^{-3}$ we have $N_{He} \approx 30$. The absorption coefficient at the Lyman limit is $6.3 \times 10^{-18} \text{ cm}^2$. As the diameters of the filaments are of the order of 1" or $1.5 \times 10^{16} \text{ cm}$, their optical depths at the Lyman limit are about equal to three. This optical depth, which decreases very quickly in the Lyman continuum, should not affect our ionization results very much.

With $\gamma = 1.5$ we obtain $N_{He^0}/N_{He^+} \approx 0.2$ and $N_{O^0}/N_{O^+} \approx 0.1$. Hydrogen, helium and oxygen are thus all predominantly ionized.

From the abundances in Table 7 we obtain that the optical depth in the Lyman continuum of HeII is about four times larger than the optical depth derived above for hydrogen. As we derived the ultraviolet emission mainly from the OIII/OII ratio, which is hardly affected by this optical depth, our results are not influenced very much.

17. The individual filaments. Possible revision of the distance of the nebula.

Up till now we have mainly discussed the mean spectrum of the nebula. We shall now investigate the details of the spectra of individual filaments. The observations of the Balmer decrement are not sufficiently accurate for this purpose, because rather large changes in physical conditions produce only small effects in the Balmer decrement. The observations of the [OIII] line $\lambda 4363$ are not accurate enough to make detailed determinations of the electron temperature. But it seems that useful information may be obtained from other lines. According to the

formulae in Tables 5 and 10 we have, for small values of x :

$$\frac{[\text{O III}] \lambda 4959 + \lambda 5007}{[\text{O II}] \lambda 3727} = 0.398 e^{0.97/t_e} \frac{N_{O^{++}}}{N_{O^+}} = \frac{4.02 t_e^{0.3} e^{-0.97/t_e} (12.03)^{-\gamma}}{r^2 x \gamma_c + 3} \quad (17,1)$$

This ratio is almost independent of the temperature but depends on r and N_e . The values of γ and γ_c will evidently be the same for all filaments.

The ratios [OIII]/[OII] can be found from Table 2. For every filament we determined the product $Q = r^2 [\text{OIII}]/[\text{OII}]$. This should depend on the electron density only. It appears, however, that for the filaments for which electron densities are known from Table 4, no correlation exists between the values of Q and N_e . For the same value of N_e widely different values of Q are found. There is a correlation between Q and r , and we might interpret this as indicating that the average N_e decreases when r increases. But in this case we must admit errors up to a factor five in the electron densities in Table 4, which do not seem very likely. A remarkable correlation exists between the angle filament—nebular centre—earth and the values of Q . Let us denote this angle by χ . Dividing the material into three groups according to the value of this angle we obtained the following results.

$ \chi $	Q	n	σ	σ_g	\bar{r}
$0^\circ-30^\circ$	1.66	6	± 0.59	± 0.26	1.01
$30^\circ-60^\circ$	0.79	14	± 0.18	± 0.05	0.75
$60^\circ-90^\circ$	0.48	18	± 0.16	± 0.04	0.61

Here σ is the root mean square deviation from the mean, while σ_g indicates the mean error of the mean value of Q in a group. The number of filaments in every group is denoted by n .

As the angle χ is correlated with the value of r , the correlation found earlier between Q and r might be only a consequence of the correlation between Q and χ . The results show that this correlation is very strong.

There are two ways to explain such a correlation. We may assume that the Crab nebula radiates anisotropically. This is not so unpalatable as synchrotron radiation is emitted very anisotropically. The direction of maximum radiation depends on the direction of the magnetic lines of force, and certain magnetic fields could produce a resultant anisotropy. It is somewhat suspect, however, that the anisotropy is roughly symmetrical with respect to the line of sight; moreover the amount of the anisotropy as well as its form are inconsistent with our ideas on the structure of the magnetic field (Part IV). This suggests the alternative explanation of a revision of the distance

of the nebula. We determined τ from a combination of the measured position of a filament and its radial velocity. For χ about zero the result depends only on the radial velocity; for $\chi = 90^\circ$ only the apparent position of the filament is relevant. In this case we need the distance of the nebula to convert it into absolute units. If the distance of the nebula is twice as large as we have adopted, the value of τ for $\chi = 90^\circ$ is doubled, whereas the τ values for $\chi = 0$ remain unaltered. Then the value of Q for $\chi = 90^\circ$ becomes four times the value we derived earlier. In this case the dependence on χ is removed. If this explanation is correct the nebula would approximately be a prolate spheroid instead of an oblate one, as we have assumed up till now. The large discrepancies between the electron densities in Table 4 and the values of Q have now disappeared, but this would likewise have been the case if we had assumed anisotropic radiation. It is remarkable that the remaining scatter in Q is so small. This appears to imply that the electron densities in most filaments are constant within thirty percent. OSTERBROCK'S (1957) results, however, indicate that occasionally much denser filaments may occur. The results of this discussion show that it is extremely important to have reliable measurements of the density and the value of Q for a large number of filaments. From such data an accurate evaluation of the distance of the nebula appears possible.

In view of the moderate accuracy of our results and the possibility of an alternative explanation we did not consider it justified to change already now all data which depend on the distance of the nebula. The effects of a change in the distance of the nebula is discussed in section 19.

The ratio $H_\beta/[OII] \lambda 3727$ is given by

$$\frac{H_\beta}{[OII]} = 1.39 \times 10^{-6} \frac{b_4(t_e)}{t_e} e^{4.84/t_e} \frac{N_p}{N_{O^+}} \quad (17,2)$$

Neglecting for a moment O° and O^{+++} ions we obtain

$$\frac{N_p}{N_{O^+}} = \frac{N_p}{N_O} \left(1 + \frac{N_{O^{++}}}{N_{O^+}} \right) = \frac{N_p}{N_O} \left(1 + 2.51 e^{-0.97/t_e} \frac{[OIII]}{[OII]} \right) \quad (17,3)$$

where the intensity ratio $[OIII]/[OII]$ is known from observations. The ratio $H_\beta/[OII]$ therefore depends strongly on the temperature.

The observed $H_\beta/[OII]$ ratios can be satisfactorily explained by temperature variations up to twenty percent around the mean. Such small variations seem quite plausible.

The ratio $[OIII]/[NeIII]$ depends only slightly on the temperature and not on the density. As expected, no systematic trend could be found in this ratio. The scatter around the mean is rather large, as $[NeIII]$ is a poor line.

The sulphur lines show large variations with respect to other lines. MINKOWSKI (1942) states that

the red $[SII]$ lines show large variations and are strong when $[OI] \lambda 6300 + \lambda 6363$ is strong. The ratio of the violet $[SII]$ lines to the $[OII] \lambda 3727$ lines is given by

$$\frac{[SII]_V}{[OII]} = 0.090 e^{0.34/t_e} (1 + 5.51x) \frac{N_{S^+}}{N_{O^+}} \quad (17,4)$$

If we assume that $N_{S^+}/N_{O^+} = N_S/N_O$, the above ratio depends mainly on the density. But we cannot explain the large variations observed unless we assume densities and density variations much in excess of the values derived from the other lines. We have two possibilities to account for these variations.

The filaments consist largely of rather tenuous gas producing most of the nebular lines. But a small fraction of their volume may be occupied by high-density gas, which shows up in the violet sulphur lines because of their strong dependence on the density. The red sulphur lines, however, do not depend more strongly on the density than the other forbidden lines. So their variations cannot be understood very well on this basis. The results about the ratio of the red and violet sulphur lines in Table 9 also indicate that density variations alone cannot explain the large variations of the violet $[SII]$ lines with respect to the $[OII]$ lines. The density may also influence the ratio $[SII]/[OII]$ by its effect on the degree of ionization. If, for example, $N_{S^{++}} \gg N_{S^+}$ and $N_{O^{++}} \approx N_{O^+}$, then a small decrease in ionization would have a much larger effect on N_{S^+} than on N_{O^+} . As the parameters for the ionization theory of sulphur are not available, we cannot discuss this point quantitatively.

Another possibility is the following. When the optical depth in the Lyman continuum is larger than unity for a filament, the degree of ionization of all elements that have ionization energies somewhat larger than 13.59 eV, decreases. Thus the ionization of H, N and O is reduced. In this case the intensity of the $[OI]$ lines increases. For sulphur the ionization energy is 10.36 eV and this element can still be fully ionized. But S^+ has a lower ionization potential than N^+ and O^+ . Therefore the degree of ionization of S^+ is less than that of O^+ and N^+ because of the large optical depth. The result of larger optical depth in the Lyman continuum is therefore to increase the intensity of $[OI]$ and $[SII]$ lines and to decrease most other lines. When $N_{O^{++}} \gg N_{O^+}$ and $N_{S^{++}} \gg N_{S^+}$, the effect of the optical depth on the strength of $[OI]$ and $[SII]$ lines will be considerable. No quantitative discussion can be given, as the ionization cross-sections of S^+ are not known.

These two possibilities are evidently interrelated. For example, an increase of the density may make the optical depth in the Lyman continuum larger. The preceding discussion also shows that assumptions like $N_{S^+}/N_{O^+} = N_S/N_O$ may be quite erroneous.

It thus appears that all variations in line intensities in the Crab nebula may be ascribed to changes in excitation conditions. There is no reason to assume differences of composition among the filaments.

18. *The mass of the filamentary shell.*

The nine spectra which were at our disposal cover about one third of the nebula. It is therefore possible to obtain a rather reliable estimate of the total line emission from the filaments.

On all spectra we made a number of tracings perpendicular to the dispersion in the [OII] $\lambda 3727$ line. In this way we found that the total intensity in the [OII] $\lambda 3727$ line on the nine spectra is equal to 9.66×10^{33} erg/sec.

According to BAADE (1942) the filamentary shell is elliptical with semi-axes of $178''$ and $120''$. As the location of MAYALL's spectra in the nebula is known we can determine for every spectrum the area of the part of the filamentary shell which fell on the slit of the spectrograph. We found that the nine spectra together covered 35.1 per cent of the area of the shell. As the spectra are well distributed over the nebula we simply divided the result for the emission in the nine spectra by 0.351 and thus obtained for the total emission from the filaments in the [OII] $\lambda 3727$ line 2.75×10^{34} erg/sec.

The emission in the other lines may be obtained from the mean spectrum in Table 6. The total emission from all spectral lines between 3700 Å and 5100 Å is about equal to 3.0 times the [OII] $\lambda 3727$ emission or about 8×10^{34} erg/sec. The total continuous emission in this wavelength interval is equal to 1.1×10^{36} erg/sec. The filamentary emission in the photographic region of the spectrum is therefore less than ten per cent of the continuous emission, in agreement with the earlier estimates of BAADE and MNKOWSKI (1942).

From the data in Table 6, combined with the above result for the [OII] $\lambda 3727$ emission, it follows that the total emission in H_{β} is equal to 2.83×10^{33} erg/sec. Using the formula for the emission of H_{β} in Table 5 and the b_4 values of section 14 we obtained the total number of protons in the filaments. We assumed that the average electron density is equal to 1000 electrons cm^{-3} . The results in Table 8 show that the filaments contain 3.30 atomic mass units per proton if hydrogen is fully ionized. The total number of protons is 3.36×10^{55} for $T_e = 17000^\circ$. Thus the mass of the filaments is equal to 1.85×10^{32} gram, or 0.093 solar masses. For $T_e = 10000^\circ$ the mass of the filaments becomes 0.064 m_{\odot} and for $T_e = 8000^\circ$, 0.057 m_{\odot} . The mass of the filaments is thus rather insensitive to changes in the temperature.

Our results are in good agreement with the results

of OSTERBROCK (1957), who obtained a mass between 0.05 m_{\odot} and 0.10 m_{\odot} .

It should be noted that the mass obtained above refers only to the visible filaments. It cannot be excluded that a considerably larger mass might be present between the filaments. To illustrate this point we consider the following case: We assume that the nebula is surrounded by a shell with a thickness equal to one tenth the present radius of the nebula. The volume of this shell is then about 10^{55} cm^3 . We distribute one solar mass with the composition of the filamentary matter throughout this volume. As this mass contains 4×10^{56} protons the density of the protons becomes 40 cm^{-3} . The line emission from this mass is only four per cent of the emission from the filaments, if the temperature in this shell is the same as that in the filaments. This emission is so low, because the line emission for low densities varies as the square of the density. This example demonstrates that the filaments give only a lower limit for the mass of the shell of the nebula (cf. section 38).

19. *The effects of a change of the distance of the nebula.*

It was shown in section 17 that it might be necessary to increase the distance of the nebula by a factor two. We shall now discuss how such a change would affect our results.

If the distance of the nebula is multiplied by a factor g the length of the two axes of the nebula perpendicular to the line of sight must also be multiplied by g . The third axis, which is found from the radial velocities, remains unaffected and the volume of the nebula must be multiplied by g^2 .

The total optical and radio emission from the nebula must evidently also be multiplied by g^2 , but the surface brightness is not affected. The diameters of the filaments must be multiplied by g . The square of the electron density is proportional to the ratio of the surface brightness to the diameters of the filaments. Therefore, the electron densities in Table 4 must be divided by $g^{\frac{1}{2}}$. The mass of the filaments is proportional to the ratio of the total emission of the filaments to the electron density and therefore has to be multiplied by $g^{\frac{5}{2}}$. Two components of the velocity are to be multiplied by g . The mean velocity is then about proportional to $g^{\frac{2}{3}}$. The kinetic energy of the visible filaments must be multiplied by $g^{\frac{23}{6}}$.

The ultraviolet emission from the nebula as derived in section 16 is proportional to the product of the square of the radius vector for a number of filaments and the electron density in these filaments. The increase of the radius vector depends on the angle χ . We found that the ultraviolet emission derived from

the [OIII]/[OII] ratios has to be multiplied by 1.57 if the distance of the nebula is doubled. The ratio of the optical to the ultraviolet emission thus depends on the distance of the nebula.

The temperature and the composition of the nebula are not affected, as they are almost independent of the electron density.

PART III. THE CONTINUOUS RADIATION

20. *The continuous spectrum.*

Some data on the continuous spectrum of the

nebula were obtained in sections 4 and 16. They are summarized in Table 11, together with the corrections that may arise from changes in the adopted values of the distance and the interstellar reddening. In the fifth and in the last column of the table the corrections are given which have to be applied if the colour excess of the nebula has been overestimated by 0^m.10.

The optical spectral index refers to the projected centre of the nebula. The ultraviolet radiation might be somewhat smaller than the value in the table if the central star contributes to the ultraviolet radiation field.

TABLE II
The spectrum of the continuum.

ν	$J(\nu)$	correction factor for double distance	correction factor for $\Delta CE = - 0^m.10$	spectral index	correction for $\Delta CE = - 0^m.10$
radio 4.00×10^8	1.38×10^{24}	4		0.35	
optical 5.45×10^{14}	6.54×10^{21}	4	0.76	0.39	+ 0.36
ultraviolet 1.20×10^{16}	6.9×10^{19}	1.57	0.96		

21. *The energy spectrum of the electrons.*

In this section we shall discuss the main features of the energy spectrum of the relativistic electrons that are responsible for the continuous emission of the nebula. We assume that the radiation is due to the synchrotron mechanism (SHKLOVSKY 1954, OORT and WALRAVEN 1956): An electron, when gyrating in a magnetic field emits linearly polarized radiation with the electric vector parallel to the radius of curvature of the orbit. The radiation is emitted in a very narrow cone around the velocity vector of the electron.

ERICKSON (1957) has suggested that the radiation might be "bremsstrahlung" produced in collisions of clouds with velocities of about 1000 km/sec. This "bremsstrahlung" does not differ very much from free-free transitions in a gas at a temperature of 10⁵ degrees, except for the fact that polarization effects are now possible. All the other difficulties inherent to free-free radiation—such as the large mass needed and the impossibility to explain the ratio of the optical and the radio emission—remain valid.

OORT and WALRAVEN (1956) have given the formulae which are needed in a convenient form. Their equations are based on the work of SCHWINGER (1949). In the following we denote the energy of a relativistic electron in units of 10⁹ ev by E . Let this electron gyrate in a magnetic field \mathbf{H} with a component H_{\perp} perpendicular to the velocity vector of

the electron. The energy radiated by a single electron in erg sec⁻¹ (c/s)⁻¹ is then given by

$$P(\nu) = 2.343 \times 10^{-22} H_{\perp} F(\alpha) \tag{21,1}$$

Here $F(\alpha)$ is a function tabulated by OORT and WALRAVEN and $\alpha = \nu/\nu_c$; ν_c is a critical frequency given by

$$\nu_c = L H_{\perp} E^2 \tag{21,2}$$

and L is equal to 1.608×10^{13} . The electron emits little radiation at frequencies much larger or much smaller than ν_c . The total energy emitted in erg sec⁻¹ is given by

$$\frac{dE}{dt} = - A H_{\perp}^2 E^2 \tag{21,3}$$

where $A = 3.79 \times 10^{-6}$.

If E_0 is the initial energy of an electron, the time in which the electron loses half its energy is given by

$$T = \frac{0.00835}{H_{\perp}^2 E_0} \text{ years} \tag{21,4}$$

We now assume that the number of electrons with energy E is given by

$$\begin{aligned} n(E) dE &= k E^{-\beta} dE & E_1 < E < E_m \\ n(E) dE &= 0 & E > E_m \text{ or } E < E_1 \end{aligned} \tag{21,5}$$

Then the combined emission from these electrons is given by

$$J(\nu) = 1.17 \times 10^{-22} L^{\frac{1}{2}(\beta-1)} k \nu^{-\frac{1}{2}(\beta-1)} H_{\perp}^{\frac{1}{2}(\beta+1)} \int_{\alpha_m}^{\alpha_1} \alpha^{\frac{1}{2}(\beta-3)} F(\alpha) d\alpha \tag{21,6}$$

where

$$\alpha_1 = \frac{\nu}{\nu_{c_1}} = \frac{\nu}{L H_1 E_1^2} ; \alpha_m = \frac{\nu}{\nu_{c_m}} = \frac{\nu}{L H_1 E_m^2} \quad (21,7)$$

For values of ν in the interval $\nu_{c_1} < \nu < \nu_{c_m}$ and well between the limits of the interval the integral does not vary very much. Therefore for these frequencies we have roughly $J(\nu) \propto \nu^{-\frac{1}{2}(\beta-1)}$. This spectrum is of the same form as the observed spectrum in the radio region and between the radio and the optical frequencies.

The spectrum in the radio region is characterized by a spectral index equal to 0.35. Therefore we have $\beta = 1.70$. The spectral index increases as we pass to the ultraviolet (Figure 1). We interpret this as an indication of a cut-off in the energy spectrum. In any acceleration mechanism for electrons where a magnetic field is involved such a cut-off must be expected, as at a certain energy the radiative energy losses become equal to the energy gain from the acceleration mechanism. The electron can then no longer be accelerated.

The presence of a high-energy cut-off affects only the optical and ultraviolet spectrum, because for small values of ν the value of α_m in (21,6) is near zero. The presence of a low-energy cut-off can be discovered only in the radio spectrum. As the radio spectrum around 50 Mc/s still does not show systematic deviations from a spectrum with a constant spectral index, any such cut-off is clearly not important in the following calculations. This permits us to put $\alpha_1 = \infty$ for all relevant values of ν .

In the following we will express the ratios of the emissions at various frequencies in a function $\psi(\alpha_m)$ given by

$$\psi(\alpha_m) = \frac{\int_0^{\alpha_m} \alpha^{-0.65} F(\alpha) d\alpha}{\int_0^{\infty} \alpha^{-0.65} F(\alpha) d\alpha} \quad (21,8)$$

This function was determined by numerical integration. It is shown in Figure 5.

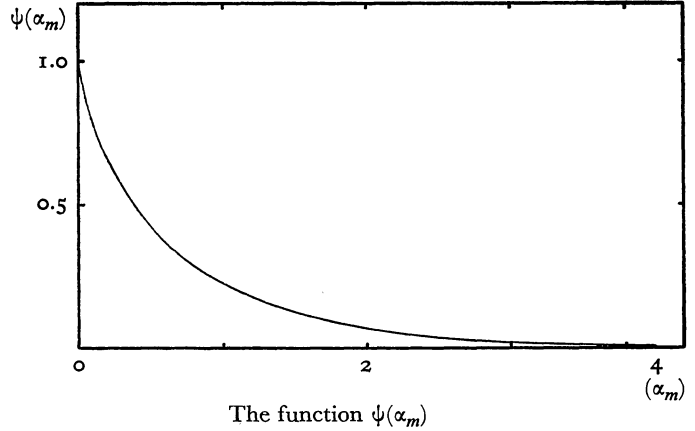
If the spectral index in the radio region is equal to 0.35 the ratio of the ultraviolet emission to the radio emission is given by

$$\frac{J(u)}{J(r)} = 2.41 \times 10^{-3} \psi(\alpha_{m_u}) \quad (21,9)$$

The ratio of the visual emission to the radio emission is given by

$$\frac{J(v)}{J(r)} = 7.16 \times 10^{-3} \psi(\alpha_{m_v}) \quad (21,10)$$

FIGURE 5



The ratio of the photographic to the visual emission is given by

$$\frac{J(p)}{J(v)} = 0.914 \frac{\psi(\alpha_{m_p})}{\psi(\alpha_{m_v})} \quad (21,11)$$

As $\alpha_m \propto \nu$ we have the relations

$$\alpha_{m_u} = 22 \alpha_{m_v} ; \alpha_{m_p} = 1.29 \alpha_{m_v} \quad (21,12)$$

The three ratios (21,9), (21,10) and (21,11) are known (Table 11). The two ratios involving $J(v)$ are evidently dependent on the interstellar extinction. Thus if we consider E_{max} and the interstellar extinction as unknowns we have three equations for two unknowns.

22. Space distribution of the emission.

The preceding analysis cannot be applied directly to the nebular continuum because it does not yet take into account the different space distributions of the optical and radio emission (cf. section 5).

It follows from (21,8) that the ratio $J(u)/J(r)$ depends on the magnetic field strength because α_{m_u} depends on H . When H decreases α_{m_u} increases and the value of $\psi(\alpha_{m_u})$ becomes smaller. Hence the ratio $J(u)/J(r)$ also decreases. Thus $J(u)$ depends more strongly on H than $J(r)$. From (21,10) the same is true for the optical emission.

OORT and WALRAVEN ascribed the different space distributions of the radio and optical radiation to a different dependence on H . The foregoing discussion shows that if the energy spectrum is constant through the nebula and if the field decreases outwards, the radio emission falls off less steeply than the optical emission. The radio emission therefore will show the flatter distribution; this agrees qualitatively with the observations.

However, as will be shown below, the data on the radio spectrum which have become available since the

writing of OORT and WALRAVEN'S paper, indicate that much larger variations in H are needed than was assumed by these authors. This leads to serious difficulties. It seems probable, therefore, that the radio electrons and the optical electrons have different space distributions.

The space distributions of the radio and optical emission can be derived from the strip brightness distributions in Figure 3.

If the nebula had rotational symmetry around an axis well inclined to the line of sight, the space distribution may be derived from the surface distribution. The nebula is probably a spheroid, but we are not certain whether it is a prolate or an oblate one. The isophotes for the optical radiation (Paper I) show an elliptical outline, but the orientation of the major axis for the inner and outer isophotes shows large differences. Because of all these uncertainties we neglected the ellipticity entirely and treated the strip distributions as if the nebula had spherical symmetry. The errors made by this assumption will probably be similar for the optical and the radio distribution.

For the case of spherical symmetry the true volume emissivity $D(r)$ is derived from the strip brightness distribution $L(x)$ by the relation

$$D(r) = -\frac{1}{2\pi r} \left(\frac{dL(x)}{dx} \right)_{x=r} \quad (22,1)$$

We are interested in the emission $P(\rho)$ which originates in a sphere with radius ρ . We have

$$P(\rho) = 4\pi \int_0^\rho D(r) r^2 dr \quad (22,2)$$

Substituting (22,2) into (22,1) and integrating by parts we obtain

$$P(\rho) = -2 \left[\rho L(\rho) - \int_0^\rho L(\rho) d\rho \right] \quad (21,3)$$

The integral is directly given by the occultation curve. We determined relative values of $P(\rho)$ for ρ equal to one, two and three minutes of arc. By subtraction we then find the values of the emission in the two shells $1' < \rho < 2'$ and $2' < \rho < 3'$. The results are given in Table 12, together with the emission per unit volume for the optical and radio radiation. In the sixth column the relative ratios of the optical to the radio emission for the three regions are given. The radio results were derived from the strip brightness distributions given by SEEGER and WESTERHOUT. The results from the Cambridge observations at 81 Mc/s are given in the last column for comparison.

TABLE 12

Relative values of the total emission and the volume emissivity in three regions of the nebula.

region	optical		radio		optical radio	radio (Cambridge)
	total	per cm ³	total	per cm ³		
$\rho < 1'$	0.252	1.00	0.099	1.00	1.00	0.145
$1' < \rho < 2'$	0.439	0.25	0.355	0.51	0.49	0.290
$2' < \rho < 3'$	0.309	0.065	0.546	0.29	0.22	0.565

We shall first investigate whether the changes of the ratio of optical to radio emission can be ascribed to a change in H . In the calculations we shall assume that the three regions may be characterized by their average values of the magnetic field H_1 , H_2 and H_3 and by their average densities of the relativistic electrons n_1 , n_2 and n_3 .

The changes in the ratio $J(v)/J(r)$ are thus assumed to be due to the variations of $\psi(\alpha_{m_p})$. If we adopt a value for α_{m_p} in the inner region, the α_{m_p} 's in the other regions are determined. Because of the equations (21,9) — (21,12) the relative values of $J(r)$, $J(v)$, $J(p)$ and $J(u)$ are all determined. The ratio $J(u)/J(r)$ is known from Table 11. If the computed ratio $J(u)/J(r)$ is not correct we must choose a better value for α_{m_p} in the inner region. The relative values of H can be determined as $\alpha_{m_p} \propto H^{-1}$. The relative values

of n are found from the volume emissivities at the radio frequencies.

From the values of $J(p)$ and $J(v)$ in the three regions we derived the total visual emission and the spectral index at the optical frequencies at the projected centre of the nebula. With the spectral index we correct the value of the interstellar absorption and thus obtain the "observed" value of the total optical emission from Table 11. The results of the calculations are given in Table 13. We made the calculations for the $J(u)/J(r)$ ratio following from Table 11, as well as for two and four times smaller values for this ratio. If the distance of the nebula is doubled and if the central star also contributes to the ultraviolet radiation field, the latter value is probably most nearly correct. The value of the spectral index in the radio region was taken to be 0.35 or 0.30. In Table 13 we express H and n in terms of the values which these quantities

have in the central sphere. In the column headed Δm_v we give the difference in magnitudes between the observed visual emission, corrected for interstellar absorption, and the values computed from the model. The last column gives the difference of the colour indices at the projected centre of the models and in the outer parts. The calculations were rather simple as it appeared that the ultraviolet emission is wholly concentrated in the central sphere in all models.

It appears that for all models computed with a spectral index equal to 0.35 in the radio region, the computed visual emission is too low. The decrease of H and the increase of n with increasing distance from the centre are very strong in these models.

These difficulties are partly removed if the spectral index in the radio region is assumed to be equal to 0.30. Because of the large frequency difference between optical and radio radiation this has a strong influence on the results. The first effect of a small decrease of the radio spectral index is a decrease of

$\psi(\alpha_{m_u})$, which is necessary to keep the ratio $J(u)/J(r)$ constant. The decrease of $\psi(\alpha_{m_v})$ is less strong and the computed optical emission is increased. Because of the stronger effect of the cut-off in this case the changes of the magnetic field and the particle density in the different regions become smaller. A slight change of the radio spectral index is certainly compatible with the observational data. For it was shown in section 4 that the uncertainty in the radio spectral index derived from the Tau A/Cas A ratios is about ± 0.05 and that if the Tau A observations are used directly a spectral index equal to 0.31 is obtained.

There is, however, one more result from the models which can be verified observationally. All models predict a difference of 0^m.35 in the colour index at the projected centre and the outer parts of the nebula. The outer parts should thus be rather red. WALRAVEN (1957) has made some colour measurements of the nebula. His results indicate that the outer parts of the nebula are bluest. WALRAVEN suggests that this may be due to the influence of the

TABLE 13
Models for the continuous emission in the Crab nebula.

spectral index radio continuum	$J(u)/J(r)$	$r < r'$			$r' < r < 2'$			$2' < r < 3'$			optical spectral index at centre	ΔCE	Δm_v (O - C)	ΔCI (centre-limb)
		α_{m_v}	H_c/H	n/n_c	α_{m_v}	H_c/H	n/n_c	α_{m_v}	H_c/H	n/n_c				
0.35	5.00×10^{-5}	0.048	1	1	0.49	10.2	11.7	1.13	23.5	20.6	0.64	m - 0.07	m - 0.53	m - 0.34
0.35	2.50×10^{-5}	0.075	1	1	0.54	7.1	7.2	1.18	15.7	11.9	0.69	- 0.08	- 0.55	- 0.34
0.35	1.25×10^{-5}	0.103	1	1	0.58	5.6	5.3	1.24	12.0	8.3	0.73	- 0.09	- 0.59	- 0.34
0.30	5.00×10^{-5}	0.077	1	1	0.50	6.5	5.9	1.14	14.9	9.8	0.63	- 0.07	+ 0.11	- 0.34
0.30	2.50×10^{-5}	0.107	1	1	0.56	5.2	4.4	1.20	11.3	6.8	0.68	- 0.08	+ 0.07	- 0.34
0.30	1.25×10^{-5}	0.136	1	1	0.61	4.5	3.6	1.23	9.0	5.1	0.75	- 0.10	+ 0.07	- 0.34

filaments. It seems therefore not improbable that the nebular colour could be more or less constant over the nebula. The data on the total [OII] $\lambda 3727$ emission from the nebula given in section 18 show, however, that the filaments are much too weak to mask a 0^m.35 reddening of the continuum. We must therefore conclude that the models discussed cannot be correct.

The colour difference between the inner and outer parts of the nebula is not an accidental property of our models, which could be removed by an appropriate slight change of the parameters. We assumed that the differences between the radio and the visual emission are due to a cut-off at high energies in the electron energy spectrum. As the cut-off has the largest influence on the highest frequencies the photo-

graphic emission will be affected more strongly than the visual emission. The colour difference between central and outer parts is thus inherent to our approach.

Moreover, from the theoretical point of view, the concentration of the particles in the outer parts of the nebula seems prohibitive. It is very implausible that a situation where the particle pressure in the outer parts is about ten times larger than in the inner parts could be approximately stationary.

OORT and WALRAVEN (1956) analysed the scale difference between the radio and the optical nebula, assuming an energy spectrum closely resembling the cosmic-ray spectrum observed near the earth. As a consequence of their adopted spectrum they obtained $J(r) \propto H^{0.66}$ and $J(p) \propto J(v) \propto H^{2.15}$. Because the

change in the exponent of their energy spectrum occurred at an energy corresponding to a frequency somewhere between the radio and the optical spectrum, the integration limits in (21,6) are effectively 0 and ∞ in this case and no colour variations occur.

From (21,6) and (21,7) we see quite generally that, irrespective of the details of the energy spectrum, a spectral variation according to $\nu^{-\alpha}$ implies that the emission depends on the magnetic field as $H^{\alpha+1}$. Thus $J(r) \propto H^{0.66}$ would imply that in the radio region $J(\nu) \propto \nu^{+0.34}$. But the observations of the radio spectrum which now are available suggest $J(\nu) \propto \nu^{-0.35}$ and therefore $J(r) \propto H^{1.35}$. This means that the difference in the dependence on H of $J(r)$ and $J(\nu)$ is seriously reduced. Accordingly, the changes of H required to account for the difference between the radio and the optical nebula become much larger, and, as $J(r)$ now depends more strongly on H , we need a large concentration of particles in the outer regions. Because of the result for the radio spectral index the change in the exponent of the energy spectrum must occur quite near to the optical frequencies and thus colour effects are again expected. Moreover, in order to account for the optical and ultraviolet spectrum with one spectral index, as is necessary if no cut-off is present, we must change all observational data more than the uncertainties seem to allow.

The situation may be summarized in a general way. The spectral indices in the radio and optical spectrum do not differ very much. Therefore the dependence on H of $J(r)$ and $J(\nu)$ is not very different. Thus large variations of H are necessary to account for the scale difference of the radio and the optical nebula. Very probably a cut-off is present in the energy spectrum. This appears evident from the data on the ultraviolet spectrum as well as from the theoretical considerations in section 25. But strong changes of H imply strongly different values of α_m in (21,11) and therefore strong colour effects, which have not been observed. We conclude that the variations of H cannot be very large and therefore the somewhat different dependence of $J(r)$ and $J(\nu)$ on H cannot explain the scale difference between the radio and the optical nebula. We must, therefore, look for an alternative solution.

23. *Alternative interpretation of the space distributions.*

The discussion of the preceding section was based implicitly on the assumption that all electrons circulate freely through the nebula. If this is not the case it would be possible that the radio electrons and the optical electrons have different space distributions; formulated in another way, we might say that the energy spectra of the electrons in the inner and outer parts of the nebula may be different. This seems the only possible interpretation after the failure of the

more attractive models of the preceding section. When we allow the electrons to have different energy spectra in different parts of the nebula we introduce a large degree of arbitrariness, as we have then in principle an arbitrary number of free parameters. But the suggestion that the electrons cannot circulate quite freely through the nebula is not wholly unfounded. As can be seen from the picture of the magnetic lines of force constructed by OORT and WALRAVEN (1956) the magnetic field lines tend to run parallel to the contours of the brighter part of the optical nebula. Such a structure of the field can greatly restrict the exchange of electrons between the inner and outer parts, as the radius of gyration of the most energetic electrons is of the order of only 10^{-6} parsec. At some places the lines of force appear to diffuse outwards and here the electrons could perhaps move from the inner to the outer parts and vice versa. We can thus picture a plausible model in which there is some exchange of electrons between the inner and outer parts but where this exchange is so slow that a different energy spectrum can be maintained for a time interval of the order of a thousand years. The dark bays which are found at some places in the nebula also suggest that there are places where the electrons cannot circulate freely (cf. section 30).

We now construct the following model. We divide the nebula again into three parts, but we now allow the electrons to have different energy spectra in the various regions of the nebula. For the inner sphere the calculation of the spectrum is the same as in the preceding section. The radio spectral index is taken as 0.30, otherwise the visual emission is too low. An intermediate value of the ultraviolet emission is adopted. Thus for the whole nebula we take $J(u)/J(r) = 2.5 \times 10^{-5}$. From $J(u)$ we again obtain the value of α_m in the inner sphere. We adopt values for the ratio between the field strength in the inner sphere and that in the outer shells, and compute the relative values of the densities of the radio and optical electrons in these shells from the known values of the volume emissivities. The results are given in Table 14.

TABLE 14

The density of optical and radio electrons in the outer shells of the nebula expressed in the density in the inner sphere, for various values of the ratio of the magnetic field strength in the inner sphere to that in the outer shells.

H_c/H	$1' < r < 2'$		$2' < r < 3'$	
	n_{opt}	n_{radio}	n_{opt}	n_{radio}
1.5	0.47	0.86	0.12	0.49
2.0	0.75	1.25	0.20	0.71
3.0	1.54	2.13	0.40	1.21
4.0	2.64	3.10	0.69	1.76

In this calculation we assumed that the value of the cut-off energy was the same in all three regions. To determine the relative values of H we make the following assumptions. We suppose that, although the particles cannot circulate freely through the nebula, there is a slow diffusion of electrons from the inner to the outer parts and vice versa. We further assume that the radio electrons were formed more or less homogeneously throughout the nebula, but that the electrons in the inner sphere were subject to subsequent acceleration. Thus, after some time, there was an appreciable density of optical electrons in the inner part but none in the outer parts. These optical electrons diffused slowly outwards and at present emit the optical radiation in the outer parts. As the total number of optical electrons in the outer parts is probably larger than in the inner parts the time scale of this diffusion process must be shorter than the age of the nebula, but not much shorter, as otherwise the densities of the optical electrons in both parts would have become comparable. The density of the radio electrons cannot increase very much outwards. For if this were the case these electrons would diffuse inwards and tend to make the densities equal in not too long a time, because of the small volume of the inner part. Putting the density of radio electrons in all three shells exactly equal we obtain from Table 14 $H_c/H_2 = 1.7$ and $H_c/H_3 = 2.6$. The outer parts of the nebula in this model are only a few hundredths of a magnitude redder than the inner parts. It will appear in the following section that there is some support for the assumption that the acceleration of particles occurs mainly in the inner parts. Evidently the division of the nebula into three parts is highly schematical, and the results obtained should be considered as tentative.

The results of this section might be confirmed by photographing the nebula in the far infrared. On the basis of our models in this section we expect that the infrared nebula closely resembles the optical nebula,

whereas the models of the preceding section predict that it is more like the radio nebula.

24. The total energy of the relativistic particles.

Using the model described in the preceding section we now calculate the total energy of the relativistic electrons. The number of particles may be found from (21,6). We take $\beta = 1.60$ for all parts of the nebula, corresponding to a radio spectral index equal to 0.30. The energy of the electrons between energies E_{min} and E_{max} is given by

$$\mathcal{E} = \int_{E_{min}}^{E_{max}} E n(E) dE = k \int_{E_{min}}^{E_{max}} E^{-\beta+1} dE = k \frac{E_{max}^{2-\beta} - E_{min}^{2-\beta}}{2-\beta} \quad (24,1)$$

For the radio electrons we assume $E_{min} = 0$, as a low-energy cut-off hardly influences their energy and as nothing is known about such a cut-off. The maximum energy of the radio electrons is taken such that the critical frequency corresponding to this energy is 10^{12} c/s in the inner sphere. The minimal energy of the optical electrons is taken equal to the maximum energy of the radio electrons and their maximum energy is derived from the value of α_{mv} in the inner sphere, which is equal to 0.107 in the present model. The exact value of the maximum energy of the radio electrons is not very critical. The relative values of H in the three shells also follow from the model in the foregoing section. Thus the only free parameter on which the results depend is the value of H in the inner sphere. In table 15 the calculated energies are given for a few values of H_c . The root mean square value of H in this model is equal to 0.48 H_c . It may be recalled that, strictly, all values of H discussed up till here should be written H_{\perp} . As the volume of the nebula is equal to 5.9×10^{55} cm³ the total magnetic energy \mathfrak{M} is equal to 5.40×10^{53} $H_c^2 = 8.75 \times 10^{53}$ $H_{c\perp}^2$, if we assume that the orientation of the velocity vectors of the electrons is random.

TABLE 15

The energy of the optical and the radio electrons and of the magnetic energy contained in the nebula for a few values of $H_{c\perp}$.

$H_{c\perp}$	E_{max}	\mathcal{E}_{opt}	\mathcal{E}_{radio}	\mathcal{E}_{tot}	\mathfrak{M}
10×10^{-4}	560	7.67×10^{46}	4.18×10^{46}	1.19×10^{47}	8.75×10^{47}
3×10^{-4}	1030	4.61×10^{47}	2.54×10^{47}	7.15×10^{47}	7.90×10^{46}
1×10^{-4}	1780	2.45×10^{48}	1.21×10^{48}	3.66×10^{48}	8.75×10^{45}

It is seen from the table that the total electron energy is about a factor five smaller than the values given by OORT and WALRAVEN (1956). This is due mostly to the different form for the energy spectrum which these authors used. If the distance of the nebula

is doubled all values in the table must be multiplied by four. It will be shown in section 34 that it is difficult to understand the origin of a magnetic energy larger than 10^{46} erg. We therefore consider the numbers for $H_c = 10^{-4}$ as the most probable, if

the homogeneous model on which the table is based is correct.

The present discussion does not take into account possible inhomogeneities in the distribution of the field and the electrons. It will be shown in section 32 that considerable hydromagnetic activity is probably going on in the nebula. In a hydromagnetic wave the lines of force are compressed, which causes the magnetic field strength to be much stronger. If a large number of such waves is travelling in the nebula we might expect that at some places the field is much stronger than would correspond to $H_c = 10^{-4}$, but at other places much weaker.

Let us assume for instance that the nebular lines of force are compressed by these hydromagnetic waves into a volume equal to one third the nebular volume. The field corresponding to the last line of Table 15 ($H_c = 10^{-4}$) then is changed into one having the total magnetic energy 2.6×10^{46} erg. The energy of the hydromagnetic waves is thus equal to 1.7×10^{46} erg, which corresponds to the energy supply of about 20 years if the average energy input in these waves is equal to 4×10^{37} erg/sec (cf. section 25). It appears not unreasonable to assume that this amount of energy in the form of hydromagnetic waves may be present in the nebula.

If we now compute the total particle energy, assuming that the electrons are compressed with the lines of force, we obtain 7.15×10^{47} erg, the value corresponding to the homogeneous model for $H_c = 3 \times 10^{-4}$.

Evidently this model is very schematical and we might expect that the electrons are somewhat less compressed than the field. On the other hand the variations in the magnetic field may be somewhat stronger than we have assumed. Therefore the figure of about 7×10^{47} erg for the total electron energy may be considered as the best estimate at present.

25. *The acceleration of the electrons and the origin of the energy spectrum.*

It has been suggested by some authors that the electrons are accelerated in or very near to the central star of the nebula (OORT and WALRAVEN 1956, PIKELNER 1956). This does not seem very likely to us. If the central star produces these electrons, the most plausible assumption is that they are accelerated by rapidly varying magnetic fields. From the work of RIDDIFORD and BUTLER (1952) it appears that the energy attained by a proton in a typical sunspot, where the field increases in 10^4 seconds to 3000 oersted, is about 1700 Gev. As the energy attained is proportional to $m^{1/4}$, an electron could obtain in this process an energy of about 260 Gev if there were no radiation losses. But from (21,5) we see that a 260 Gev electron loses half its energy in 110

microseconds. As this time is several orders of magnitude smaller than the time scale for acceleration this process is not possible for electrons. It is easily shown that if the time scale for acceleration is not very much shorter than a few days the only place where the electrons can be accelerated sufficiently is the nebula itself. Even in a field of one oersted the time scale for acceleration must not exceed 250 seconds if energies of a thousand Gev are to be attained.

The loss and gain of energy of an electron depends on the physical parameters of the nebula. To describe the energy balance of an electron completely we have to make some assumptions concerning the variation of the relevant parameters during the history of the system. The time will be counted from the moment of the supernova explosion in which the nebula originated. If we disregard the ellipticity of the shell and the acceleration of its motion, the radius of the shell is given by $R = Vt$. The magnetic field strength depends on the radius; we suppose that $H \propto R^{-n}$. Denoting the present value of H by H_p and the present age of the nebula by T we have $H = (t/T)^{-n} H_p$.

At the low density in the nebula the energy loss of a relativistic electron in the form of "bremsstrahlung" and inelastic collisions may be neglected. The electron loses energy mainly by the expansion of the shell and in synchrotron radiation. It may gain energy from a FERMI mechanism.

The energy loss in the form of synchrotron radiation is given by

$$\left(\frac{dE}{dt}\right)_{syn} = -AH^2E^2 = -AH_p^2\left(\frac{T}{t}\right)^{2n}E^2 \quad (25,1)$$

The expansion of the shell causes an average energy loss given by (cf. e.g. PIKELNER 1956)

$$\left(\frac{dE}{dt}\right)_{exp} = -\frac{E}{t} \quad (25,2)$$

The energy gain from a statistical acceleration mechanism is given by

$$\left(\frac{dE}{dt}\right)_{acc} = -g(t)E \quad (25,3)$$

It seems plausible that statistical acceleration was strongest in the early stages of the nebula. For this reason and for mathematical simplicity we assume

$g(t) = \frac{q+1}{t}$, where q is a constant. The energy

equation for a single electron now becomes

$$\frac{dE}{dt} = -AH_p^2\left(\frac{T}{t}\right)^{2n}E^2 + \frac{g}{t}E \quad (25,4)$$

This equation can be written as

$$t^q \frac{d}{dt} (Et^{-q}) = -AH_p^2 \left(\frac{T}{t}\right)^{2n} t^{2q} (Et^{-q})^2 \quad (25,5)$$

After integration we obtain for the present value of the energy E_p of an electron which at time t_0 had an energy E_0

$$E_p = \frac{(T/t_0)^q E_0}{1 + \frac{AH_p^2 T}{q - 2n + 1} \left\{ \left(\frac{T}{t_0}\right)^q - \left(\frac{T}{t_0}\right)^{2n-1} \right\} E_0} = \frac{a E_0}{1 + b E_0} \quad (25,6)$$

For very large values of T/t_0 we have approximately $E_p = a/b$, independent of the initial energy. Effective acceleration may occur when q is positive and larger than $2n - 1$. If the electrons are accelerated in the nebula the maximum energy they can attain is given approximately by

$$E_{max} \approx \frac{q - 2n + 1}{AH_p^2 T}, \quad (25,7)$$

for $T/t_0 \gg 1$ and q somewhat larger than $2n - 1$.

In section 33, n will be shown to be about 2. The value of q is rather uncertain, but is estimated below as 5.3. Then $q - 2n + 1 = 2.3$, and for $H_p = 3 \times 10^{-4}$ oersted we obtain $E_{max} = 240$ Gev. Because of the inhomogeneities in the field we might expect to reach somewhat higher values. These results agree well with the values derived from the ultraviolet emission of the nebula.

We shall now discuss the value of q more closely. It will be shown in section 32 that certain moving details in the nebula, for instance the light-ripples observed by BAADE (OORT and WALRAVEN 1956) may be interpreted as hydromagnetic waves. These hydromagnetic waves might be very effective in the acceleration of relativistic particles, as has first been suggested by PIDDINGTON (*unpublished*). These light-ripples have a velocity of about $0.1 c$. If the motion is inclined to the plane of the sky the real velocity might be even larger. The average energy gain of a relativistic particle in a collision with such a hydromagnetic wave is given by $\Delta E/E = (v/c)^2$ (e.g. BIERMANN 1953), and is thus about $0.01 E$.

The width of a light-ripple perpendicular to its motion may amount to about six seconds of arc. Let us assume for a moment that such a ripple exists for a year. The inner part of the nebula, where the electrons are supposed to be accelerated, has a diameter of about 1.5 minutes of arc. We then find that a fraction 7.2×10^{-4} of the particles in this inner sphere has made a collision with this ripple if it is assumed that the electrons move at random with velocity c . However, the electrons move not quite at random because of the magnetic field. The number of encounters thus depends on the local structure of the field. Perhaps this estimate must therefore be

slightly reduced. BAADE estimates that there may be one ripple every three months. Thus these ripples give on the average a yearly gain $\Delta E = 4 \times 7.2 \times 10^{-4} \times 0.01 E = 2.9 \times 10^{-5} E$. The yearly energy loss due to the expansion is about $1.1 \times 10^{-3} E$. We must expect that such a ripple becomes more extended after some time. It is easily shown that the damping time arising from the finite conductivity and viscosity is much longer than the age of the nebula. It is therefore probable that we have underestimated the energy gain by a large factor. It appears plausible to assume that the waves are appreciably damped by this process of particle acceleration and that they thus convert a large part of their energy into the kinetic energy of the relativistic electrons.

The energy of such a light-ripple may be estimated to be of the order of 10^{43} or 10^{44} erg. Thus, if there are four such light-ripples a year the present energy input into the nebula would be of the order of 10^{36} or 10^{37} erg per second. As these light-ripples are certainly not the only type of hydromagnetic waves in the Crab nebula, it appears that their energy could be sufficient for the acceleration of the relativistic particles.

If the nebula contains about 7×10^{47} erg in the form of the relativistic electrons, the loss of energy due to the expansion amounts to about 2.5×10^{37} erg at present. The energy loss due to the synchrotron radiation is about 2×10^{37} erg/sec. Thus an energy supply of about 4.5×10^{37} erg/sec is needed to maintain the nebula.

Effective acceleration is supposed to occur in the inner sphere with radius $r'_{.5}$. The value of q is determined by the conditions in this part. Let us assume that of the available energy about 4×10^{37} erg may be used to accelerate electrons in the inner sphere. The total energy of the electrons in this inner sphere is equal to 1.9×10^{47} erg. We then find that q is equal to 5.3. The precise value of q is evidently very uncertain.

It is in general not possible to accelerate electrons effectively which do not have a certain initial energy, as the energy losses by inelastic collisions are prohibitive for very slow electrons. It is thus necessary that electrons with a certain minimum energy are injected into the nebula. The electrons might be injected by radioactive matter or they might be slightly accelerated by an inductive mechanism in a weak magnetic field.

Let us assume that electrons with energy E_0 are continually injected into the nebula and that the number injected per unit time is N . Let us start with the assumption that N is constant. The electrons injected at t_0 will at the present time (T) have an energy E_p given by (25,6). The number per unit interval of energy is then evidently

$$n(E_p) = N (dE_p/dt_0)^{-1} \quad (25,8)$$

Using the relation (25,6) between E_p and t_0 we can eliminate t_0 and thus obtain the energy spectrum provided that the constants n and p are known. A very simple case occurs if n is equal to 0.5. The function a can then be expressed explicitly in E_p . After some reductions we obtain for this case

$$n(E) \propto E^{-\frac{p+1}{p}} \left(1 - \frac{E}{E_{max}}\right)^{-\frac{p-1}{p}} \quad (25,9)$$

where E_{max} is given by (25,7) and where we have dropped the index p .

The other case for which an explicit solution can be given is characterized by $p = 2(2n - 1)$. For values of E not too close to E_{max} or to E_0 , equation (25,9) is approximately valid. Thus if p is larger than 1 the exponent of the energy spectrum is limited to values between 1 and 2, in good agreement with the observed value of β . Evidently the assumption of a constant injection of electrons, all with the same energy, is too radical a simplification. If the injected electrons are due to a radioactive substance, we would expect the number of injections per second, N , to vary as $\exp(-t/\tau_{1/2})$, where $\tau_{1/2}$ represents the half life of the radioactive element. This would produce an exponential factor in the energy spectrum. On the other hand the energy spectrum is also affected by the escape of electrons from the inner part. This also tends to produce an exponential factor in the energy distribution, but the sign of the exponent in this case is opposite to that for the variation of the number of injections. For the gradual decrease of the injection causes the number of younger electrons to be smaller than in the case of constant injection; the escape of electrons causes a relative decrease of the older ones. From the density distribution in the nebula derived in the preceding section we found that the time scale for escape from the inner part is of the order of 300 years. In Part V we shall show that the injected electrons might be derived for a large part from radioactive elements with a half life of about 300 years. Then the two exponential factors would tend to cancel each other.

Equation (25,9) shows that $n(E)$ tends to infinity for values of E close to E_{max} . This is due to the fact that all electrons which have been accelerated sufficiently must approach E_{max} but cannot pass it. To investigate the influence of this effect we have computed the total number of electrons with energies between E_{max} and $0.5 E_{max}$ for the energy distribution (25,9), with and without the second factor. The complete distribution gives about 1.9 times more electrons in this energy interval than the pure power law distribution. Such a small deviation does not greatly affect the synchrotron spectrum emitted by these electrons.

PART IV. THE MAGNETIC FIELD IN THE NEBULA

26. The nature of the field.

A relativistic electron emits linearly polarized radiation with the electric vector perpendicular to the local direction of the magnetic field. From the polarization picture in Paper I we may therefore obtain some information on the structure of the magnetic field. The interpretation of this picture is complicated by the fact that it gives the integrated result of regions along the line of sight with different directions of \mathbf{H} .

The first thing evident from an inspection of the polarization picture is that the magnetic field represents a large-scale structure. It is very probable therefore that the field is a property of the nebula as a whole. It should be noted that it is absolutely impossible that the field could be due to the central star. The origin of the nebular field, however, may be related to the field of the central star.

Frequently there is a relation between the filaments and the polarizations in the continuum.

Plate 2 shows the polarization results from Paper I projected against a reproduction of the photograph that BAADE obtained in the light of the [SII] lines. We used this plate as it shows the filaments very clearly. Although there are large intensity differences between the sulphur lines and other emission lines in the filaments, the general structure of the filaments on this plate is the same as on plates taken in the light of these other lines. In many places, particularly in the outer parts of the picture, the relation between the filaments and the polarization is clearly visible. This connection between the field and the filaments will be discussed later on.

In the inner parts of the nebula, where no filaments are present, the magnetic field is strongest (cf. section 23). Thus, there are large internal magnetic pressures, but there is probably not much matter with sufficient inertia to compensate these pressures. The only types of fields which may be stable under these circumstances are the force-free fields and we shall now first discuss the general aspects of such fields.

27. Force-free fields.

Force-free magnetic fields are defined as fields in which the Lorentz force vanishes. They therefore satisfy the relation

$$\text{curl } \mathbf{H} \times \mathbf{H} = 0 \quad (27,1)$$

This is equivalent to the condition

$$\text{curl } \mathbf{H} = \alpha \mathbf{H} \quad (27,2)$$

where α is a scalar function of the space coordinates. Fields of this type have first been studied by LUND-

QUIST (1950) and subsequently by LÜST and SCHLÜTER (1954) and CHANDRASEKHAR (1956). LUNDQUIST investigated the axisymmetric field in an infinite cylinder, whereas the latter authors discussed axisymmetric fields in a sphere. In all cases the discussion was limited to cases where α is a constant. This is evidently a severe restriction and there is no direct reason why fields with α strictly constant should be realized in nature. But the analytical difficulties for variable α are in general insurmountable.

LÜST and SCHLÜTER and CHANDRASEKHAR solved equation (27,2) by separating the field into a toroidal and a meridional part. Each of these fields can be characterized by a scalar function. In this way the full analytical solution of (27,2) under the conditions of axial symmetry and constancy of α could be obtained. For cases without axial symmetry the representation of \mathbf{H} as the sum of a toroidal and a meridional field is not very practical. We therefore discuss first the general solutions of (27,2) in spherical polar coordinates for a field with constant α .

28. The complete solution for constant α *.

Taking the curl of (27,2) we obtain

$$\text{curlcurl } \mathbf{H} = \alpha^2 \mathbf{H} \quad (28,1)$$

$$\mathbf{M}_{nm}^e = \frac{-}{+} \frac{m}{\sin \theta} z_n(\alpha r) P_n^m(\cos \theta) \begin{matrix} \sin \\ \cos \end{matrix} m \varphi \mathbf{e}_\theta - z_n(\alpha r) \frac{dP_n^m(\cos \theta)}{d\theta} \begin{matrix} \cos \\ \sin \end{matrix} m \varphi \mathbf{e}_\varphi \quad (28,4)$$

$$\begin{aligned} \mathbf{N}_{nm}^e = & \frac{n(n+1)}{\alpha r} z_n(\alpha r) P_n^m(\cos \theta) \begin{matrix} \cos \\ \sin \end{matrix} m \varphi \mathbf{e}_r + \frac{1}{\alpha r} \frac{d}{dr} \left\{ r z_n(\alpha r) \right\} \frac{d}{d\theta} P_n^m(\cos \theta) \begin{matrix} \cos \\ \sin \end{matrix} m \varphi \mathbf{e}_\theta \\ & - \frac{m}{\alpha r \sin \theta} \frac{d}{dr} \left[r z_n(\alpha r) \right] P_n^m(\cos \theta) \begin{matrix} \sin \\ \cos \end{matrix} m \varphi \mathbf{e}_\varphi \end{aligned} \quad (28,5)$$

where the indices e and o refer to the even and odd solutions.

Now we expand \mathbf{H} in a series of these characteristic vector functions. The general solution of (28,1) may then be written as

$$\mathbf{H} = \sum_n^e \sum_m^e a_{nm}^e \mathbf{M}_{nm}^e + b_{nm}^e \mathbf{N}_{nm}^e \quad (28,6)$$

Inserting this expression in (27,2) and remembering (28,2) and the relation $\mathbf{M} = \frac{1}{\alpha} \text{curl } \mathbf{N}$ we obtain

$$\begin{aligned} \alpha \sum_n^e \sum_m^e \left(a_{nm}^e \mathbf{N}_{nm}^e + b_{nm}^e \mathbf{M}_{nm}^e \right) = \\ = \alpha \sum_n^e \sum_m^e \left(a_{nm}^e \mathbf{M}_{nm}^e + b_{nm}^e \mathbf{N}_{nm}^e \right) \end{aligned} \quad (28,7)$$

*) The solution discussed in this section was found independently by CHANDRASEKHAR and KENDALL. (Private communication by PROF. CHANDRASEKHAR.)

Every solution of (27,2) is also a solution of (28,1), although the reverse statement is not true. Therefore, once we have determined the complete solution of (28,1), we can find the solution of (27,2) by retaining the appropriate part of this solution. Equation (28,1) has the same form as the time-independent part of the vector wave equation for a solenoidal vector in the theory of electromagnetic waves. We recall briefly the method of solution for this equation in spherical polar coordinates (STRATTON 1941, Chapter 8).

We introduce two vectors as follows

$$\mathbf{M} = \text{curl}(\mathbf{r} \psi) \quad ; \quad \mathbf{N} = \frac{1}{\alpha} \text{curl } \mathbf{M}, \quad (28,2)$$

where ψ is a solution of

$$\nabla^2 \psi + \alpha^2 \psi = 0 \quad (28,3)$$

It is easily verified that the vectors \mathbf{M} and \mathbf{N} satisfy (28,1). The solutions of (28,3) are found in terms of spherical Bessel functions z_n and associated Legendre polynomials P_n^m . The characteristic vector functions are now given by

The solutions of (28,1) which also satisfy (27,2) are therefore characterized by $a_{nm}^e = b_{nm}^e$. The general solution of (27,2) is thus given by

$$\mathbf{H} = \sum_n^e \sum_m^e a_{nm}^e \left(\mathbf{M}_{nm}^e + \mathbf{N}_{nm}^e \right) \quad (28,8)$$

In the case of axial symmetry we have $m = 0$ and from (28,4), (28,5) and (28,8) our fundamental solutions for \mathbf{H} are found to be

$$\mathbf{H}_n = \frac{n(n+1)}{\alpha r} z_n(\alpha r) P_n(\cos \theta) \mathbf{e}_r + \quad (28,9)$$

$$\frac{1}{\alpha r} \frac{d}{dr} \left[r z_n(\alpha r) \right] \frac{dP_n(\cos \theta)}{d\theta} \mathbf{e}_\theta - z_n(\alpha r) \frac{dP_n(\cos \theta)}{d\theta} \mathbf{e}_\varphi$$

This solution should be compared with the solution given by CHANDRASEKHAR, who expresses his results in terms of Bessel functions and Gegenbauer polynomials. Remembering the relation between the Gegenbauer polynomials and the Legendre polynomials, $(n+1) P_n(\mu) = C_n^{3/2}(\mu) - C_{n-1}^{3/2}(\mu)$, we easily

find that a field \mathbf{H}_{n-1} in CHANDRASEKHAR'S treatment is identical with a field \mathbf{H}_n in our notation.

29. Boundary conditions.

If we suppose that no current can flow outside the sphere with radius R , the boundary conditions in the absence of a surface current are

$$r = R; H_r = 0; H_\theta \text{ and } H_\varphi \text{ continuous.}$$

When a surface current \mathbf{K} is allowed on the surface of the sphere, we have

$$r = R; H_r = 0 \text{ and } \mathbf{e}_r \times (\mathbf{H}^e - \mathbf{H}^i) = \mathbf{K}, \quad (29,1)$$

where \mathbf{H}^e and \mathbf{H}^i denote the external and internal field respectively.

$$\mathbf{H}^e = \text{grad} \left[\sum_n^e \sum_m \left\{ c_{nm}^e r^n + d_{nm}^e r^{-(n+1)} \right\} P_n^m(\cos \theta) \frac{\cos m\varphi}{\sin} \right] \quad (29,3)$$

The radial component of \mathbf{H}^e is therefore

$$H_r^e = \sum_n^e \sum_m \left\{ n c_{nm}^e r^{n-1} - (n+1) d_{nm}^e r^{-(n+2)} \right\} P_n^m(\cos \theta) \frac{\cos m\varphi}{\sin} \quad (29,4)$$

To have $H_r^e(R) = 0$ it is necessary that

$$n c_{nm}^e R^{2n+1} = (n+1) d_{nm}^e \quad (29,5)$$

The continuity of H_θ requires

$$c_{nm}^e = \left(\frac{n+1}{2n+1} \right)^2 \frac{z_{n-1}(\alpha R)}{R^{n-1}} a_{nm}^e \quad (29,6)$$

At large distances from the centre $r \gg R$, H_r^e approaches asymptotically to

$$H_r^e \approx \sum_n^e \sum_m n c_{nm}^e r^{n-1} P_n^m(\cos \theta) \frac{\cos m\varphi}{\sin} \quad (29,7)$$

For $n = 1$ the radial component approaches a definite

From (28,4), (28,5) and (28,8) we obtain

$$H_r = \sum_n^e \sum_m \frac{n(n+1)}{\alpha r} z_n(\alpha r) P_n^m(\cos \theta) \frac{\cos m\varphi}{\sin} \quad (29,2)$$

For $r = R$ we must satisfy $H_r = 0$ for all values of θ and φ . Therefore we must have $z_n(\alpha R) = 0$. This equation limits the possible values of α for a given R to a discrete set. Moreover, we see that we can use only one term of the sum over n . For, when $z_n(\alpha R) = 0$, we have $z_{n'}(\alpha R) \neq 0$ for $n' \neq n$.

To discuss the other boundary conditions we first investigate the outer fields that can be adapted in the absence of a surface current. The general solution for the field in the outer region where no current flows is given by

value for large r and for other values of n it increases with increasing r . Thus these fields are not acceptable, as they should vanish at infinity at least as quickly as a dipole field if the current distribution is confined to a finite volume. Therefore, if we do not fit the field to an outer field caused by currents outside the sphere $r < R$, we must require $c_{nm}^e = 0$. This also implies $d_{nm}^e = 0$. Therefore the outer field must vanish entirely. But in this case a surface current must flow. For otherwise at the boundary $H_r = H_\theta = H_\varphi = 0$, which means that the whole field inside the sphere would vanish. Using (29,1) we can derive the surface current appropriate for a field \mathbf{H}_n from the condition $\mathbf{H}^e = 0$. The result is given by

$$\mathbf{K}_n = \sum_m^e a_{nm}^e z_{n-1}(\alpha R) \left[- \frac{m}{\sin \theta} P_n^m(\cos \theta) \frac{\sin m\varphi}{\cos} \mathbf{e}_\theta - \frac{d P_n^m(\cos \theta)}{d\theta} \frac{\cos m\varphi}{\sin} \mathbf{e}_\varphi \right] \quad (29,8)$$

We thus see that the field determines the surface current uniquely and vice versa.

30. Application of force-free fields to the Crab nebula.

The results of the previous sections show two important properties of force-free fields. Firstly, at the border of a region containing a force-free field such a field has no radial components. Secondly, if

the field is confined to a finite volume the boundary conditions require that the field is surrounded by a surface current. These conclusions are also valid if the ratio of field strength to current is not a constant. These two features of the force-free fields appear to be realized in the nebula. The picture of the magnetic field lines constructed by OORT and WALRAVEN and the polarization results in Paper I demonstrate

that the field is largely tangential at the apparent border of the optical nebula. Moreover, the fact that the nebula seems to be able to retain the relativistic particles demonstrates that the field cannot have an appreciable radial component at the border of the nebula.

As the field strength in the nebula is appreciably higher than in interstellar space it is improbable that the field in the nebula can be fitted to the interstellar field. Thus the nebula must be surrounded by a surface current. The influence of the filaments on the field in the nebula demonstrates that they carry current. At a number of places in the outer parts the polarizations on Plate 2 appear all to emerge radially from a certain point and this point is then situated in a filament. The most noticeable example of such a configuration is the dark bay at the east side of the nebula, but more to the north two similar cases are seen. The very thick filament at the south side of the nebula represents another case and about half a dozen more may be distinguished. Polarization arrows which point radially imply circular lines of force. If a filament carries current such circular lines of force are to be expected. We should see the effect most clearly if the filament's orientation is along the line of sight, and this evidently occurs most frequently at the border of the nebula. For those filaments which could be located in space (cf. section 3) this can be seen more directly. For instance we see on the space picture of the filaments on Plate 3 that the filament which on Plate 2 has approximately the coordinates $x = -1$, $y = +8$ is just emerging from the back side of the nebula to the front side. The same is probably the case with the filament at $x = -3$, $y = -6$. However, in most cases we have no sufficiently accurate information on the exact location of the filaments.

The idea that the filaments are associated with currents is supported by the fact that these polarizations are frequently accompanied by intensity changes in the continuum. For instance the large dark bay at the east side of the nebula is clearly related to the polarization distribution. We interpret these features as due to the circular lines of force around the filament, which prevent that the relativistic electrons enter this region.

As the filaments form a sheet surrounding the whole nebula, their identification with a surface current around the inner force-free field appears plausible.

In the mathematical model of a force-free field the current is distributed smoothly over the surface. The field vanishes entirely outside the surface and the influence of the current is not seen in the field lines. But in the nebula the currents are probably concentrated in filaments. This makes no difference for the large-scale structure of the field, but when we come

near to a filament its direct influence becomes marked. We must therefore expect that there will be a weak field outside the nebula; but this becomes negligible at some distance from the filaments, because it arises from more or less random structures on a rather small scale. These fields around the filaments might give some relativistic particles the opportunity to leak out of the nebula.

The general structure of the nebula thus appears consistent with the idea that the field is force-free. A more detailed comparison between the nebular field and a force-free field meets severe difficulties. The theory of the force-free fields developed in the preceding sections deals only with cases for which α is a constant, which may not be true for the nebular field, even if it is force-free. Moreover, these fields have their boundary conditions prescribed on a spherical surface, whereas the nebula is a spheroid with an axial ratio differing appreciably from unity.

Finally we do not expect that the nebula is already in a stationary state, and we expect locally rather strong deviations from a strict force-free condition.

In view of these difficulties we have restricted ourselves to the construction of some models for the nebula. Such a model consists of some force-free field in which relativistic electrons circulate with a prescribed density distribution. For such a model we may calculate the polarization and intensity distribution we would observe when we look at the model from a certain direction. We are interested to see whether such a model shows some resemblance to the actual nebula.

31. The construction of some models.

We introduce a system of Cartesian axes, with the y -axis along the line of sight from the model to the observer. As the radiation from the relativistic electrons is polarized with the electric vector perpendicular to the direction of \mathbf{H} , we obtain for the intensities observed through a nicol with maximum transmission along the x -axis, the z -axis and their bisectrix, respectively,

$$\begin{aligned} I_x &= \frac{H_z^2}{H_x^2 + H_z^2} I \\ I_z &= \frac{H_x^2}{H_x^2 + H_z^2} I \\ I_{xz} &= \frac{0.5 (H_x + H_z)^2}{H_x^2 + H_z^2} I \end{aligned} \quad (31,1)$$

where I represents the total intensity given by

$$I = c N_{re} H^s F(\chi) \quad (31,2)$$

Here N_{re} denotes the density of the relativistic electrons. The spectrum of these electrons is taken

constant through the model. $F(\chi)$ is a function of the angle between \mathbf{H} and the line of sight. This factor represents the anisotropy of the radiation. The angle χ is given by the relation

$$\sin^2 \chi = \frac{H_x^2 + H_z^2}{H^2} \quad (31,3)$$

On integrating the expressions (31,1) along lines parallel to the y -axis we obtained the surface distributions of polarization and intensity. The magnetic

field adopted was the axisymmetric field characterized by $n = 1, m = 0$. The z -axis is taken as the axis of symmetry. We assumed that the boundary of the region containing the field coincides with the first zero which is reached at $\alpha r = 4.49$. Results were obtained for $s = 1$ and $s = 2$, and for $F(\chi) = 1$ and $F(\chi) = \sin^2 \chi$. The polarizations along the x - and z -axis are given for a few cases in Table 16. The polarizations are mostly parallel to the x -axis, but are indicated by a negative sign, if parallel to the z -axis.

TABLE 16
The degree of polarization in the emission of some models.

x	z	$F(\chi) = 1, s = 1$	$F(\chi) = 1, s = 2$	$F(\chi) = \sin^2 \chi, s = 2$	x	z	$F(\chi) = \sin^2 \chi, s = 2$
0	0	11	22	22	0	0	22
1	0	7	16	14	0	1	22
2	0	- 4	- 3	- 9	0	2	29
3	0	49	47	56	0	3	42
4	0	99	99	99	0	4	72

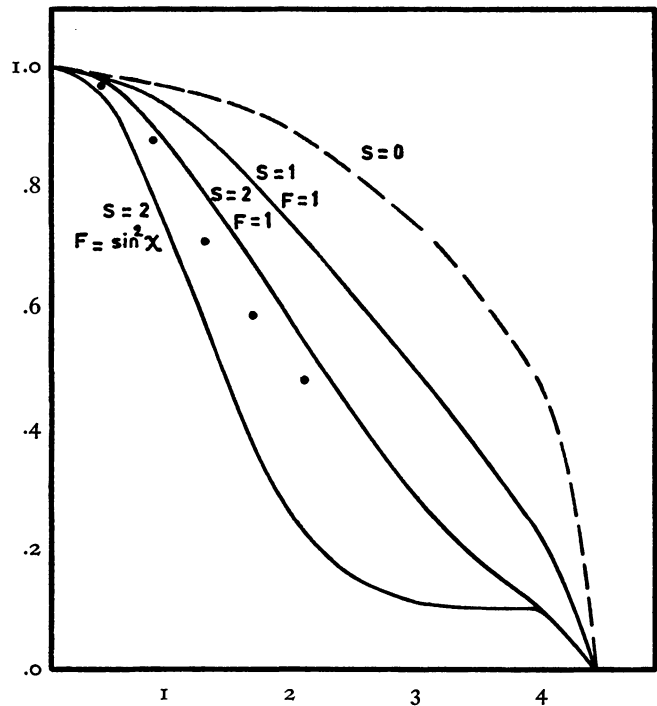
It is seen that the results do not depend very much on the anisotropy. If we suppose that the density of the relativistic electrons slightly decreases outwards, the case $s = 2$ corresponds best to the optical radiation. The main direction of the polarization shows that in the comparison with the Crab nebula the z -axis must be taken parallel to the minor axis of the nebula.

The computed polarizations cannot be compared directly to the observed ones. As is indicated in the next section, the nebula consists of a seemingly amorphous part, on which are superposed a number of light-concentrations, which are almost completely polarized. In this "amorphous" part the detailed structure appears to have been obliterated by the superposition of a large number of structures. Therefore it probably gives a rather good picture of the basic field of the nebula. It is in general rather difficult to separate the two components. At the centre of the nebula we estimate the polarization in the amorphous part as about 18 per cent and almost parallel to the major axis of the nebula. This agrees well with the results from the models. The large polarizations near the borders of the models are in the nebula completely obliterated by the irregularities due to the filamentary currents.

The intensity distribution along the x -axis for some models is shown in Figure 6. It is seen that the introduction of the anisotropy has a strong influence on the results. For comparison we have also indicated the intensity distribution for a sphere filled uniformly with light.

In the nebula we take along the major axis the boundary of the force-free field at z' from the central star. We have chosen this value for two reasons.

FIGURE 6



The intensity distribution on the x -axis for some models of a force-free field. The dots indicate the equivalent intensities in the nebula along the major axis.

Firstly it was shown in section 23 that the electrons in the sphere $\rho > z'$ may have a spectrum differing appreciably from the energy spectrum in the inner part of the nebula. Secondly, this distance corresponds approximately with the inner limit of the filamentary shell. Along the major axis, to the north of the central star, we were able to derive the intensity

in the amorphous part of the nebula up to about one minute of arc from the central star. Beyond this distance it is not possible to derive the intensity for this "amorphous" part very well; so a useful comparison cannot be made. The points obtained are shown in Figure 6. It is seen that the results are compatible with an emission proportional to H^2 and a slight anisotropy.

Although no definite conclusions may be drawn from this rough comparison between a simple model of a force-free field and the actual nebula, the results demonstrate that the nebula is not very different from what could be expected if the nebular field were force-free.

32. *The variable structures in the nebular continuum.*

Although the general structure of the nebula has not changed in a fundamental way during the last fifty years, considerable local variations have occurred in the continuous light.

The most remarkable temporary features are the light-ripples discovered by BAADE, which a few times a year appear at a small distance from the central star and then move away from this star with a velocity of about a tenth of the velocity of light (OORT and WALRAVEN 1956).

We have made a detailed photometry of such a ripple on the polarization plates taken by BAADE (cf. Paper I). The correction for the background intensity was rather difficult, as the ripple was situated in a region where the background varied steeply. The surface brightness of the ripple was less than twenty per cent of the background.

The polarizations in the ripple are very high, reaching ninety per cent in part of it. The lines of force in the ripple are perpendicular to its motion. The emission of the ripple was equal to 8.4×10^{-5} of the emission of the whole nebula. We find that for this ripple the volume emissivity was about 4 times the average in the region within $1'$ from the central star.

It is plausible to assume that such a ripple represents a hydromagnetic wave travelling in a tenuous medium, as has first been suggested by PIDDINGTON (*unpublished*). If we assume that the density of the relativistic electrons is roughly equal in and outside the ripple and if we assume that the undisturbed field in the region close to the central star where the ripples appear is 3×10^{-4} oersted, the energy in the ripple is found to be 1.2×10^{43} erg.

The fact that these ripples originate each time at about the same spot indicates that they are correlated with some details of the structure of the field in the neighbourhood of the central star. The field in this region might be somewhat higher and the particle density somewhat lower than we have assumed. For each ripple has a tendency to remove the electrons

and the path of a ripple is thus already cleaned to a certain extent by previous ripples. We may therefore estimate the average energy of such a ripple to be of the order of 10^{43} or 10^{44} erg; but it should be kept in mind that this estimate is very uncertain.

If we compare plates taken with an interval of about ten years, changes on a larger scale become apparent. We have made a photometry of a plate taken by HUBBLE in 1924, which was kindly put at our disposal by Dr BAADE. The detailed results of these measurements and of the measurements on other plates will be described elsewhere, but a few results may be noted. Locally the intensity changes may reach fifty per cent. The results suggest that the continuous radiation of the nebula consists of two parts; a more amorphous part showing little variation in time, and a number of intensity concentrations which appear superposed on the amorphous part. Evidently this seemingly amorphous part may consist of a large number of superposed structures. This is suggested by the fact that at the edge of the nebula more rather sharp structures become visible, probably because here less structures are superimposed on each other. These concentrations seem to move through the nebula in the course of time.

In the analysis of the polarization measurements it appeared that the nebula possibly consists of an amorphous part which is weakly polarized. Superposed are a number of almost fully polarized intensity peaks (OORT and WALRAVEN 1956 Figure 8).

These moving light-concentrations should probably be considered as hydromagnetic waves on a far larger scale than the light-ripples. These waves have an appreciable width and we consider them not as a single wave but as an assembly of waves moving in the same direction. Their occurrence may indicate that the central star has sometimes periods of several years in which its activity is more violent. A detailed interpretation must wait for the measurement of a larger number of plates, which is in progress, and from which we hope to derive the velocities and the paths of these features.

PART V. THE DYNAMICS AND ORIGIN OF THE NEBULA

33. *The expansion of the nebula.*

The magnetic field and the relativistic particles exert a force on the shell of the nebula. The shell must therefore be in accelerated expansion, in agreement with observations (section 3). Evidently the present value of the acceleration is not known; the observed acceleration depends on the history of the system. The kinetic energy of the shell increases continuously and it follows from the conservation of

energy that the magnetic energy m and the particle energy U must decrease unless new energy is fed into the nebula. The expansion is most easily discussed by using the virial theorem derived by CHANDRASEKHAR and FERMI (1953). The theorem as derived by these authors involves some volume integrals extended over an infinite volume. If we wish to apply this to a finite volume, two surface integrals have to be added and it is easily shown that the complete theorem becomes

$$\frac{1}{2} \frac{d^2}{dt^2} \int r^2 dm = 2T + 3(\gamma - 1)U + m + \Omega + \frac{1}{4\pi} \int_s (\mathbf{r} \cdot \mathbf{H})(\mathbf{H} \cdot \mathbf{n}) da - \int_s \left(P + \frac{H^2}{8\pi} \right) \mathbf{r} \cdot \mathbf{n} da \quad (33,1)$$

Here T and Ω represent the kinetic energy and the gravitational energy, respectively. At present the gravitational energy may be neglected, as it is several orders of magnitude smaller than the other types of

$$\frac{R}{8\pi} \int_s (H_r^2 - H_t^2) da = -\frac{R^3 H_{is}^2}{4} \int_0^\pi (\cos^2 \theta - \sin^2 \theta) \sin \theta d\theta = -\frac{R^3 H_{is}^2}{6} = -m_{is} \quad (33,3)$$

Here m_{is} is the magnetic energy the nebula would contain if the field inside the nebula were the interstellar field. As the sum of U and m is much larger than m_{is} , the influence of the interstellar field on the dynamics of the nebula cannot be very large. This does not exclude the possibility that the filaments in the outermost regions of the nebula could be locally influenced by the interstellar field.

It is not improbable that the central star of the nebula has a strong magnetic field. To investigate the influence of this field we evaluate the surface integral over the surface of the star. If we assume that the star has a dipole field this integral becomes

$$-\frac{R_s^3 H_s^2}{4} \int_0^\pi (\cos^2 \theta - \frac{1}{2} \sin^2 \theta) \sin \theta d\theta = 0, \quad (33,4)$$

where R_s represents the radius of the star and H_s the polar strength of the field. If, however, on the entire surface of the star the field is directed almost purely radially the integral becomes

$$-\frac{R_s}{8\pi} \int H_{rs}^2 da = -\frac{R_s^3 \overline{H_{rs}^2}}{2} = -m_s, \quad (33,5)$$

where H_{rs} is the field strength of the radial field at the stellar surface and m_s the magnetic energy the central star would have if it had a homogeneous field $H_{rs}/\sqrt{3}$. Hence, if m_s were equal to the magnetic energy in the nebula, the magnetic field would not

influence the expansion at all. Physically this means that the lines of force all connect the expanding shell with the central star and therefore tend to compensate by their tension the outward magnetic pressure.

$$MR\ddot{R} = 3(\gamma - 1)U + m + \frac{R}{8\pi} \int_s (H_r^2 - H_t^2) da, \quad (33,2)$$

where H_r and H_t represent the components of \mathbf{H} in the radial direction and perpendicular to this direction, respectively. If the system is also bounded by a spherical surface at its inner side, the surface integral must be taken over this surface with opposite sign.

If there is a homogeneous interstellar field \mathbf{H}_{is} , the integral over the outer surface is evaluated by introducing spherical polar coordinates with the axis parallel to \mathbf{H}_{is} . We obtain

The stellar field cannot be strong enough to have an appreciable influence on the *present* dynamics of the nebula. It may, however, have been of importance in the past in connection with the origin of the nebular field (see next section). For in a magnetic field where the lines of force all point radially outwards the field strength varies as r^{-2} . Thus, if the central star had a radius of 10^{10} cm and a radial surface field of 10^{10} oersted—a field which would bring the star near magnetic instability—the field in the nebula, at a distance of 10^{18} cm from the centre, is only 10^{-6} oersted. This is certainly too small, although not by many orders of magnitude. There must therefore be an additional field in the nebula which was not originally connected with the central star.

We now proceed with the discussion of (33,2). Let us first disregard the particle energy U , in order to obtain a minimum estimate for the acceleration of the shell. The virial theorem then can be written as follows

$$MR\ddot{R} + \frac{1}{2}MR\dot{R}^2 = \frac{1}{2}MR\dot{R}^2 + m - m_s = E - m_s, \quad (33,6)$$

where E represents the total energy of the system

which, for the moment, we assume to be a constant. Equation (33,6) may be written as

$$\frac{M}{2R} \frac{d}{dt} (R\dot{R}^2) = E - m_s, \quad (33,7)$$

After integration we obtain

$$\frac{1}{2} MR\dot{R}^2 = E - m_s + \frac{A}{R} \quad (33,8)$$

Therefore the magnetic energy is given by

$$m = m_s - \frac{A}{R} \quad (33,9)$$

The constant of integration A is given by the condition that the equation must also be valid at an arbitrary initial time t_0 , when the radius of the nebula was R_0 and its magnetic energy m_0 . Hence we obtain

$$m = m_s + (m_0 - m_s) \frac{R_0}{R} \quad (33,10)$$

At present m is much larger than m_s and (33,10) shows that it has been even larger in the past. This equation shows that the magnetic energy rapidly decreases during the expansion of the nebula. Thus, if at present m is equal to 10^{46} erg, it was equal to 10^{49} erg when the radius of the nebula was 0.001 times the present radius. All this energy has been transformed into kinetic energy of the shell.

If the mass of the shell is equal to that of the sun, its present kinetic energy is 10^{49} erg. Therefore the magnetic pressure would have been sufficient to give it its present kinetic energy if starting from rest. If the field had ever been confined within a region having a still smaller radius, the present kinetic energy of the shell would be much larger than the value which is actually observed. We, therefore, conclude that, unless there has been a subsequent supply of magnetic energy, the field cannot have been enclosed in a region with a radius smaller than one thousandth of the present radius. This leads once more to the conclusion that the field cannot have resulted from the simple dilution of a stellar field. This also follows from the following consideration. The magnetic energy varies as R^{-1} during the expansion. The gravitational energy of the system varies in the same way. At present the gravitational energy of the system is much smaller than the magnetic energy. The same situation should then have existed during the whole history of the system. But such a configuration could never have originated because it is unstable.

The only possibility to escape these difficulties is to assume that the field was mainly formed at a time when the radius of the nebula was equal to at least a thousandth of the present radius.

34. *The origin of the magnetic field.*

The origin of the magnetic field in the nebula is the most difficult problem in the study of the system. The results of the preceding section demonstrate that it is not possible simply to dilute a stellar field over the volume of the nebula, and that it is likewise impossible to produce the field by a shell moving through the magnetic field of the star from which it was expelled. The first process increases the distance between all lines of force, which decreases the magnetic energy too strongly. In the second process all lines of force are connected with the central star. As shown in the previous section this gives too small a field at large distances from the centre.

The preceding arguments show that we need not only a lengthening of the lines of force, but the number of field lines passing through a cross-section of the nebula must be increased. This may occur in a turbulent medium. The lines of force are stretched as on the average neighbouring elements tend to drift apart. Because the turbulent elements move in many directions the number of the lines of force through a given surface may be increased.

Under the present conditions in the Crab nebula it does not appear possible to increase the magnetic energy in this manner. It is highly improbable that in the present phase a sufficient number of high-velocity turbulent elements is present in the nebula. Small-scale turbulence is excluded by the regularity of the present nebular field, as has been remarked by OORT and WALRAVEN (1956). However, it cannot be excluded that important turbulence occurred in the earlier history of the nebula. In the time elapsed since this turbulence ceased the lines of force could have somewhat straightened themselves and a field with a large scale could have been produced.

We tentatively suggest the following picture. We assume that a shell was ejected by the supernova. This shell moved through the field of the star, thereby producing a field consisting of lines of force which connect the stellar remnant and the shell. In the region inside this shell strong, large-scale motions were caused by eruptions from the central star. This seems not implausible, because even at present strong activity persists near this star.

The field formed between the shell and the star was greatly increased by this "turbulent" motion. At the same time a field in the shell was set up, by motions on a smaller scale. In general, turbulent elements reaching the shell suffered elastic collisions but occasionally a turbulent element moved some distance through the shell, thereby connecting the field lines of the nebula with the field in the shell. This had a stabilizing influence on the field after the turbulence had gradually died down. As it was shown

in the previous section that the present magnetic field cannot have been confined in a volume with a radius smaller than a thousandth of the present radius of the nebula, we must assume that the turbulence was important at least one or two years after the outburst.

We shall now make some rough numerical estimates of the parameters involved in this process. We assume that during the first years after the outburst the shell had a velocity of about 700 km/sec. If the sum of the turbulent and magnetic energy was maintained at about 3×10^{48} erg during the second and third year after the outburst and if finally most of the turbulent energy was converted into magnetic energy, the present value of the magnetic field energy becomes 7×10^{45} erg. This appears sufficient to account for the emission of the nebula. In this case the shell would have obtained a kinetic energy of about 6×10^{48} erg from the turbulent and magnetic pressures. The pressure exerted by the relativistic particles follows from the amount of radioactive energy (section 36) which is supplied to the nebula. This energy is partly used to accelerate the relativistic electrons. If we neglect the radiative losses of these electrons we find that the shell would have acquired an energy of about 10^{48} erg by this process since the first year after the outburst. Even if this input of energy were a few times larger, the pressure on the shell due to the combined effect of the magnetic field and the particle pressure need not have been prohibitive.

Because of the short time during which the energy supply was sufficient to produce strong turbulence, the initial field must have been quite strong before turbulence started. Let us suppose that the mean random velocity of the turbulent elements was equal to 10 000 km/sec. Then these elements may have moved about ten times across the nebula. If we assume that all lines of force are connected with turbulent elements, the number of field lines through a given cross-section of the nebula may have been doubled ten times. Thus we would have a maximum gain of a factor 1000. Since the number of field lines depends on H and the magnetic energy on H^2 , the magnetic energy could be increased by a factor 10^6 at most.

The turbulence is not important in the inner part of the nebula dominated by the field of the central star. If we assume that the process occurs mainly in the space between the shell and a sphere of half its radius, the initial field must have been 0.04 oersted at a distance of about 10^{15} cm from the central star in order to obtain a final magnetic energy of 3×10^{48} erg. Assuming that the radius of the star was equal to 10^{10} cm, the surface field must have been 4×10^8 oersted. If the field were more or less homogeneous through the star, the magnetic

energy would have been about 10^{47} erg, i.e., a factor thousand less than the energy at the limit of magnetic stability.

Obviously the present discussion is very rough, but a more elaborate theory would be exceedingly complex.

35. *The pre-supernova.*

It appears from the preceding discussion that the star which became a supernova had a strong magnetic field. We shall now investigate how this fits in with current evolution theories.

It appears that supernovae of type I are population II objects. This is indicated by their rather frequent occurrence in elliptical galaxies.

According to HOYLE and SCHWARZSCHILD (1955) a population II star first evolves slowly to the top of the giant sequence in the HR diagram. The energy is derived mainly from the burning of hydrogen. Afterwards the star probably starts burning its helium and evolves rather rapidly along the horizontal branch in the HR diagram. E. M. BURBIDGE, G. R. BURBIDGE, W. A. FOWLER and F. HOYLE (1957) have developed a theory in which they suppose that all elements have been formed in stars. Most of the heavy elements should have been formed in a very short time in a star which has exhausted most of its hydrogen and helium. BURBIDGE *et al.* give reasons for supposing that this last stage of element formation occurs in a star which has lost its stability and produces a supernova explosion. According to this view the supernova is one of the latest evolutionary stages of a star. Therefore it seems plausible that most of the stars reaching the end of the horizontal branch in the HR diagram become supernovae. After the supernova process probably a white-dwarf structure remains and the star becomes much fainter. It seems necessary to assume such a catastrophic ending of these stars, as the horizontal branch terminates rather abruptly and no stars have been found in the neighbourhood of its last part.

Thus every star passes along the horizontal branch of the HR diagram and must also traverse the cluster variable gap. If the suggested evolution is correct, the frequency of supernovae may be predicted from the observed frequency of the cluster variables.

No reliable evolutionary tracks have been computed along the horizontal branch of the HR diagram, but some order-of-magnitude estimates may be obtained from the preliminary models of stars in this region constructed by HOYLE and SCHWARZSCHILD (1955).

In their models a star evolves in about 10^8 years from the model characterized by $q = 0.70$ to the model characterized by $q = 0.80$. As the luminosity of their models is about one magnitude brighter than the luminosity of the stars on the horizontal branch,

we multiply the evolution time by a factor two. The colour indices of these two models differ by about $0^m.5$ and, assuming a uniform motion of the stars in the magnitude colour-index diagram, the rate of change of the colour index is found to be about $0^m.25$ per 10^8 years. The cluster gap has an average width of about $0^m.2$ and a star would spend 8×10^7 years as an RR Lyrae star. PARENAGO (1948) has estimated the total number of RR Lyrae stars in the Galactic System as 1.7×10^5 . Thus in a steady state every 500 years a star enters the cluster gap and another star leaves it. Also, once every 500 years a star reaches the end of the horizontal branch and may become a supernova. This figure agrees well with the frequency of supernovae observed in extragalactic systems.

The possible connection between RR Lyrae stars and supernovae is important as it can give us some estimate of the magnetic fields we have to expect in a pre-supernova. For RR Lyrae itself BABCOCK (1956) has measured the magnetic field and found a polar strength of about 4000 oersted. Assuming a homogeneous field this corresponds to a total magnetic energy of 3×10^{41} erg, as the radius of the star is 5×10^{11} cm. For a decay field in a SCHWARZSCHILD stellar model we obtain 6×10^{42} erg (WRUBEL 1952), but we must bear in mind that the magnetic field may be still more concentrated towards the centre.

If the star contracts in a period of time which is short compared with the decay time of the field, the field is compressed and the magnetic energy increases as R^{-1} (section 33). Adopting the decay field in a SCHWARZSCHILD model for RR Lyrae we then obtain for a pre-supernova with radius 10^{10} cm a magnetic energy of 3×10^{44} erg. We found in the preceding section that the magnetic energy in the supernova remnant is about 10^{47} erg if its radius is 10^{10} cm. The uncertainty in both figures amounts to at least a factor hundred and they can be easily made to agree.

These strong magnetic fields introduce a serious complication in the theory of stellar structure and evolution. In the evolutionary models of HOYLE and SCHWARZSCHILD a large fraction of the models has a rather extensive convection zone and it is possible that the presence of the field may change the results materially because of its stabilizing effect.

The discussion of this section is highly speculative, but nevertheless demonstrates that the physical parameters we have adopted are not incompatible with current ideas on stellar evolution.

36. *The supernova and the source of energy in the nebula.*

G. R. BURBIDGE, E. M. BURBIDGE, W. A. FOWLER and F. HOYLE (1957) have presented a rather elaborate theory of the supernova phenomenon. The general

results of this theory appear compatible with our results concerning the nebula.

The supernova process, in which a large number of heavy elements is formed, requires a stellar composition deficient in hydrogen and helium. In section 14 it was shown that the composition of the filaments is rather normal, with no large excess of the other light elements with respect to hydrogen and helium. However, helium is overabundant with respect to hydrogen and this demonstrates that nuclear activity has also taken place in the material which is now in the filaments. The fact that hydrogen and helium are not underabundant appears to imply that the pre-supernova consisted of various shells in different states of evolution and with almost no mixing between these shells. This is plausible, as the magnetic field may inhibit any large-scale circulation in the star.

In their theory of the element abundances BURBIDGE *et al.* show that it is necessary that a very small fraction of the elements synthesized in the supernova outburst (*r*-process elements) must spend some time in a medium rich in hydrogen and react there (*p*-process) to produce some proton-rich isotopes of the heavy elements. The advantage of a supernova with an outer shell rich in hydrogen, is that the *r*-process and the *p*-process may occur in the same star, as during the explosion some mixing of the *r*-process elements with the material of the shell is likely to occur.

According to BURBIDGE *et al.* in the *r*-process an amount of Cf^{254} is formed and the decay of this element produces the energy needed to account for the exponential part of the supernova light-curve after the maximum, with a half-time of 55 days. But at the same time a considerable amount of other radioactive elements is formed. Some of these have a rather long half-life and it is to these elements that we attribute the present energy supply for the nebula. A radioactive energy supply has been suggested by various people, e.g. W. H. RAMSEY and in more recent times P. MORRISON. We shall now make a quantitative estimate of this energy.

From the data given by BURBIDGE *et al.* the initial rate of the energy production by Cf^{254} in the supernova which produced the Crab nebula is found to be 1.45×10^{41} erg/sec. The energy production of any radioactive element at any time may be computed from the data in Table VIII, 1 in the book by BURBIDGE *et al.* The total energy production at any time may then be found by adding the results for all elements. The greatest uncertainty in these calculations arises from the estimates of the abundances. If we assume that the neutron flux was sufficient to transport all the processed material to the region between $A = 110$ and $A = 260$ and that it cycled there, we obtain for the total energy production 10,

100 and 1000 years after the outburst respectively 2.1×10^{38} , 1.2×10^{37} and 0.52×10^{37} erg/sec. At the present moment most of the energy is then due to Cm^{250} .

If we assume, however, that steady flow was reached in the r -process, producing abundances similar to the abundances in the solar system, we obtain for the energy released after 10, 100 and 1000 years respectively 4.0×10^{38} , 8.6×10^{37} and 1.3×10^{37} erg/sec. In the present stages of evolution the energy is now mainly derived from the β decay of Si^{32} and A^{39} , which have a half-life of about 300 years.

The energy which is needed at present has been estimated in section 25 to be 4.5×10^{37} erg/sec. As all calculations are rather uncertain, the agreement with the above figures is reasonable.

37. *The remnant of the supernova.*

Because of the high gravitational potential it does not appear plausible to assume that all the elements formed in the supernova outburst can leave the star. An appreciable fraction of the radioactive energy might, therefore, be liberated inside the star. The core is probably a pure neutron core and the radioactive elements are likely to be concentrated near the outer part of the star. These elements liberate their energy partly by β decay. By this process electrons with an energy of the order of 1 Mev are continually being formed. If the magnetic field at the surface of the star is of the order of 10^8 oersted, these electrons radiate half their energy in a time of the order of 10^{-8} sec (cf. equation 21,4). The critical frequency for an electron with 1 Mev energy in a field of 10^8 oersted is about 10^{15} c/s. It follows that the supernova remnant may emit strong synchrotron radiation in the ultraviolet. The number of electrons produced in β decay is small for low energies, reaches a maximum at intermediate energy and subsequently decreases again, dropping to zero beyond the maximum energy. Accordingly, this synchrotron radiation may have a positive spectral index between the optical and the ultraviolet part of the spectrum. As discussed in section 10 the ultraviolet radiation from the supernova remnant might thus have an important influence on the temperature of the filaments.

38. *The structure of the filaments.*

In section 30 it was shown that the filaments are

$$\left. \begin{aligned} H_{\theta} &= 2\pi j_0 r & r < r_0 \\ H_{\theta} &= 2\pi j_0 \left(\frac{T}{T_0}\right)^{3/2} \left[r + r_0 \left\{ \left(\frac{T_0}{T}\right)^{3/2} - 1 \right\} \right] & r_0 < r < r_1 \end{aligned} \right\} \quad (38,5)$$

The pressure may be found by integrating (38,3):

$$\left. \begin{aligned} p &= p_0 - \pi j_0^2 r_0^2 & r < r_0 \\ p &= p_0 - \pi j_0^2 \left(\frac{T}{T_0}\right)^3 \left[r - r_0 \left\{ 1 - \left(\frac{T_0}{T}\right)^{3/2} \right\} \right]^2 & r_0 < r < r_1 \end{aligned} \right\} \quad (38,6)$$

associated with a system of currents. We shall now consider the structure of an individual filament.

If a current flows through a filament, the magnetic field due to the current tends to compress the filament to a small cross-section. This effect is known as the pinch effect (cf. SPITZER 1956). In a stationary state the cross-section of the filament is adjusted so that the outward gas pressure is equal to the force exerted by the magnetic field. If gravitational effects are disregarded, the structure of such a pinch is easily derived, and it is found that the total current is related to the gas pressure at the axis of the filament by the relation

$$I^2 = \pi r^2 p_0. \quad (38,1)$$

The diameters of the stronger filaments are about 3×10^{16} cm. The pressure in the filament is 7×10^{-9} dyne cm^{-2} , if $N_e = 1500 \text{ cm}^{-3}$ and $T_e = 17000^\circ$. The corresponding current is $I = 2.2 \times 10^{12}$ emu. Assuming that the mean field strength is 10^{-4} oersted in the central parts of the nebula, and that the field is the simplest axisymmetric force-free field (characterized by $n = 1$) and assuming that the whole surface current is distributed over five filaments, each forming a closed loop around the nebula, we find from (29,8) that the current in each of these filaments must amount to 3.26×10^{13} emu in order that it can yield a proper boundary for the force-free magnetic field. This is considerably larger than the result derived from (38,1).

The central pressure in the filament would appear to be rather well determined. The only possibility to produce a larger current is to increase the radii of the filaments.

Let us suppose that we have a filament in which the temperature is T_0 for $r < r_0$ and T_1 for $r_0 < r < r_1$. As the conductivity is proportional to $T^{3/2}$, and since Ohm's law is satisfied in this case, we obtain for the current in the outer region

$$j_1 = j_0 \left(\frac{T}{T_0}\right)^{3/2} \quad (38,2)$$

The hydromagnetic equations are for this case (SPITZER 1956)

$$\frac{dp}{dr} = -j H_{\theta} \quad (38,3)$$

$$\frac{1}{r} \frac{d}{dr} (r H_{\theta}) = 4\pi j \quad (38,4)$$

Integrating (38,4) and making use of (38,2) we find

From the condition that the pressure must vanish at $r = r_1$ we obtain the following expression for the total current

$$I^2 = \pi r_1^2 \rho_0 \left[1 + \frac{r_0}{r_1} \left\{ 1 - \left(\frac{T_0}{T} \right)^{3/2} \right\} \right]^2 \quad (38,7)$$

If we suppose that the filaments are surrounded by a medium of rather low density and high temperature, the current required by the boundary conditions of the nebula's general magnetic field may be obtained if the cross-section of the whole filament including this less dense medium, has a radius about 15 times larger than the visible part. Because of their low density these outer parts emit only a small amount of radiation and are, therefore, unobservable (section 18). If we suppose that the temperature in the filaments proper is $17\,000^\circ$ and in the surrounding cylinders $400\,000^\circ$, the total mass of the filamentary system becomes roughly one solar mass.

The reason for the low temperature in the inner parts of the filaments is that the radiation is large in these parts because of the relatively high density. The situation resembles the solar corona, where the prominences are surrounded by the hot coronal gas.

These considerations find some support in the observed structure of the filaments. Although they appear to represent continuous structures when considered on a large scale, a more detailed consideration shows that they may be more adequately described as an assembly of loose pieces of matter. Frequently a filament appears to have sudden interruptions and the diameter of a filament may vary greatly over a rather small distance. If we compute the current in different parts of such a filament from (38,1) we find large variations. This indicates that currents also flow outside the observable parts of the filaments. Therefore, the general picture of the shell consists of a rather high-temperature medium which, as a consequence of the mutual attraction of the currents in the shell, is split up into a number of diffuse filaments. In these low-density filaments condensations occur which, because of their higher emission rate, cool rapidly. These condensations correspond to the observed filaments.

This discussion neglects the effects of gravity. It was pointed out to us by Dr SCHLÜTER that the acceleration of the shell has exactly the same effect as gravity. In their theory of the solar filaments SCHLÜTER and KIPPENHAHN (1957) have taken into account the effects of gravity and were thereby able to explain the small width of these filaments. In their case a considerable simplification arose from the fact that the height of the filaments was very large. If the filament is more circular in cross-section, the differential equation which determines the structure of the filaments is very difficult to solve. It is probable

that, because of the acceleration of the shell, the filaments, including the low-density parts, have a more elongated form, but the area of the cross-section will not be altered very much.

It may be expected that in the outer parts of the filamentary shell, where the magnetic field is weak, the detailed structure of the filaments may be influenced by the interstellar field.

39. *The escape of relativistic electrons and the production of cosmic-ray particles.*

At the present time radioactive energy is probably still being liberated in the nebula. We estimate that about 10^{48} erg, or slightly more, is still available. The actual magnetic energy in the nebula is of the order of 10^{46} erg. It will continue to decrease because of the expansion of the shell. The energy of the relativistic electrons is of the order of 10^{48} erg. Part of this energy may be transformed into kinetic energy of the expanding shell, but after some time, when the field of the nebula is still weaker and no longer very different from the interstellar field, the relativistic particles will start to escape and contribute to the relativistic-particle energy of the Galactic System. The kinetic energy of the shell is about 10^{49} erg, if its mass is equal to that of the sun. Probably this energy will finally be added to the turbulent energy of the interstellar medium.

As shown by BALDWIN (1955) the greater part of the long-wave radio-frequency radiation originates in a more or less spherical volume around the Galactic Centre, with a radius of about 15 kpc. If we assume that this radiation is synchrotron radiation from electrons which spiral in the weak magnetic fields of the halo (SHKLOVSKY 1953) and if we assume that the spectral index of this radiation is equal to 0.50 (ADGIE and SMITH 1956) we find that the total number of electrons, per energy interval of 1 Gev, and with an energy of 1 Gev, is 1.2×10^{57} . We assumed that the field in the halo is 10^{-6} oersted (cf. G. R. BURBIDGE 1956). The electrons producing the high-frequency part of the radio spectrum have an energy of about 10 Gev and a half-life of the order of 10^9 years. The electrons with lower energy are probably eliminated in about the same time by collisions with the interstellar medium. If we assume that a supernova occurs every 300 years and that the electron production is the same as in the Crab nebula the total number produced, per Gev energy interval, and with an energy of 1 Gev is about 7×10^{55} in 10^9 years. If the distance of the Crab nebula should be doubled this number becomes four times larger. In view of the uncertainties in these estimates the approximate agreement with the 6×10^{56} electrons which should be renewed in 10^9 years is satisfactory. It is not necessary, therefore, to assume much additional acceleration in the Galactic halo. This some-

what weakens the results obtained by FAN (1956) on the acceleration of cosmic-ray particles and relativistic electrons in interstellar space.

No information is available on the relativistic ions which might be present in the Crab nebula, but their energy may not be much larger than the energy of the relativistic electrons. For the available energy appears insufficient to accelerate many more particles; moreover the pressure on the shell would then become too large. We therefore adopt a total cosmic-ray production of 10^{48} erg as an upper limit for the Crab nebula. OORT and WALRAVEN (1956) have shown that the total energy of the cosmic-ray particles which has to be supplied, is of the order of 10^{48} erg per year. The production of objects like the Crab nebula is therefore much too small. It may be, however, that the supernovae produce a larger amount of cosmic-ray particles shortly after the explosion. If these particles were able to leave the nebula the pressure difficulty could be avoided. But even then, the energy needed seems rather large.

40. Suggestions for future work.

The present investigation demonstrates that much observational work remains to be done on the Crab nebula. We shall summarize here a few of the data which are most urgently needed.

The distance of the nebula is evidently a datum of fundamental importance. The discussion in section 17 indicates that it may be derived from the [OIII]/[OII] ratios of a large number of filaments, combined with data on the densities in these filaments. If a sufficient amount of data is obtained the effects of a possible anisotropy could probably be eliminated. If the densities are derived from the [OII] $\lambda 3727$ doublet ratio, only relative intensities are needed and a high accuracy may be obtained.

The uncertainty of the temperature could be largely removed if the presence or absence of iron lines could be settled. Spectra with moderate dispersion would be sufficient for this purpose. Spectra with a fair dispersion, covering the whole region from 3700 Å to 7400 Å — thus including the red and violet [OII] and [SII] lines, the [NII] and the [OIII] lines — would be valuable to obtain independent estimates of the temperature and the density. They could thereby give us valuable information on the variations of these parameters in a filament, which is of importance for the theory of the structure of the filaments and for the determination of accurate abundances.

The determination of the infrared emission of the nebula is of interest as it would give information on the spectrum of the nebula which cannot be obtained very well from the visual or photographic observations because of the effects of interstellar absorption.

Colour measurements in the continuum at various points in the nebula are needed to determine the change of the energy spectrum of the relativistic electrons across the nebula. The filamentary emission should be carefully eliminated in such measurements.

I wish to express my sincere thanks to Dr W. BAADE and Dr N. U. MAYALL, who very kindly sent us a large number of valuable plates and spectra. This beautiful material forms the basis of the whole investigation. I wish to thank especially Prof. Dr J. H. OORT for many stimulating discussions and valuable criticism. Prof. Dr H. C. VAN DE HULST kindly read the manuscript and made many valuable suggestions. My thanks are also due to Dr D. E. OSTERBROCK, who communicated his data on the electron densities in advance of publication, to Dr J. H. PIDDINGTON for showing us a draft of a paper on the Crab nebula and to Dr A. SCHLÜTER for a discussion on the filaments. Lastly I should like to thank my wife whose help in performing part of the measurements and reductions was of great value.

REFERENCES

- R. ADGIE and F. G. SMITH 1956, *Observatory* **76**, 181.
 L. H. ALLER 1953, *Ap. J.* **118**, 547.
 W. BAADE 1942, *Ap. J.* **96**, 188.
 J. G. BAKER and D. H. MENZEL 1938, *Ap. J.* **88**, 52.
 J. E. BALDWIN 1955, *M. N.* **115**, 690.
 D. BARBIER 1944, *Ann. d'Ap.* **7**, 80.
 D. BARBIER 1945, *Ann. d'Ap.* **8**, 35.
 D. R. BATES, R. A. BUCKINGHAM, H. G. W. MASSEY and J. J. UNWIN 1939, *Proc. R. Soc. London A.* **170**, 322.
 D. R. BATES 1946, *M. N.* **106**, 423.
 D. R. BATES and M. J. SEATON 1950, *M. N.* **109**, 698.
 L. BIERMANN, 1953, in "Kosmische Strahlung", edited by W. HEISENBERG, Chapter 1, 4. Springer Verlag, Berlin.
 A. BOISCHOT, E. J. BLUM, M. GENAT and E. LE ROUX 1956, *C. R.* **242**, 1849.
 E. M. BURBIDGE, G. R. BURBIDGE, W. A. FOWLER and F. HOYLE 1957, "Synthesis of Elements in Stars", Pasadena, California.
 G. R. BURBIDGE 1956, *Ap. J.* **123**, 178.
 J. W. CHAMBERLAIN 1953, *Ap. J.* **117**, 387.
 S. CHANDRASEKHAR 1956, *Proc. Nat. Acad. of Science* **42**, 1
 S. CHANDRASEKHAR and E. FERMI 1953, *Ap. J.* **118**, 116.
 C. H. COSTAIN, B. ELSMORE and G. R. WHITFIELD 1956, *M. N.* **116**, 380.
 A. N. DEUTSCH and V. V. LAVDOVSKY 1940, *Pulk. Circ.* No. 30, 21.
 J. C. DUNCAN 1939, *Ap. J.* **89**, 482.
 W. C. ERICKSON 1957, *Nature* **179**, No. 4563, 773.
 C. Y. FAN 1956, *Ap. J.* **123**, 491.
 R. H. GARSTANG 1951, *M. N.* **111**, 114.
 L. GOLDBERG 1953, in "The Sun", edited by G. P. KUIPER, p. 19, University of Chicago Press.
 J. L. GREENSTEIN 1946, *Ap. J.* **104**, 414.
 W. A. HILTNER 1956, *Ap. J. Suppl.* No. 2, 389.
 F. HOYLE and M. SCHWARZSCHILD 1955, *Ap. J. Suppl.* No. 2, 1.
 K. HUNGER and G. E. KRON 1957, *P.A.S.P.* **69**, 347.
 N. U. MAYALL 1937, *P.A.S.P.* **49**, 101.
 N. U. MAYALL and J. H. OORT 1942, *P.A.S.P.* **54**, 95.
 J. S. MATHIS 1957, *Ap. J.* **125**, 318.
 D. H. MENZEL and L. H. ALLER 1941, *Ap. J.* **94**, 30.
 R. MICHARD 1950, *B.A.N.* **11**, 227 (No. 416).
 R. MINKOWSKI 1942, *Ap. J.* **96**, 199.

- M. MINNAERT 1953, in "The Sun" edited by G. P. KUIPER, Chapter 3.
- J. H. OORT and TH. WALRAVEN 1956, *B.A.N.* **12**, 285 (No. 462).
- D. E. OSTERBROCK 1957, *P.A.S.P.* **69**, 227.
- P. P. PARENAGO 1948, *Astr. Journal U.S.S.R.* **25**, 123.
- H. A. PELS-KLUYVER, 1949, "Problems of cosmical aerodynamics", p. 89. CADO, Dayton, Ohio.
- S. P. PIKELNER 1956, *Astr. Journal U.S.S.R.* **33**, 785.
- L. RIDDIFORD and S. T. BUTLER 1952, *Phil. Magazine* **43**, 447.
- A. SCHLÜTER and R. KIPPENHAHN 1957, *Zs. f. Ap.* **43**, 36.
- J. SCHWINGER 1949, *Phys. Rev.* **75**, 1912.
- M. J. SEATON 1954, *M. N.* **114**, 154.
- C. L. SEEGER, G. WESTERHOUT and H. C. VAN DE HULST 1956, *B.A.N.* **13**, 89 (No. 472).
- C. L. SEEGER 1957, *Report U.R.S.I.* at Boulder, Colorado.
- C. L. SEEGER and G. WESTERHOUT 1957, *B.A.N.* **13**, 313 (No. 478).
- I. S. SHKLOVSKY 1953, *Doklady Akad. Nauk. U.S.S.R.* **90**, 383.
- I. S. SHKLOVSKY 1953, *Doklady Akad. Nauk. U.S.S.R.* **91**, 475.
- L. SPITZER 1956, "Physics of fully ionized gases", pp. 41 ff. Interscience Publishers, New York.
- J. STEBBINS, C. M. HUFFER and A. E. WHITFORD 1940, *Ap. J.* **91**, 20.
- J. A. STRATTON 1941, "Electromagnetic theory". McGraw-Hill, New York.
- SU-SHU HUANG 1948, *Ap. J.* **108**, 354.
- TH. WALRAVEN 1957, *B.A.N.* **13**, 293 (No. 478).
- L. WOLTJER 1957, *B.A.N.* **13**, 302 (No. 478).
- M. WRUBEL 1952, *Ap. J.* **116**, 291.